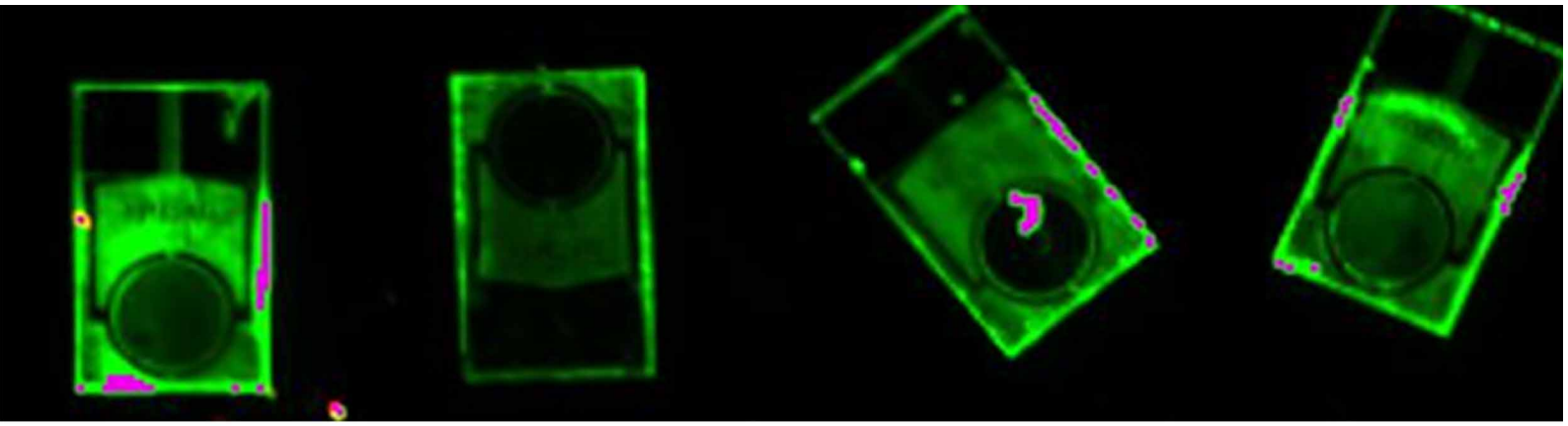

Characteristics of BioMEMS thin-film polymers

Silvana van der Voort

TU Delft PHILIPS TU/e

Characteristics of BioMEMS thin-film polymers

A study towards the biocompatibility

by

S. van der Voort

Student Name	Student Number
Silvana van der Voort	4398912

Supervisor:	J. van Beek
	R. Dekker
	R. de Kooi.
	E. Timmering.
Project Duration:	February, 2022 - December, 2022
Faculty:	Faculty 3ME and EEMCS, Delft

Cover: Fluorescence SU-8 chips and crystalline structure on polymer layer

TU Delft

Contents

List of Figures

List of Tables

Acknowledgement

While completing this thesis assignment, I was able to dive into the business world. I would like to thank all the people and colleagues who helped me throughout this assignment. My supervisors (J. van Beek and R. Dekker), as well as my cleanroom mentor, E. Timmering, for his assistance in setting up, running, and dismantling the experiments and assisting with sample production. And the PhD students (M. Klimopoulou and R. Kooi) for the cell culturing procedures and tests. Last but not least, I want to thank my family and friends for assisting me in completing my studies one step at a time. Thank you all for the lessons you have taught me.

Abstract

Biomedical micro-electromechanical systems, or BioMEMS are microdevices with an actuation or sensory function in biomedical applications. In this process, polymers are widely used as material layers. Polymers have significant advantages for applications in BioMEMS, such as low cost and ease of fabrication. The problem at the moment is the lack of information needed to compare polymers with each other in order to identify their characteristics and properties. These characteristics are particularly important for the biocompatibility of the BioMEMS. Therefore, the optical characteristics, surface characteristics, adhesion etching, and cytotoxicity are investigated. For the optical characteristics, the polymers were examined for fluorescence and transmission of light. For the surface characteristics, hermeticity (non-permeable) and wettability (hydrophilic or hydrophobic surfaces) were examined. Furthermore, adhesion and etching were studied for their (chemical) resistance. Finally, the polymers were examined for their toxicity to cells (cytotoxic).
Through these tests, more information about the polymers and their characteristics has been obtained through these tests. The results of these different tests cannot be combined into a single polymer showing the best results from all tests. The fluorescence test showed that the layers of the final device are important as they can be responsible for a different intensity of fluorescence. Furthermore, it was found that perminex is the most hydrophilic but may fracture in saline solution. It was noteworthy that the polymers, which are already widely used in BioMEMS applications (SU-8 and parylene-C), appeared to be the only ones to exhibit negative effects on cells (toxicity and cell growth inhibition). The other polymers tended to do significantly better there. Even though a number of properties that are important for biocompatibility were evaluated here, to ensure that the polymers and BioMEMS devices are fully compliant, testing will be required to meet the ISO standard 10993.

1

Introduction

1.1. Background information

Since the 1980s, there have been many developments in the field of Micro-Electro-Mechanical Systems (MEMS). MEMS technology has gained popularity in applications requiring actuation and sensing due to its excellent performance at low power and small dimensions. These microsystems are called BioMEMS when they are designed to operate for biological, medical, and chemical applications. BioMEMS has a lot of overlap with microfluidics where fluids are manipulated at sub-millimeter dimensions and microTAS(μTAS) which involves microsystems performing chemical/biological analysis of desired samples.Due to this overlap a wide variety of polymers are often tested and researched for improving the micro device's properties such as optical absorption, cell toxicity etc. Philips is performing research in the area of both BioMEMS and microfluidics. Research in the field of microfluidics and BioMEMS are gaining popularity, as everything is getting smaller to the micro- and nanometer scale, and there are more opportunities to obtain data. The field of BioMEMS involves diverse topics such as the fabrication of micro-sized sensors, miniaturized drug delivery systems, organ-on-chip, etc. There is often an overlap between lab-on-chip devices, microfluidic devices, and BioMEMS. During this project, a number of polymers used for BioMEMS devices are evaluated, but they can and sometimes are also applied in microfluidics and microTAS.

1.2. Research goal and outline

The aim of the assignment is to evaluate the biocompatibility of a selected set of polymers, which are available for processing of BioMEMS in the Philips MEMS foundry. The polymer SU-8 is a widely used epoxy-photoresist but has some downsides when used in a production environment. For example, the adhesion of su-8 is often unsatisfactory, but also has problems creating bulk structures. Therefore, other polymers are studied and their performances will be compared with SU-8. With that, an overview can be created to gain more insight into application possibilities for future clients regarding BioMEMS applications. Research question:

How biocompatible are the polymers that can be used for BioMEMS processing at Philips MEMS foundry *in-vitro* applications in comparison with SU-8?

To answer this question, we will first discuss what BioMEMS entail and how they are made. Moving further, important properties and applications of BioMEMS are discussed. Finally, the research conducted in various areas to ascertain the biocompatibility of various polymers is discussed. This report will highlight the following topics: optical properties, surface properties, adhesion and etching characteristics, and cytotoxicity of the polymers.
The goals for the project are as follows:

- Study the optical characteristics of the polymers.
- Evaluate the hermeticity of the polymers.
- Evaluate if the polymers are cytotoxic according to ISO-10993-5.

Chapters 2 and 3 will consist of background information providing insight into various material properties and production processes conducted in this work. Chapter 2 discusses the definition and function of a BioMEMS device. Next, Chapter 3 introduces the various polymers to be studied. ”Chapter 4 explains various processing steps involved in the production of samples which were used for testing in this work. Chapter 5 discusses the optical characteristics of these polymers along with the tests performed to determine these properties. Chapter 6 will cover the surface properties of the polymers, followed by the adhesion of the polymers in Chapter 7. Chapter 8 will conclude the series of tests by studying the cytotoxicity. Chapter 9 discusses the characteristic results of the tests performed on these polymers while Chapter 10 addresses the answer to the research question of this thesis.

2

BioMEMS devices

2.1. Introduction

The Bio in BioMEMS stands for biomedical or biological-MEMS. As the name suggests it encompasses a wide variety of technologies including but not limited to biomedical engineering, electrical microsystems, electromechanical systems, material sciences, chemical engineering, etc. In this chapter, BioMEMS devices are discussed in detail. The chapter begins with the definition of BioMEMS and Micro-fabrication techniques used to fabricate these devices. The chapter is then concluded with some examples of BioMEMS applications.

For a few decades now, Integrated Circuit (IC) technology has grown from fabricating a few thousand transistors to a hundred billion transistors in a single integrated circuit. In IC technology silicon substrates are subjected to various processes to manufacture electrical elements such as BJT transistors, CMOS transistors, diodes, etc. This same technology is also used to fabricate MEMS devices which are essentially micrometer sized actuators and sensors that are often used in many electronics including a smartphone. MEMS devices are fabricated using a series of IC technology processing steps called micro-fabrication techniques. These techniques include for example lithography, deposition processes and etching processes. These techniques are further discussed thoroughly in Section 2.1.1.

The materials used to produce a BioMEMS device can be distinguished in three classes:
• Materials that are often used in IC technology (silicon, glass, photoresists etc.);
• Plastics and polymers;
• Biological materials (cells, tissues, proteins);
In this report, all of these materials will play a role, but the focus will be on the role of the polymers in BioMEMS. The benefit of polymers for BioMEMS is the mass production, low cost, ease of fabrication, flexibility, transparency, etc. These benefits are highlighted in later sections of this report.

2.1.1. Micro-fabrication techniques

During the fabrication of a BioMEMS, sacrificial and structural layers will be used to form the required 3D-structure for the MEMS devices. The difference between these two layers is, the sacrificial layer will be removed in a later stage whereas the structural layer remains. The desired shape of the MEMS device can be produced with the structural layers.

To create these MEMS, micro-fabrication techniques are used in the industry to create structures, layer by layer. They can be distinguished into two subdivisions: *surface micro-machining* and *bulk micro-machining*. The difference between these two is that surface micromachining creates structures layer by layer and removes parts to create freestanding structures, whereas bulk micromachining removes parts of the material through etching methods such as wet or dry etching. Figure 2.1b shows a schematic representation of the structural and sacrificial layers during a surface micromachining process. To create a BioMEMS, the same microfabrication techniques are used to create a MEMS. Therefore, if a polymer is used to create a BioMEMS, it should withstand and be able to be used during

the following microfabrication techniques:

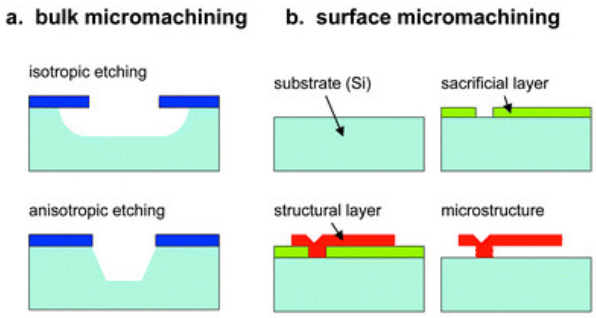

Figure 2.1: The difference between a.) Bulk micromachining and b.) Surface micromachining to produce the structure of a MEMS device.

- *Deposition*
  Dropping or deposit material on a wafer. This could either be a metal or a polymer. There are multiple ways to deposit a material on the substrate layer. Figure 2.2 shows two examples of how a material can be deposited on a wafer. Chemical vapor deposition (CVD) is a coating method that uses gaseous reagents to supply thermally induced chemical reactions at the surface of a heated substrate.

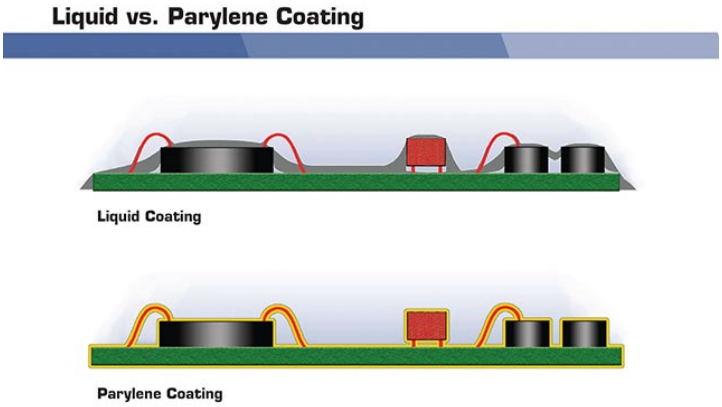

(a) Chemical vapour deposition, as the name suggests, the polymer will be deposited on the wafer when reactants are in vapour phase.

(b) Spin coating a polymer evenly on a wafer.

Figure 2.2: Two examples of how a material can be deposited on a substrate.

- *Lithography*
  With the use of UV light and a mask, patterns can be made on the material. The photoresist will be developed by immersing the wafer in a solution.
- *Etching*
  After the lithography, an etching step is needed to remove parts of the material. There are two types of etching: dry etching and wet etching. Dry etching is the process where reactive ions are targeting the material. The process of how it targets the material is dependent on the type of dry

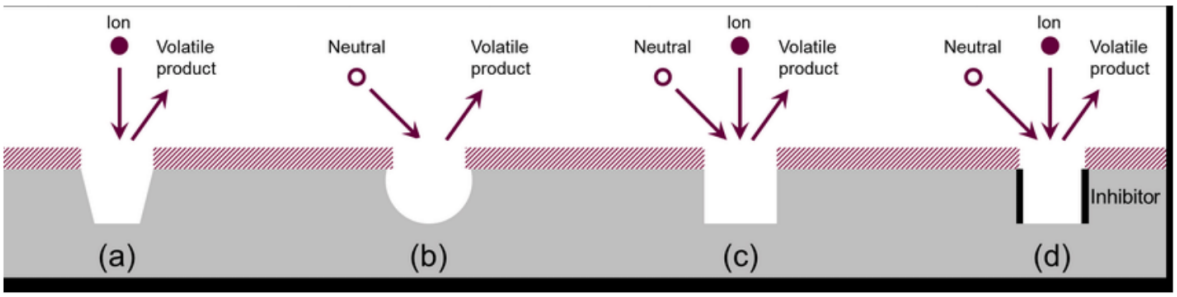

14: Description of basic etching processes: (a) sputtering, (b) pure chemical etching, (c) ion-assisted etching, and (d) ion-enhanced inhibitor etching.

Figure 2.3: Different ways of dry etching.

etching. Figure 2.3 shows different types of dry etching creating different structures. With wet etching, the wafer is placed in a bath of a chemical solution to cause the reaction. The type of etching and chemical solution depends on the materials involved.

- *Curing*
  With polymers, the curing step creates stability in the material by crosslinking it. Dependent of the polymer the crosslinking will be performed with exposure or with a post-bake.

Focus on BioMEMS

During this thesis, the focus will be on BioMEMS applications where polymers are involved. BioMEMS devices have an overlap with microfluidics and μTAS devices. At Philips, there are projects working on MEMS (e.g. capacitive micromachined ultrasonic transducers, CMUTs), BioMEMS, microfluidics, and more [1]. For this reason, some of the polymer applications can have applications in a more microfluidic field. The efficiency of a device's performance is dependent on the characteristics and applications. In this section, some BioMEMS examples will be highlighted and the scope will be on the role of the polymers in these examples.

Examples of BioMEMS

BioMEMS refer to biomedical micro-electro-mechanical systems which involves measuring, sensing, changing or creating biological functions.

- Microneedles:
  Microneedles can be used as an interface device between an organ and a micro device on the outside (see Figure 2.4b). These microdevices can be used to deliver drugs, proteins, or other liquid substances toward the organ or for analyzing purposes of the organic system [2].
- Cantilever beams:
  A MEMS device for biochemical sensoring. Meaning it can be used to detect proteins or other biochemical substances. The cantilever beam with its mass is made of a polymer, see Figure 2.4a. The mass is connected to a chip to transfer the information from the sensor to its destination [3].
- Organ-on-chips:
  Organ-on-chips are devices consisting of cells in a micro-environment, where the cells represent the organ and the micro-environment is the chip. The types of cells are dependent on the organ, but since an organ itself consists of different types of cells, the mimicking purpose of the organ-on-chip should be clear. The chip part needs to be made to look like the cells' natural surroundings. The chip is primarily a 3D culture environment with round tubes in order to mimic a vessel structure.

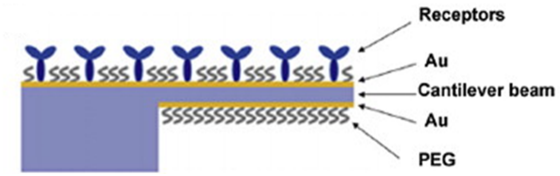

(a) A cantilever of a polymer called SU-8, which can be used for protein detection methods [3].

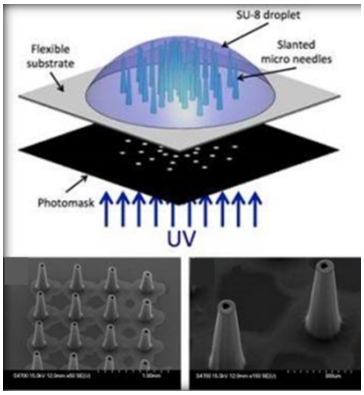

(b) Microneedle as interface communication between the organic system and outside device [2].

Requirements of BioMEMS polymers

The polymers that will be looked into are polymers that are currently used by companies to create BioMEMS devices and are therefore applicable in the aforementioned micro-fabrication techniques. However, for the current and future applications, there is a lack of information about their characteristics compared to other polymers. That will be one of the goals of this thesis: investigating what their characteristics are compared to other polymers that are being used. As one cannot investigate every single characteristic of a material, we will look at characteristics that are of importance for potential clients in deciding what polymers are the right fit for their application. To investigate the performance of a BioMEMS, fluorescence measurements are needed, which is why the optical characteristics of the polymers will be studied. When polymers with a low autofluorescence are used, the signal will improve as it will reduce the amount of noise that can exhibit during fluorescent imaging or detection, as it reduces the signal-to-noise ratio. Moreover, since BioMEMS applications can involve *in vitro* and *in vivo* contacts, the device should still work in these environments. Therefore not only the cytotoxicity will be tested, but since the polymers can also be used to encapsulate devices, they should prevent potential corrosion, causing dysfunctional BioMEMS devices.

3

Polymers used for BioMEMS applications

3.1. Introduction

Polymers used in BioMEMS have functions regarding encapsulation, wafer bonding, transparency, flexibility, microlayer structure building, and more. A polymer is an organic compound composed of more than 100 repeated sub-units of monomers, which are chemically coupled due to the process of polymerization. Because of their wide range of attributes, synthetic and natural polymers are part of our everyday lives. Polymer-based technologies introduced in the 1990s have played a large role in advancing MEMS into new applications, especially in the area of BioMEMS. The application of polymers in BioMEMS devices is beneficial due to their increased biocompatibility, abundance, ease of fabrication, low cost, low protein absorption, rapid prototyping, low thermal and electrical conductivity, and ability to integrate functional hydrogel materials. This chapter discusses the types of polymers used in this work while introducing the bio-compatibility of polymers.

3.2. Types of polymers

SU-8 is one of the main polymers in the market. This will be our reference polymer, to study the fluorescence of others which will be discussed further in Chapter 5.1. There are a variety of polymers that are typically used for BioMEMS, but this project will focus on the key polymers of interest to Philips. Polymers such as SU-8, polyimide, and parylene-C are widely used in the fields of BioMEMS, microfluidics, and microTAS. Therefore, there is also more information available on these polymers compared to the other polymers which are lesser known. Below will be a list of these polymers, with the polymer SU-8 as a point of reference. An overview of the polymers and their structures can be seen in Table 3.1. Passivation is the technique of applying a thin, inert coating to a microdevice's surface in order to significantly enhance its electrical properties.

- **SU-8**: It is an epoxy-based polymer and is widely mentioned in studies as a polymer for diverse applications, especially for cantilever beams (as seen in Figure 2.4a). The SU-8 that will be used in this report is SU-8 2002. According to Kayakuam (manufacturer), this type of SU-8 will create a layer thickness of 0.8-3 μm with one spin coat and can create an optimum layer from 10 -100 μm [4].
- **BCB**: A polymer that stands for benzocyclobutene. It is good for high-frequency applications due to its high resistivity and low dielectric constant. It's mainly used to bond two wafers to each other. It is a polymer that is used frequently to bond the top and lower level pieces of a microfluidic system together, due to its high bonding strength (see Figure 3.1a)
- **Parylene**: A polymer that is not spin-coated on a wafer, but chemically vapor deposited. This polymer is used for encapsulating devices due to its biocompatibility and the way it is deposited on the wafer. In Figure 2.2a, one can see how chemical vapor deposition will cover it conformally over the whole target. There are four types of parylene: N, D, C, and HT. Only parylene-C is

Polymer	Type	Structure	Application	Layer thickness[μm]
SU-8 2002 [4]	Negative epoxy photoresist	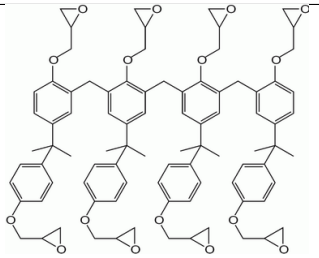	Structural, passivation[1] layer	0.8-3 (single layer); 10-100 (optimal)
BCB 3000[5]	Negative photoresin	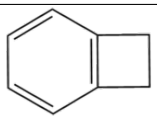	Dielectric, passivation, covering and adhesive layer,	2.35-5.46
Parylene-C [6]	Gas coating	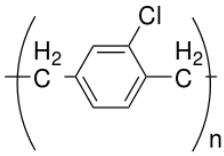	Covering layer	2-25
Perminex 2005[7]	Negative epoxy photoresist	N/A	Adhesive layer	1-25
Polyimide 2610[8]	Positive photoresist	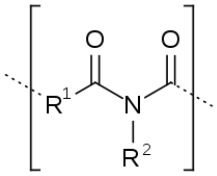	Dielectric and structural layer	1-2.5
TMMR [9]	Negative epoxy photoresist	N/A	Adhesive layer	10-50

Table 3.1: Summarized overview of the polymers. Type, layer applications and thickness as mentioned by the manufacturers.

of importance due to its low permeability. In addition to having an extremely low permeability to moisture and corrosive gases, parylene-C also possesses a desirable mix of electrical and physical properties. When parylene is mentioned throughout this report, it will be about parylene-C.

- **Perminex**: Another negative epoxy photoresist is perminex. It is used to bond wafers together and used for Lab-on-Chip applications. The application of perminex and the number of studies on it are sparse. Given the reliance on research, the manufacturing company provides the majority of the information about perminex, which is not entirely objective [10].
- **Polyimide**: A polymer that has a high thermal stability of more than 300°C. This polymer is also widely used as tape in electrical devices. In the same manner, it is used in BioMEMS for its flexible characteristics. In applications, it is often used in combination with parylene-C (see Figure 3.1b) [11].
- **TMMR**: produced by TOK, a company from Japan. It is an epoxy-based polymer that is sold in liquid and film structures. The dry film version, known as TMMF, is up to 55 μm thick. These dry films are delivered with protective PET films. According to Wangler, N. et al. (2011), TOK-TMMF is non-cytotoxic with the ISO-10993 criteria tested. This also means that TMMR is non-cytotoxic. The TMMR version is spin-coated on a wafer [9].

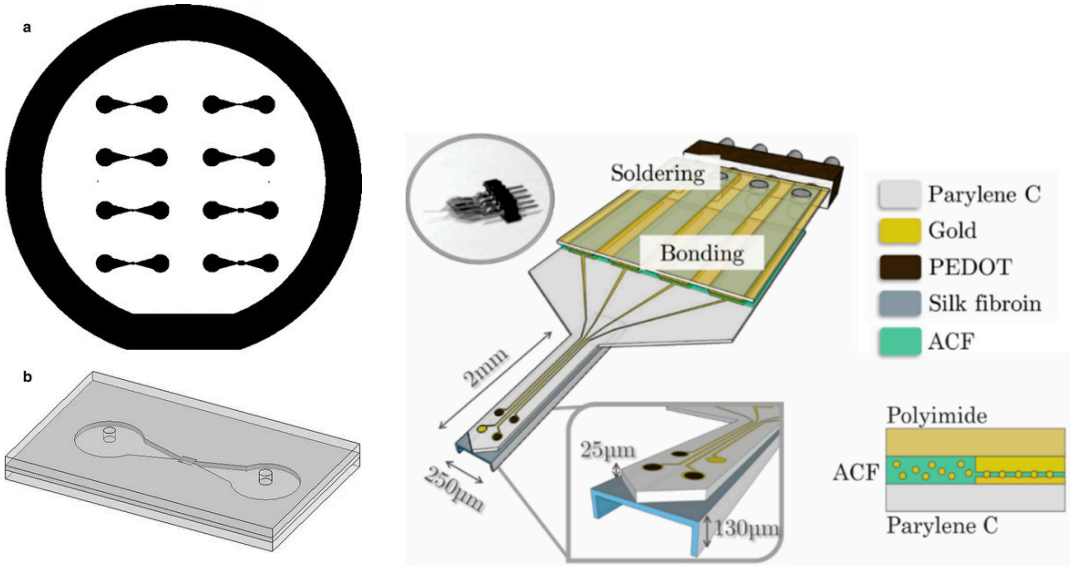

(a) Microfluidic device where top and bottom layer are bonded together with BCB to create a chamber [12].

(b) A neural probe made of a Parylene-C basis, with electrodes and attached to a polyimide cable [11].

Figure 3.1: Applications of polymers.

Only the polymers that are available at the MMD cleanroom of Philips will be included, though, as this study is being conducted on their behalf. Therefore, only the polymers SU-8, BCB, parylene-C, perminex, polyimide, and TMMR will be covered.

3.2.1. Bio-compatibility and dependencies

Biocompatibility can have different meanings. In this context, a device or material is biocompatible if it does not cause harmful effects to the body and has the desired optical characteristics. This is a broad term, as something can be partially harmful but not in this application. ISO 10993 includes a range of tests to validate the biocompatibility of a medical device. These tests investigate different biological effects, with the most critical tests being: cytotoxicity, sensitization, and irritation, or intracutaneous reactivity [13]. Depending on the application, contact with the body, and duration, more biocompatibility tests may be required or recommended. In this case, there is no specific device or application other than it being BioMEMS. On top of that, since this is a thesis and not an official ISO biocompatibility test, no guinea pigs, lymph nodes (sensitization), or blood tests (irritation) were performed.

As the purpose of these polymers is their usage in BioMEMS, it is important to mention factors that can affect a polymer's biocompatibility with its surroundings. According to Constatin, C.P. et al. (2019) a number of material-related aspects can influence the biocompatibility of polymers [14]. These factors are:

- *Bulk characteristics* - composition morphology;
- *Surface features* - chemical composition, wettability, mechanical features and roughness;
- *Degradation*- their reaction mechanism and products and their resistance in different surroundings and how they respond;
- *Leachables, extractables and potential toxicity*- cell viability, proliferation and adhesion.

For this reason, some of these topics will be investigated. This will include at least the following: research on the surface of the polymers, their resistance in a saline solution, and cell toxicity.

4

Production of samples

4.1. Introduction

This chapter will discuss the production of the samples needed for the experiments. Since this project studies diverse topics, different samples were needed to study the characteristics. Even though these samples were initially produced for the fluorescent and hermeticity measurement, due to the area of the wafers (fluorescent samples) and amount of the samples (hermeticity) they were used in multiple experiments.

4.2. Fluorescence

The fluorescence samples started with collecting samples of polymers of interest from other people of the Philips MMD department. However, after analyzing the early results on fluorescent measurements, a more steady approach was needed. As a result, the goal was to obtain wafers with no polymer structures on them, resulting in blank polymers on wafers. Most of the polymers are spin-coated on a wafer. This means that the polymers from the chemical bottles are poured onto the wafer. The wafer is placed on a spinning plate and draws a vacuum. Due to the speed of the spinning plate, the polymer will be evenly spread over the wafer. As previously stated, only parylene-C is not spin-coated. The blank parylene-C wafers were prepared by people in the cleanroom working with the CVD machine. The flows of the spin-coated blank wafers are also described in Section 4.3.6, but they can be summarized briefly as follows:

1. Clean a silicon wafer in the oxygen plasma to remove organic contaminants.
2. Prepare the spinner, place the wafer and apply water on the wafer to make it hydrophilic for good adhesion, until the wafer is spin dry. Some primers need to attach to OH groups. For an HMDS primer, it's not as necessary as it is for the other primers, but it will be executed. HMDS is deposited by gas and is therefore also applied on both sides of the wafer.
3. Add a primer (adhesion promoter) if needed to ensure the adhesion of the polymer to the wafer. : It depends on the type of primer if it can be deposited with a spin coating step or a machine. The machine that is only used for the HMDS-primer, is needed for the perminex ans SU-8.
4. Next, the primer has been added and baked. The polymer was spun on the wafer with a spin coater, as in Figure 4.1.
5. The wafer underwent a soft bake, to bake any solvent away.
6. After that, the wafer only needs an exposure step and a post-bake or other curing method to complete the total process.

Figure 4.1: An illustration of how a polymer can be applied when a wafer is on a spin coater [15].

Table 4.1 summarizes which primer was used per polymer and what the spin parameters were. At this point, only the SU8, BCB, Perminex, and Polyimide blanket wafers have been created. The parylene-C wafer was already delivered during the first measurements on fluorescence. At the end of the chapter, there is a table with an overview of all the thicknesses of the different samples.

Polymer	Primers	Spin speed	Bake [°C]	Cure
SU8 2002	HMDS	1000 rpm	95	Exposure and Hotplate
BCB 3003-46	AP3000	1000 rpm	120	350 °C Chemical lab oven or oven cleanroom
Perminex 2005	HMDS	1000 rpm	95	Exposure and Hotplate
Polyimide 2610	VM562	1500 rpm	120	convection oven 275°C

Table 4.1: Overview of the primers, spin speed, bake time, and way to cure the polymers to create a blanket wafer.

4.3. Hermeticity

For the hermeticity tests, the samples were prepared in the cleanroom. The samples for the hermeticity tests were prepared in the cleanroom. The aim of the samples were defined before the production of the samples started. The goal of the tests was to see if the polymers were hermetically sealed, in which the polymers would not cause corrosion on the samples. The mask that was used was from a previous student, where meander beams were made to perform these corrosion tests. In this case, the difference of the interaction between ceramic and non-ceramic layers within the sample was not relevant. In Figure 4.2 one can see the distinctive layers of the samples, with two variables in terms of layers: the layer of encapsulation and the metal interconnects. In Table 4.2, there are two different materials for the metal layer. Aluminum tracks were used as it is sensitive to corrosion. The main purpose of the hermeticity tests was to investigate if the tracks would corrode due to the permeability of the polymers. Gold metal tracks were used to investigate potential problems of processing gold. But as the adhesion of the polymers is dependent on the substrate layer, a different metal can potentially indicate this as well.

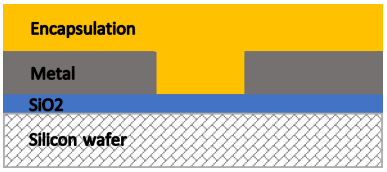

Figure 4.2: Structural layers of hermeticity samples.

		Encapsulation layers				
		SU-8	**BCB**	**Perminex**	**Polyimide**	**SiN**
Metal layer	**Al**	2	2	2	2	2
	Au	2	2	2	2	2

Table 4.2: Amount of wafers with the different layers.

4.3.1. PECVD oxide

For proper adhesion to the wafer, an oxide layer is first applied by PECVD of silane (SiH_4) and nitrous oxide (N_2O) as precursor gases. This results in Figure 4.3, consisting of the silicon wafer with the Silicon dioxide top layer.

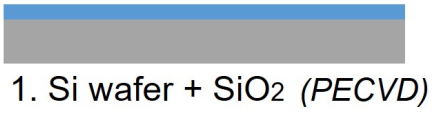

Figure 4.3: Step 1: Add an oxide layer on the wafer.

4.3.2. Metal tracks

Next, metal is sputtered. In this process, argon is supplied in a high vacuum, where it hits the target material. In the process, the positive ions of the argon collide with the negative ions of the target material, causing the desired material to be sputtered on the surface of the wafer.

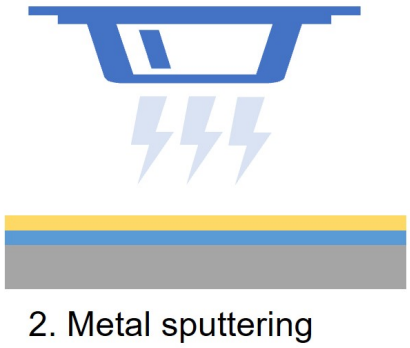

Figure 4.4: Step 2: Sputter metal

4.3.3. Lithography

The purpose of lithography is to create a pattern on the wafer, consisting of the processing steps seen in Figure 4.5. A primer of 1.3 μm HPR was added first, followed by a 50 mJ contact lithography exposure. For the contact exposure, a positive tone mask was used, which keeps the exposed parts and removes the unexposed parts. After that, the wafers were developed with a post-exposure bake step. The device seen in Figure 4.6b, performs the lithography steps except for the exposure.
The next day, the 10 wafers of aluminum went into a convection oven at 125 °C for 30 minutes. This temperature was to keep the rubber quality high and decrease the chance and amount of under-etching. When the 30 minutes were over, the wafers went into the barrel for a descum to create a hydrophilic surface. The oxygen plasma descum that exists has the goal of removing thin residual layers on the wafer. The descum is needed now to create OH-groups on the aluminum surface; if it was kept hydrophobic, bubbles of air would exist during the next steps.

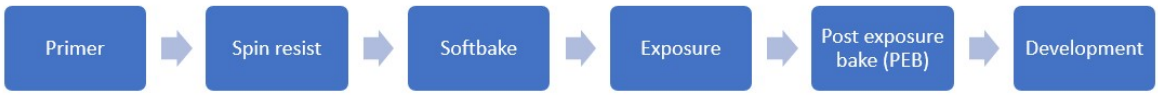

Figure 4.5: Lithography process.

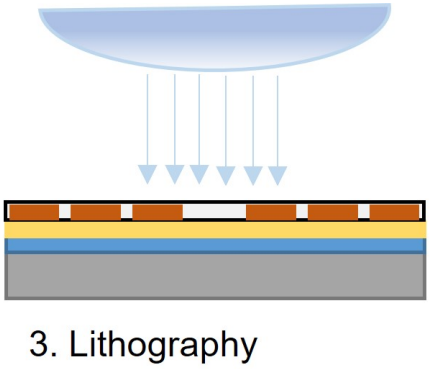

(a) Step 3: Add resist and expose with mask.

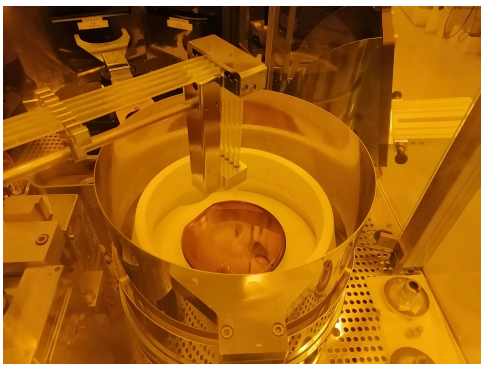

(b) One of the wafers being developed, where the structure will be visible.

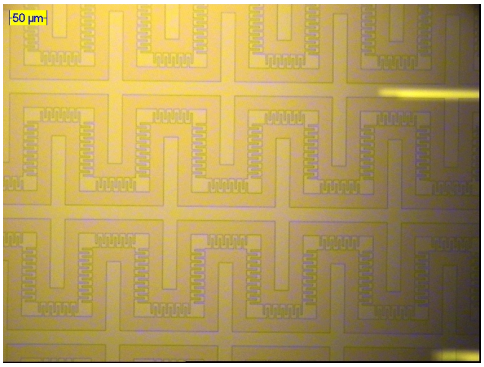

(c) The gold meander beams of the sample after lithography step (microscope).

Figure 4.6: Lithography exposure and microscopic result.

4.3.4. Etching

As there are two types of metal tracks on the design, there are two different processes performed. The wafers with aluminum tracks were etched with PES and were there for 10 minutes and 30 seconds. The gold wafers were etched with gold etching (Transveen). First, the titanium dissolving process was tested on a glass gold wafer. A glass wafer was used to observe the under-etching of gold. Titanium is gray colored whereas gold is yellow colored. With a glass wafer, the under-etching can be studied from the bottom of the wafer, as it is impossible to investigate the under-etch with a silicon wafer. The result was that 1% HF was superior to using the barrel with CF_4. The barrel needed a trial-and-error approach and has a risk where parts of the gold structures are gone. The result of the gold wafer after lithography and after etch can be seen in Figure 4.7b.

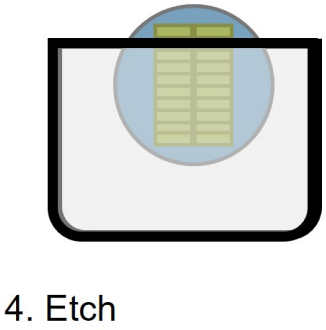

(a) Step 4: Etching the wafers.

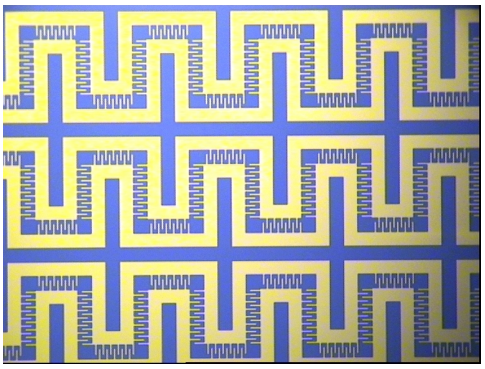

(b) The meander beams of the sample after the gold etching step.

Figure 4.7: Microscopic inspection on the gold wafer structure.

4.3.5. Strip resist

To clean the substrate layer of the resist, the wafers were placed in acetone. The result from this is shown in Figure 4.8 with the resist on the metal layer removed. This was performed for both the aluminum-coated and gold-coated wafers.

Figure 4.8: Step 5: Removing the resist.

4.3.6. Polymer coating

Coating the polymer consists of pre-treatment, spinning, and curing. During pre-treatment, the wafers are set in the barrel to give them a hydrophilic substrate and eliminate any contamination on the surface. Depending on the primer, an OH group may be required on the surface. If so, water will be spun for better adhesion. For the primer HMDS, this is not required; however, for the primers of polyimide and BCB, it is needed. Then the primers were applied to the substrate layer. The primer HMDS was required for SU-8 and perminex. With HMDS, this was conducted using a vapour primer oven, where it was deposited on the wafer as a gaseous compound. For BCB, primer AP3000 is used, and for polyimide, primer VM652 is used. The next step is to coat the wafers with the polymers that will be part of the experiments. Wafers requiring a silicon nitride Si_3N_4 layer had been sent to PECVD (plasma enhanced chemical vapor deposition), which deposited a layer of 0.5 μm of Si_3N_4. Spin coating was required to deposit the polymer layers on the wafers. Table 4.3 shows that a dynamic spin was used. In this, the lid of the spinner is open in the first part. Then the lid closes and the speed (rpm) of the spinner is increased. The exact spin speed and time can be seen in the table. These parameters determine the thickness of the polymer layer. Next, the polymers are cured to crosslink them. This curing can consist of a high-temperature baking step or an exposure step followed by a baking step.

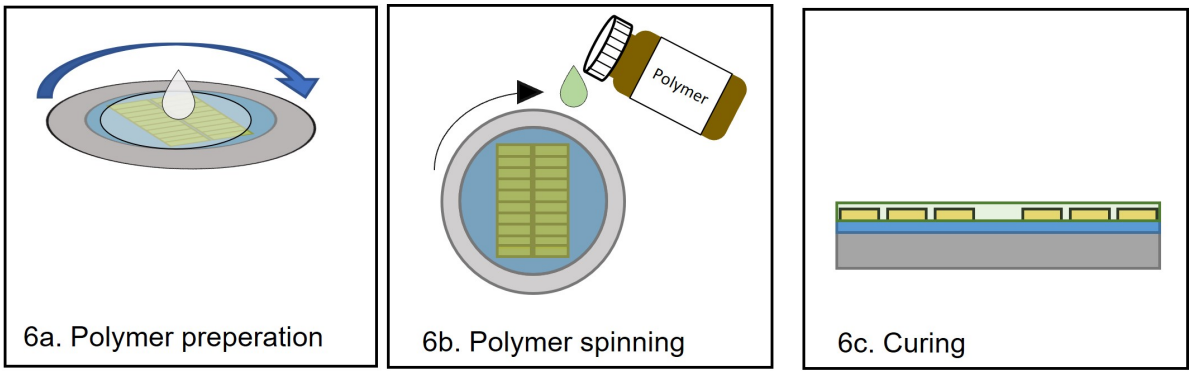

Figure 4.9: Polymer preparation, coating and curing.

	BCB	**Perminex**	**Polyimide**	**SU-8**
Pre-treatment	Barrel & water	Barrel	Barrel & water	Barrel
Primer	AP3000 10 s at 500 rpm 20 s at 1000 rpm	HMDS (primer convection)	VM652 10 s at 500 rpm 20 s at 1000 rpm	HMDS (primer convection)
Spin polymer (Dynamic)	10 s at 500 rpm 20 s at 1000 rpm	10 s at 500 rpm 20 s at 1000 rpm	10 s at 750 rpm 30 s at 1500 rpm	10 s at 750 rpm 20 s at 1000rpm
Soft bake	1 minute at 120 °C	5 minutes at 95 °C	5 minutes at 120 °C	3 minutes at 95 °C
Curing	Bake at T=225 °C	Exposure & hard bake	Bake at T=350 °C	Exposure & hard bake

Table 4.3: Summarized polymer coating parameters.

4.3.7. Dicing

After all the encapsulation layers were deposited, the wafers were ready to be diced into the correct dimensions with a width of approximately 50 mm wide and a height of 10 mm per sample. To cut the wafer, a diamond coated saw was used. Water is sprayed on the dicer. If the adhesion of the layer is not sufficient, the polymer layer will detach from the substrate layer.

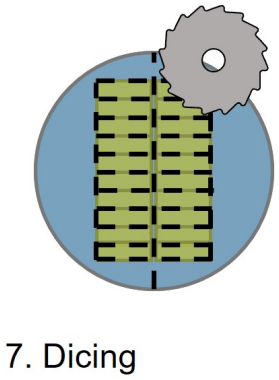

Figure 4.10: Step 7. Wafer dicing.

4.4. Overview of thicknesses different samples

The following table (Table 4.4) shows the exact type of polymers used during the whole study. Furthermore, it shows what kinds of samples were used for different tests and their thicknesses. These thicknesses were measured with a step altimeter, where a needle slides over the wafer and the thickness can be measured. To be certain of the thicknesses, they needed to be measured at least three times. For these measurements, a scratch was made on the sample to be measured.

Polymer	Structured	Blank	Glass	Cytotoxic	Hermeticity
BCB 3003-46	-	32 (old)	2.04	1.95	2.48
Parylene-C	-	4.85	-	4.99	-
Perminex 2005	4	4 (unexposed)	4.63	4.77	6.62
Polyimide 2610	-	3	3.12	3.26	4.48
SU-8 2002	5	3.10	2.51	2.10	2.66
SiN	-	-	-	-	0.5
TMMR	20	60	-	-	-

Table 4.4: Thickness of all the samples used during tests in μm.

5

Optical characteristics

5.1. Introduction

To investigate the functioning of the BioMEMS device, there are three possible detection modalities: mechanical, electrical, and optical detection. For BioMEMS, optical detection is a commonly used method to study the BioMEMS sensor, since this is also performed in biology and life sciences. Optical detection can be performed based on chemiluminescence and fluorescence [16]. Chemiluminescence refers to the emission of visible light due to a chemical reaction; as chemical reactions between the polymers and other materials are outside the scope of this thesis. Fluorescent detection can be performed due to fluorescent markers. For BioMEMS one wants to study the functioning of the BioMEMS with fluorescent detection. Therefore it is necessary that the polymers in the BioMEMS are not influencing the fluorescent detection methods. As a result, the polymers used in the BioMEMS layers should have a low to zero level of auto-fluorescence at the wavelength ranges where the detection methods are used. There are several dyes and proteins that can be used to create a fluorescent visual for these detection methods [17]; a list of these can be found in Appendix A.1. In Figure 5.1 one can see how the fluorescent dyes and proteins used are distributed over the emission wavelength spectrum. Most of them lie within the 465–600 nm range of emission wavelengths; therefore, this is the preferred range for a low autofluorescence. The dyes and proteins used by customers are between 500-520 nm, the range to avoid is 500 to 550 nm in the emission spectrum.

As some of the applications of the BioMEMS are about detecting cells or proteins with an emitted fluorescent light, it is unwanted to have a device with an auto-fluorescence caused by the polymers in this range of the emitted light. Furthermore, fluorescence is one of the ways that a BioMEMS functionality with its performance can be detected [18]. To get more insight in the optical properties of the polymers within the layer, the absorption and transmission will be studied. The absorption spectrum also shows how much of the light will be absorbed over the wavelength. It might be useful to combine this information with the fluorescence levels on the polymers, introducing potential insights. What should be noticed is that the color of the polymers may influence the absorption and fluorescent levels. When BCB is baked with too much oxygen, it might turn to a yellow/brown color. It was not in this case, but the polyimide had a yellow-colored blaze.

Principle of fluorescence

When a material is fluorescent, it means that the molecules (fluorophores) of the material, are able to absorb the energy of the photons from the incoming light and thereby turn the electrons of the molecules to a state with a higher energy. At that moment, the electron will lose some energy due to vibrations of molecules and get to the excited state. When the electron falls back to its original state it will emit light of a certain wavelength deciding its fluorescent colour. The emitted wavelength will be higher compared to the wavelength of the excited state, since it has absorbed the electromagnetic energy of the photon. Figure 5.2 shows how a molecule of a material goes into an excited stage and then emits energy. As mentioned before, the BioMEMS could have different applications with fluorescence. Some of the proteins and dyes are used for cell detection methods, where the fluorescence of the cells is measured by a laser. But also other fluorescence detection methods can be disturbed with the auto-fluorescence

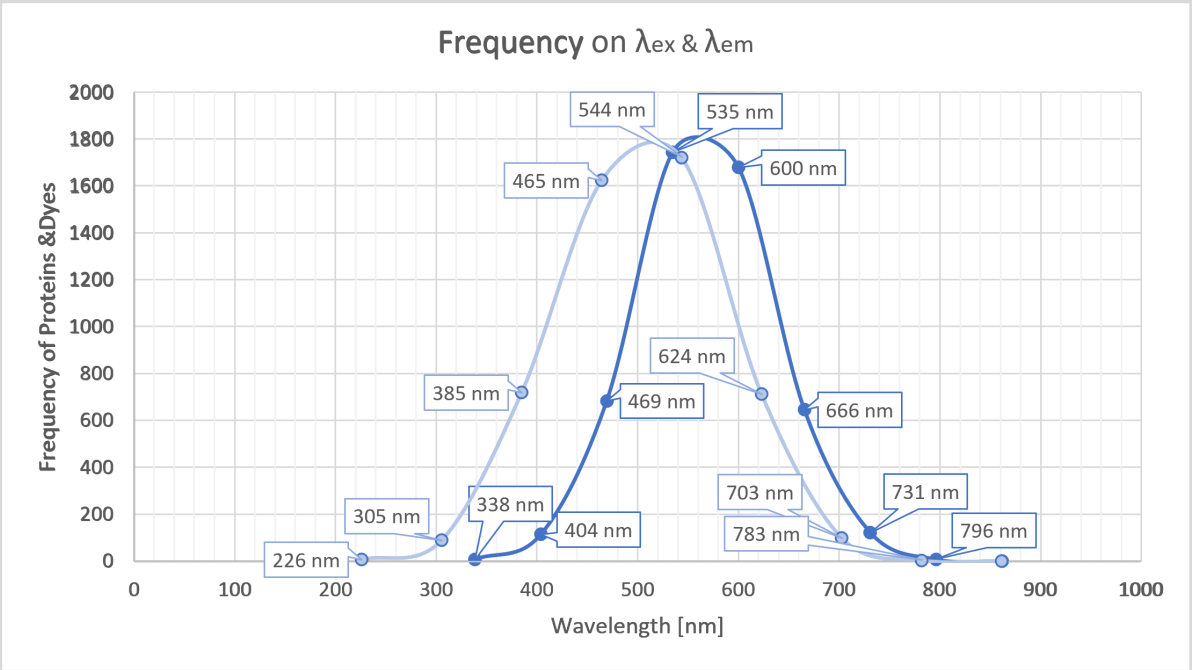

Figure 5.1: Distribution of the number of fluorescent dyes and proteins over the wavelength. The light coloured line represents the excitation wavelength and the other represents the emission wavelength.

of a polymer. Auto-fluorescence is the primary fluorescence of a material, where a natural emission of light of a material is present. In the biological sector, biological structures can absorb light and emit light such as mitochondria can. The colour of fluorescence is decided by its emitted wavelength, meaning if a polymer is blue fluorescent, the polymer absorbs the energy of a photon and reflects light with a wavelength between 450 - 495 nm.

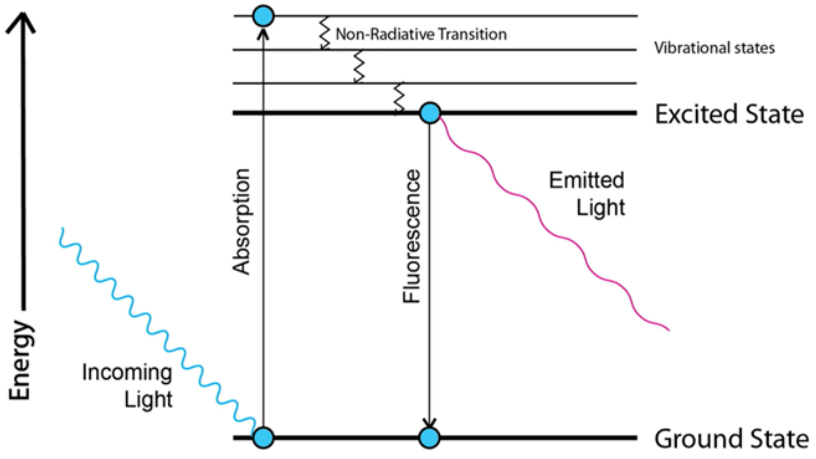

Figure 5.2: Working principle of fluorescence [19].

5.2. Auto-fluorescence polymers

There is a considerable amount of studies on the auto-fluorescence of polymers. In most studies the authors defined the intensity of the fluorescence in arbitrary units (a.u), this means that one cannot compare the values of one study with another. Moreover it should be taken into account, that the studies used different methods to measure the fluorescence in their results. Therefore, these studies will solely be mentioned subjectively or compared to another polymer of their study. Meaning, fluorescent yes/no, high/low, more or less than, and at which emission spectrum. Furthermore, the thickness of the polymer deposited on a wafer or glass substrate also influences the intensity of the auto-fluorescence. In the study of Lu, Zheng, Quoc Quach and Tai (2009) [20], the authors mention that the following assumption can be made: the initial intensity is proportional to the material thickness. They used a variety of polymers with different thickness and normalized those value to a thickness of 5 μm, by applying the following equation:

$$I_{normalized} = \frac{I_0}{t} \cdot 5\mu m \tag{5.1}$$

With $I_{normalized}$ being the new normalized fluorescent intensity (a.u.), I_0 being the measured fluorescent intensity (a.u.) and t the thickness of the layer of polymer. This is of importance when analyzing the results of the different polymers.

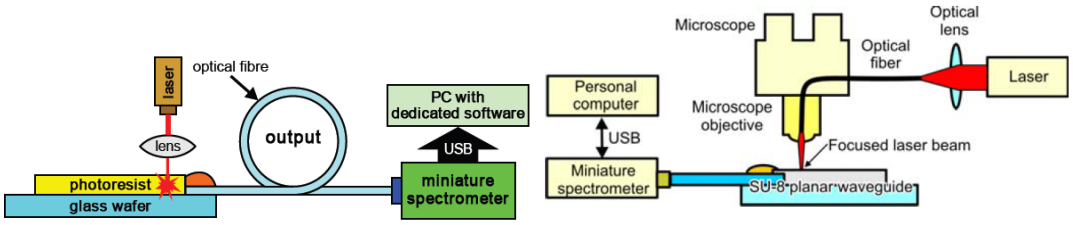

Figure 5.3: Scheme setup to measure the auto-fluorescence intensity with a laser. Left the setup of Microchem [21] and right the setup of P.Sniadek et al.[22].

SU-8

Starting with SU-8, which was originally created by Microchem. They performed a study on the auto-fluorescence of SU-8 compared with one of their other polymers perminex 1000 and 2000. During the experiments the researchers used lasers with excitation wavelengths at 488 nm, 532 nm, 643 nm. With $\lambda_{ex} = 532$ nm an auto-fluorescence signal of SU-8 was present, for the other wavelengths it was absent [21]. However, according to P.Sniadek et al. [22] who used the same excitation wavelengths, the highest intensity of fluorescence was found at $\lambda_{ex} = 488$ nm with $\lambda_{em} = 550$ nm, but they also mentioned that auto-fluorescence of SU-8 was present but lower at blue $\lambda_{ex} = 532$ nm, $\lambda_{em} = 625$ nm and at red $\lambda_{ex} = 636$ nm, $\lambda_{em} = 670$ nm. Therefore they concluded the following:"longer wavelengths cause lower auto-fluorescence, but a higher powered laser caused higher auto-fluorescence". Both studies used the same method of detection, consisting of a laser and a miniature spectrometer connected to a computer to process the results (see Figure 5.3). Furthermore, both studies were performed with researchers from Wroclaw University.

Perminex

As mentioned in the section on SU-8 fluorescence, Microchem also studied the auto-fluorescence of perminex 1000 and 2000. This polymer is highly auto-fluorescent in the visible spectrum. The study showed fluorescence at $\lambda_{ex} = 338$ nm (blue light) and $\lambda_{ex} = 532$ nm (green light), creating peaks at $\lambda_{em} = 500$ & 550 nm for blue light and 550 & 600 nm for green light [21].

BCB

For the polymer BCB, there is little information about its fluorescence. Cen et al. studied the fluorescence and absorption of BCB [23]. To measure the BCB fluorescence the authors used a fluorescence

Figure 5.4: Image of the Hitachi FL-4500, the device the authors used to measure the fluorescence of BCB [23].

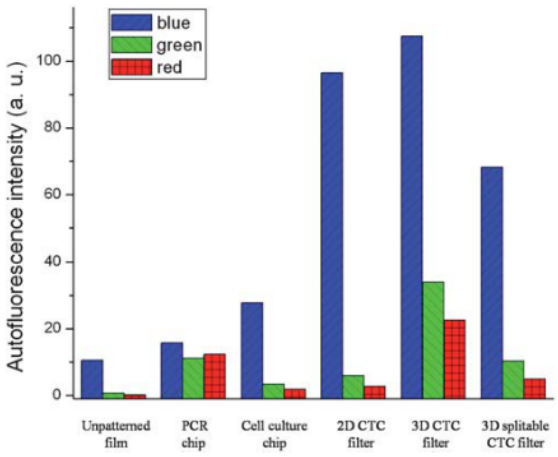

Figure 5.5: Fluorescent intensity of parylene-C per device sample [20].

spectrophotometer Hitachi FL-4500 (see Figure 5.4), with $\lambda_{ex} = 500$ nm. The polymer BCB showed a high fluorescence intensity at $\lambda_{em} = 535$ nm and a low peak at $\lambda_{em} = 650$ nm.

Parylene-C
There are four types of parylenes, but throughout this report only parylene-C will be considered. The authors B.Lu et al., compared the fluorescence of polymers as polyimide and parylene [20]. According to the article, parylene is higher fluorescent in blue. Compared with polyimide it is less fluorescent for red, but almost equally fluorescent at green. The excitation and emission wavelengths of these fluorescence are as follows: $\lambda_{ex_{Blue}} = 340 - 380$ nm, $\lambda_{em_{Blue}} = 435$–$485$ nm (Figure 5.6a), $\lambda_{ex_{Green}} = 465$–$495$ nm, $\lambda_{em_{Green}} = 515$–$555$ nm (Figure 5.6b), $\lambda_{ex_{Red}} = 528 - 553$ nm, $\lambda_{em_{Red}} = 590$–650 nm (Figure 5.6c). Their method to measure the auto-fluorescence of the polymers was with a Nikon epi-fluorescence microscope with the aforementioned wavelength range of filters. The grey-scale images from the microscope were then analyzed with a MATLAB custom-code. Another important finding that was mentioned in their report, is how the application of parylene-C has significant effects on the fluorescent intensity. Figure 5.5 shows the difference between the fluorescence of parylene-C for different applications. Parylene is more fluorescent for use in circulating tumor cell filters. Although the fluorescence increases for all colors, the increase in fluorescence intensity is strongest for blue fluorescence.

Polyimide
According to Y.Wu et al.[24], polyimide has a low fluorescence, due to its strong charge transfer effect which neutralizes fluorescence due to re-absorption in the polymer chains. In the study of B.Lu et al., it is moderately high fluorescent for green and red fluorescence, and lower fluorescent at blue [20].

TMMR
Not many studies have used TMMR, not even to measure its auto-fluorescence. Only the company

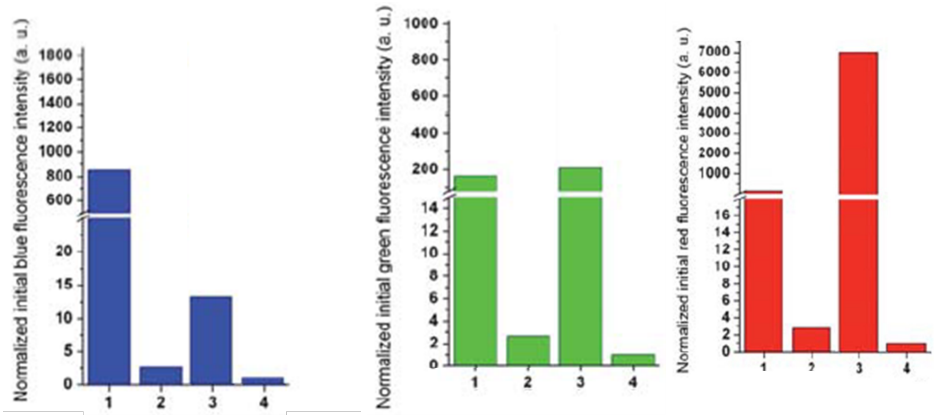

(a) Blue fluorescence
$\lambda_{ex_{Blue}} = 340 - 380nm$,
$\lambda_{em_{Blue}} = 435–485nm$

(b) Green Fluorescence
$\lambda_{ex_{Green}} = 465–495nm$,
$\lambda_{em_{Green}} = 515–555nm$

(c) Red fluorescence
$\lambda_{ex_{Red}} = 528 - 553nm$,
$\lambda_{em_{Red}} = 590–650nm$

Figure 5.6: Fluorescence of (1): 5 mm parylene-C; (2): 380 mm PDMS; (3): 50.8 mm polyimide; (4): 980 mm Corning glass slide (control). This study made the corning glass slide the reference material, thus its auto-fluorescence of Corning glass microscope slide was set as 1 (a. u.). The values are normalized to 5µm thickness and all measurements were carried out with a 20x objective.

that distributes TMMR (TOK) studied the auto-fluorescence of the polymer [9]. But other than a graph of their findings, it is unclear how the auto-fluorescence of TMMR was measured (see Figure 5.7). Looking at TMMR, the intensity of fluorescence becomes smaller as the wavelengths of excitation and emission increase.

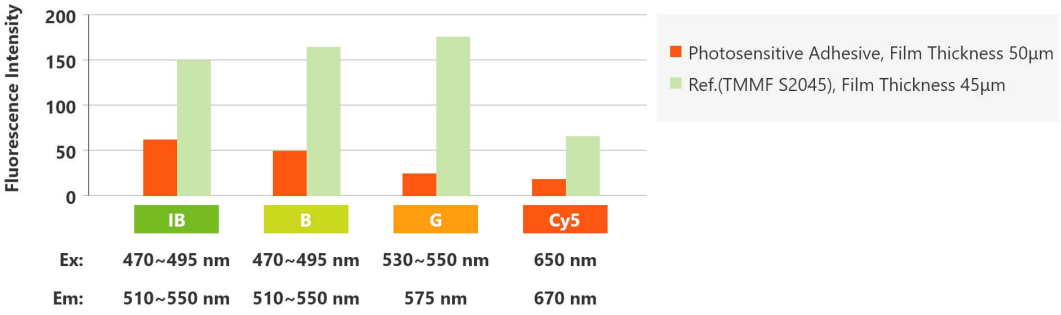

Figure 5.7: Auto-fluorescence of TMMR(orange) and TMMF(Green) [9].

Summarized literature:

Polymer	colour	Wavelength		Fluorescence	Method
		excitation [nm]	emission[nm]		
Su-8 [22]	Blue Green Red	488 532 643	550 625 670	Yes Yes Yes;low	laser and a miniature spectrometer
[21]	Blue Green Red	488 532 643		No Yes No	Laser and a miniature spectrometer
BCB [23]		500	535 & 650	Yes; Low	Fluorescence spectrophotometer
Perminex [21]	Blue Green	338 532	500 & 550 550 & 600	Yes; Low Yes; Low	Laser and a miniature spectrometer
Parylene-C [20]	Blue Green Red	340 − 380 465– 495 528 − 553	435–485 515–555 590–650	Yes Medium Medium	Epi-fluorescence microscope
Polyimide [20]	Blue Green Red	340 − 380 465– 495 528 − 553	435–485 515–555 590–650	No Medium Yes	Epi-fluorescence microscope
TMMR [9]		470-495 530-550 650	510-550 575 670	Yes low/no low/no	Unknown

Table 5.1: Overview of literature study on the fluorescence. '&' means peaks of fluorescence, and '-' means the range of the filters used for the excited or emitted light.

5.3. Absorption and Transmission

The transparency of a polymer is an important optical characteristic, as it provides an indication of how much of the light will be absorbed by the polymer, which is a valuable characteristic for lithography processes. The first ASML lithograhy systems, used a so-called g-line mercury vapour lamp where they could print structures of 1000 nm. To create smaller structures they went to i-line systems with an wavelength of 365 nm printing structures between 220-1000 nm. Thus to apply lithography to create smaller structures, photoresists (e.g. SU-8 and perminex) need to be sensitive in these ranges [25]. Therefore, for the lithography process we need to know the behaviour of absorption of a photoresist over the wavelength spectrum. If it absorbs a substantial amount of light, there will be a defined limit on the maximum thickness of the polymer, because the bottom part of the polymer would not be able to fully be cross-linked which increases the chance of a lift-off process. Figure 5.8 shows a spectrum of the light wavelengths. Absorption measurements are performed for detecting substances of importance, a method called analyte detection. The absorption of the polymers will also be studied, as it is an important property to be considered when applying the polymer for a BioMEMS device. This section will take a dive into the literature studies on the absorption of the polymers that are of interest during this project.

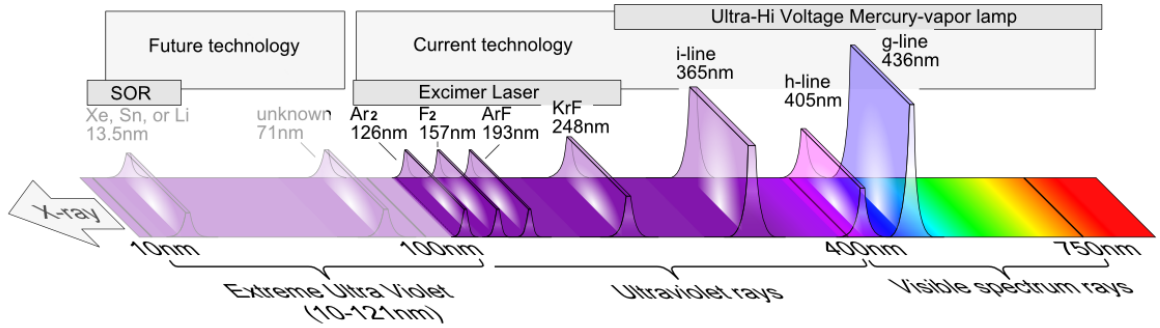

Figure 5.8: Spectrum for lithographic applications [26].

A transmittance of 100% means that the light will pass through the sample without being absorbed. Not all the polymers had sufficient information or studies about their absorbance capabilities. To measure the absorption of a polymer, a UV-VIS spectrometer is used. All the literature studies use this to measure how much of the light is absorbed by the polymer. Although there might be differences per spectrometer, these are not considered at this point.

SU-8

As previously stated, SU-8 is widely used in BioMEMS applications; thus, several studies have been conducted to investigate the absorption of SU-8. The manufacturer of the SU-8 has a transmission graph on their data sheet, which can be seen in Figure 5.9b [4]. The transmission of SU-8 does not seem to differ much when measured after exposure, whether softbake or hardbake. These are SU-8s of the Type 2000 series. All in all, it can be said that from 400 nm on, almost all light passes through it. From Figure 5.9a, it is visible that the transmission might not be as smooth as mentioned by the manufacturer, as the thickness of the layer SU-8 plays an important role [27]. These researchers found that smaller thicknesses led to a more fluctuating transmission compared to thicknesses of more than 7,0 µm.

BCB

The information on the absorption and transmission of BCB 3000 series is minor. A study was done on the transmission of BCB 3022–32, and the transmission was above 90% at about 450 nm (see Figure 5.9c [28]. This is a different type of BCB, but it will be more comparable than the BCB 4000 series absorption studies.

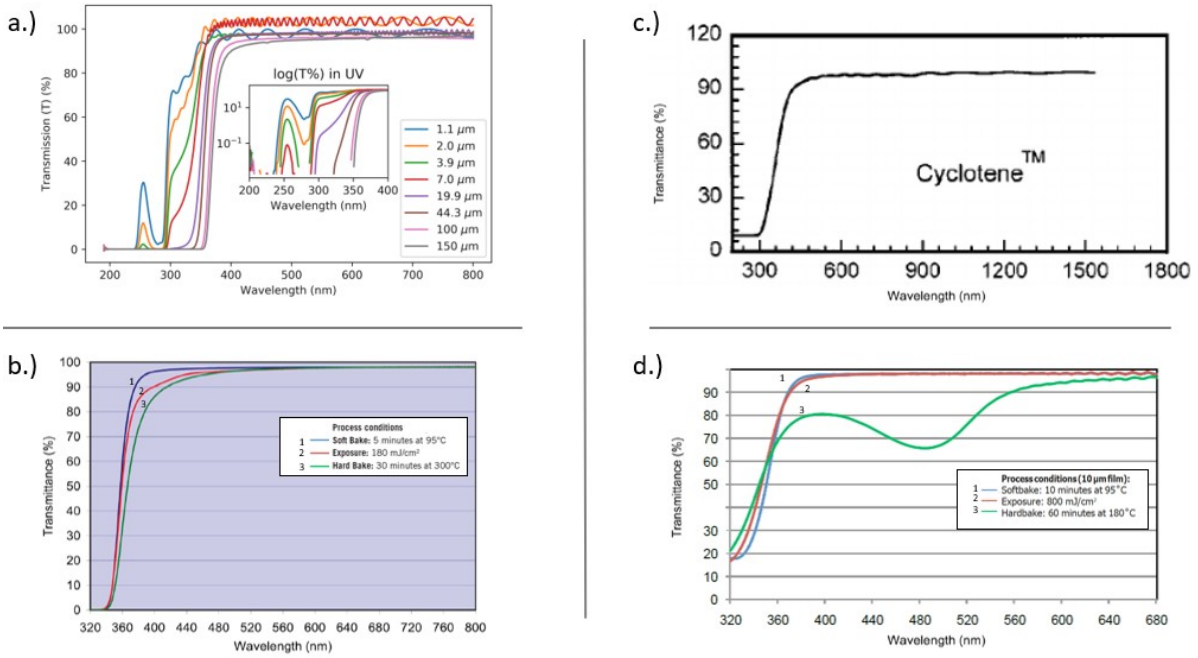

Figure 5.9: Overview of graphs on absorption and transmission of the polymers a.) SU-8 thickness [27] b.) SU-8 supplier [4], c.) BCB [28] and d.) perminex [7]

Perminex

The transmission is stated by the manufacturer in the perminex datasheet. It demonstrates that above 380 nm, the soft bake and exposure bake produce a transmission of more than 90%, whilst the hard bake only does so at 540 nm, see Figure 5.9d [7].

Polyimide

There is no information available on transmission and absorption over wavelength for polyimide types 2610 or 2611.

5.4. Method

As mentioned in the previous section, there are multiple methods to study the fluorescence. The aforementioned studies used three types of measurements for the fluorescence, with a microscope or spectrometer. In the beginning of the project, there were different types of polymer samples, therefore a different type of method was used to investigate the materials, instead of a laser fluorescence spectrometer. The studies using lasers and fluorescence spectrometers deposited the polymers on glass wafers to allow for trans-illumination. However, with silicon wafers this is not possible, thus the Amersham Imager was used. In the upcoming sections the working and usage of the microscope and imager will be explained followed by the setup for the absorption measurement, the UV-VIS.

5.4.1. Fluorescence Setup I: Leica fluorescence microscope

The microscope used to analyze auto-fluorescence was a Leica confocal microscope, with a mercury lamp. The mercury lamp was used as an excitation light source, which went from the excitation filter to the dichroic mirror where the excited light reached the object, in this case the polymer. To create an image, the fluorescent light of the object follows its way back to the dichroic mirror and reaches the emission filter (see Figure 5.10). During the setup three distinct filter cubes were used: N2.1, I3, A (see Table 5.2). These filter cubes contain the excitation filter, dichroic mirror and the emission filter. The filters are needed to block a region of wavelengths, to observe the light that is emitted due to fluorescence. To analyse the fluorescence of the polymer samples, the software provided with the Leica microscope was used to view the images on the computer and to calculate the shutter speed. For the images of the microscope, see appendix B. During the measurements with the microscope, the roller-shutters were down and the light was out, to keep the the environmental luminescence constant and low for all the microscopic measurements.

Filter	Excited colour	Emitted colour	λ_{ex}[nm]	λ_{em}[nm]
A	UV	Blue	340-380	400-425
I3	Green	Red	450-490	510-515
N2.1	Blue	Blue/Yellow	515-550	580-590

Table 5.2: Leica microscope filters including its wavelengths excited and emitted

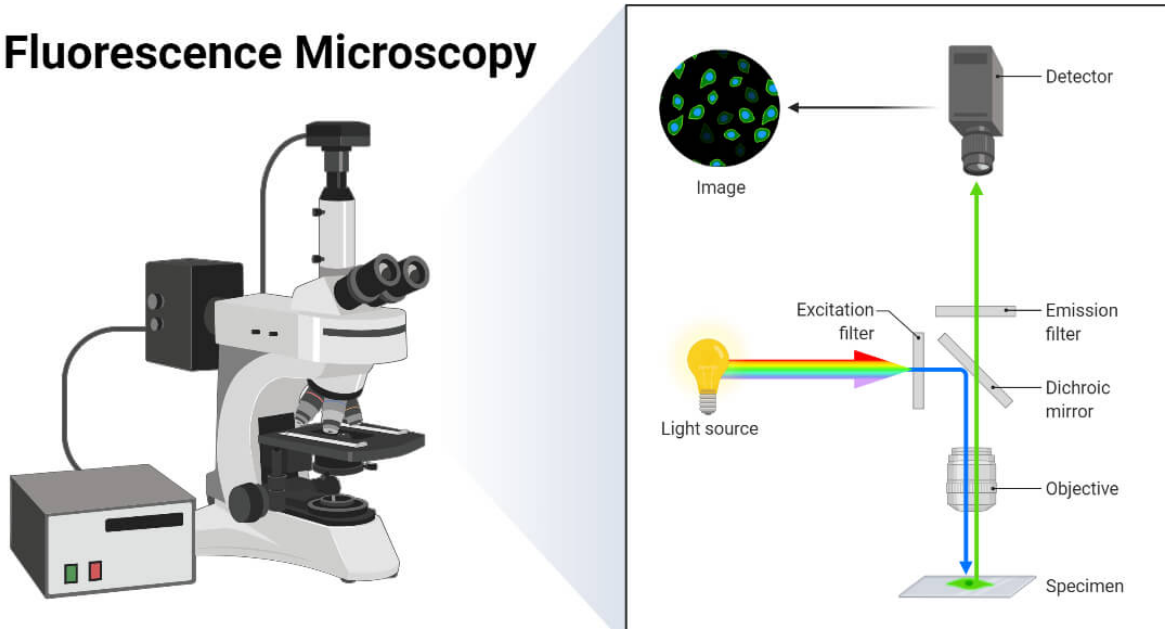

Figure 5.10: Schematic of the excited light passing through the microscope and if present how the fluorescent light passes to the detector of the microscope [29].

5.4.2. Fluorescence Setup II: Amersham Imager 600RGB

As was mentioned in the method, Setup II consists of an imager which could capture fluorescence in bio-science applications. The imager was an Amersham 600RGB from GE Healthcare life sciences, which can be used for studying the chemiluminescence and fluorescence of proteins, DNA molecules, gells and membranes (seen in Figure 5.11). The imager has three light exposure options for epi-illumination, which are seen in Table 5.5 and 5.12. The Amersham imager uses a CCD technique which stands for charge coupled device, a sensor to create a digital image.

Filter	Fluorescence colour	λ_{ex}[nm]	λ_{em}[nm]
Cy2	Blue	460	505-545
Cy3	Green	520	565-645
Cy5	Red	630	665-745

Table 5.3: Amersham 600 Imager filters including its wavelengths excited and emitted

The imager has limited dimensions of the measurement plate with 16x22 cm. Therefore, samples larger than the plate were cut to a square with maximum dimensions of 10x10 cm to fit them on the tray. The imager was set on epi-illumination, meaning that the light source would enter the surface of the sample at an angle (see Figure 5.12). During this setup a pure silicon wafer was used, besides the five polymer samples, as a non-fluorescent reference sample. The Amersham 600RGB has light sources trans-UV, white, blue, green and red. In this case, the RGB (red, green, blue) light sources were used as it involved the fluorescence of the samples with epi-illumination. Epi-illumination was required as a majority of the samples were non-transparent. The measurements were performed at separate sessions with different goals of measurements, based on the results of previous measurements session.

(a) Amersham Imager 600RGB Device [30].

(b) The inside of the Amersham Imager.

Figure 5.11: Amersham imager 600RGB.

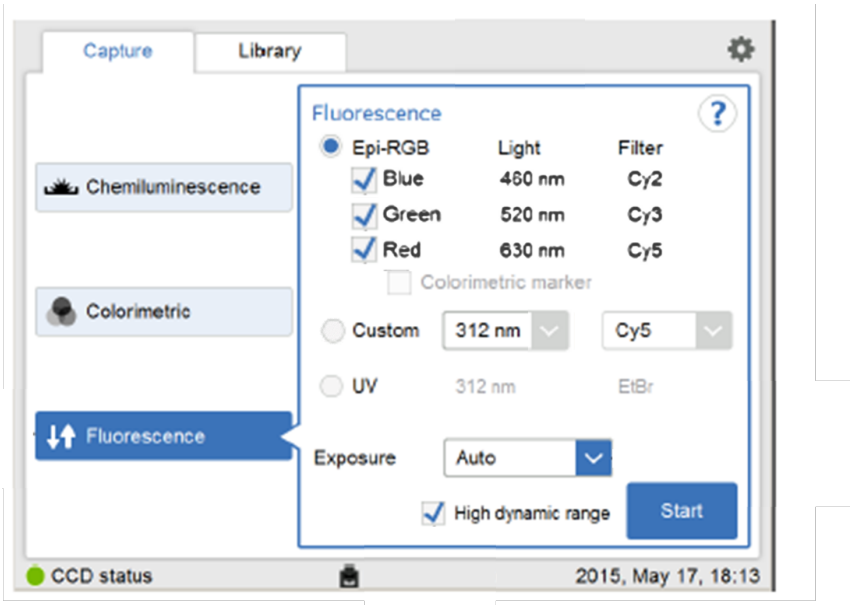

Figure 5.12: Image on the computer to set the settings of the imager

Session 1

During this session, the following samples were investigated: SU-8 structured, TMMR structured, parylene wafer, polyimide wafer, BCB wafer, and a pure silicon wafer (see Figure 5.13). Knowing that SU-8 is our reference polymer, this sample was studied first and set to automatic exposure. As the original SU-8 samples were small, the automatic exposure time was initially set at six minutes to analyze the fluorescence of SU-8. However, since the other samples were larger and had other chemical properties, they became overexposed to the red excitation light. BCB and TMMR, in particular, showed significant overexposure. Thus, the next step was to expose the whole plate, including the other samples. As not all the samples would fit on one plate, the experiment was divided into three separate measurements, where only one of the four samples would be exchanged with another to check if the measurements were comparable, as there would be no significant difference between these three. Measurement 1 contained parylene-C, BCB, SU-8, and TMMR. In measurements 2 and 3, the parylene-C was exchanged with polyimide and pure silicon wafer samples. Measurement 1 was set to auto exposure and dynamic range, so to have the same exposure times and avoid overexposures, all three measurements were taken under the same conditions. This resulted in exposure times for blue and green excitation lights as follows: 15.6 s for blue (Cy2) and 19.9 s for green (Cy3). The other two measurements were then set to manual and exposed for the same duration.

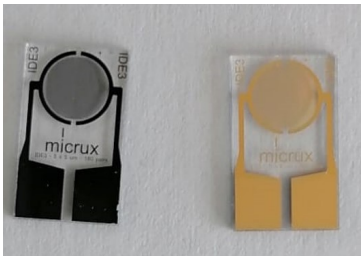

(a) SU8 micrux structured sample

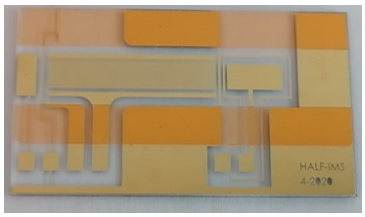

(b) TMMR structured sample

(c) BCB sample

Figure 5.13: Amersham imager 600RGB

Session 2
The goal for session number two was to study the fluorescence of the following samples: perminex wafer, SU-8 wafer, TMMR wafer, and borosilicate glass (BF-33). To confirm the results of Session 1 with those of Session 2, a couple samples from the previous session were placed on the tray to examine if there is a statistical difference between the two sessions. If that is not the case, these sessions can be compared. If there is a statistical difference, the sessions cannot be compared, and a third session is necessary. During Session 2, the light incidence on the SU-8 and polyimide chips was also studied by changing the position of the chips. The perminex structure was cured for 3 hours instead of 1 hour; however, the result of this sample will also be shown to visualize the effect of curing time on the fluorescence of perminex. Measurements were as follows:

1. **Fluorescence samples**

    (a) BCB, TMMR structure, perminex wafer
    (b) BCB, TMMR structure, perminex structure
    (c) BCB, TMMR structure, SU-8 wafer, TMMR wafer, Silicon wafer
    (d) BCB, TMMR structure, borosilicate glass (BF-33)
    (e) BCB, perminex structure, perminex wafer

2. **Angular Dependence**

    (a) Measurement chips angles at manual times
    Cy2=15.6s Cy3=19.9s
    (b) Measurement chips angles at automatic times
    Cy2=4min 39.3s Cy3=20.0s Cy5=1min 37.1s

The fluorescence measurements of this session were exposed to the same exposure as the ones in Session 1, namely 15.6 s for blue light and 19.9 s for green light exposure.

Session 3
The goal of session 3 was to study the fluorescence of the three polymers: perminex, polyimide, and SU-8. In the iteration below, it can be seen that the polymers were applied to different surfaces. The hypothesis was that there should not be a significant difference between the polymers on silicon and those on a glass surface. To exclude potential fluorescence due to the primers and the type of glass wafers, their fluorescence was also taken into account during this session.
In the previous sessions, these polymers were already studied. However, since the perminex was accidentally unexposed, this time one of the goals was to investigate the effect of the exposed perminex. The difference between exposed and unexposed perminex is that the exposure causes cross-links of polymer chains within the material. In Session 2, the patterned perminex was exposed and the blank perminex was unexposed, which created a difference between patterned and blank perminex. Furthermore, the polyimide was studied on various surfaces (glass, Si with and without an oxide layer), and a new exposed SU-8 sample. The exposure times of all the separate measurements of Session 3 were constant with the measurements of previous sessions. Specifically, 15.6 s when exposed to blue light and 19.9 s when exposed to green light.

1. **Perminex**:
   a. exposed Si
   b. exposed glass
2. **Polyimide**:
   a. on Si tox
   b. on Si
   c. on glass
3. **SU-8**:
   a. exposed Si
   b. exposed glass
4. **Primers**:
   a. AP3000
   b. HMDS,
   c. VM651
5. **Glass**:
   a.BF33
   b.AF45
6. **BCB**: on glass

Session 4
Finally, a fourth session of fluorescence measurements was performed. This was after analyzing the results from the previous sessions and after the hermeticity samples were finished. As for some polymers, not only was the fluorescence different per substrate but also the processing of the sample; this will now be constant per polymer. These will also be the samples that are used for the cytotoxicity tests. The goals of this session were as follows:

- Measure the fluorescence of the new BCB wafers.
- Measure a new parylene-C wafer.
- Measure the fluorescence of samples used for cytotoxicity and hermeticity.
- Measure the alignment and exposure influence.

During the above measurements, the same exposure times were used as in all the previous sessions, namely 15,6 s on blue light and 19,9 s on green light exposure. Furthermore, there were two automatic exposures: during the hermeticity measurement and to check the influence of exposure time. The automatic exposure times were as followed: **Hermeticity**: Cy2=18.8 s; Cy3=4.6 s, Cy5=7.2 s; **Alignment**: Cy2=18.35 s; Cy3=26.95 s, Cy5=1 min 54.6 s.

Analysis

After each measurement, the images were saved for analysis. For the analysis, a program application called Fiji was used, which is a version of ImageJ and ImageJ2 with the needed plugins pre-installed [31]. With this tool, it is possible to calculate the gray values of the images. The imager made the photos in grayscale (black and white) as they contain more details. In this case, the parameters of interest were the area, mean value, minimum value, maximum value, integrated density, and raw integrated density. The area is described as pixels/cm^2 and the other parameters are in greyscale value. The integrated density is the area times the mean gray value of the selection taken. The raw integrated density is the area times the gray values of all the pixels, thus creating a total overall value. The integrated density was examined and compared among materials in order to analyze the fluorescence intensity of each individual substance. An ANOVA one-point analysis was carried out to determine whether there was a statistically significant difference between the measures in order to confirm that the outcomes of the three measurements were equivalent. ANOVA, often known as analysis of variance, is a statistical method for comparing the averages of more than two groups. It compares the means of up to two groups and is an extension of the t-test. Furthermore, during the measurements, the background noise was also measured using the reference silicon wafer. It was compared with an empty spot on the plate, which was not significantly different, but since the silicon wafer was clean and the teflon plate could contain dust, the gray value of the silicon wafer was used for the calculations. The values without the background noise were calculated by subtracting them from the raw integrated density and then dividing by the area. Note that the gray values are dependent on the position and area of the sample; therefore, two methods have been applied to calculate with as little varieties as possible. One is that the area and position should remain constant over the three measurements. The selected areas in the first two sessions were constant, with an area of 30x30 pixels, which was equal to 0.057 cm^2. Next, the selected area was the whole sample, excluding certain areas where no polymer was present on the wafer due to scratches or bubbles. As there could be differences in fluorescence over the wafer, an example of this can be seen in Figure 5.14, where the perminex wafer shows a pattern with different values. Observe how the image was read here using Matlab to clearly investigate the pattern. This third session's observation led to a second analysis of the results utilizing the latter technique.

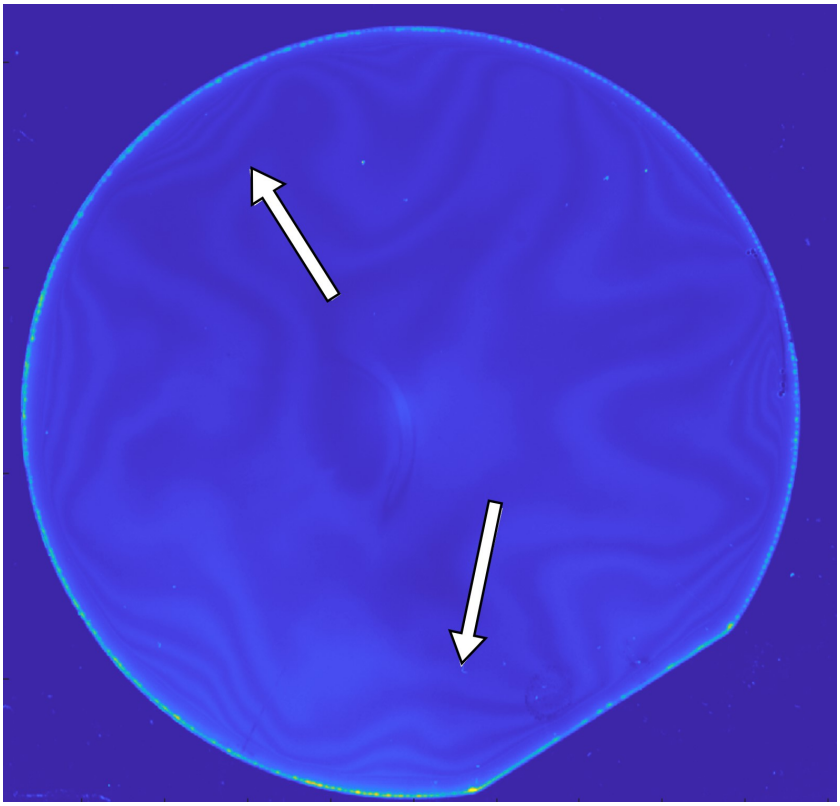

Figure 5.14: Example were fluorescent intensity differs over the wafer

5.4.3. Absorption measurement setup: Spectroscopy

The absorption measurements of the polymers are performed with Ultraviolet-visible spectroscopy (UV-VIS). The samples were placed in the UV-VIS device. To measure the absorption or transmission of the polymers, there is one requirement for the samples: they need to be deposited onto a glass substrate, which measures the amount of light passing through the sample. In Figure 5.15, the device is shown with two distinctive chambers. The samples were placed in the first chamber, where the light enters the lens, which is located in the separation between the two chambers. Figure 5.16 shows how the light is emitted from a reference side and a sample side, passes through the lens and mirrors, and enters the integrating sphere. This sphere is completely white to prevent a drop in light intensity. Perminex, SU-8, and BCB were deposited on an AF45 glass wafer, while polyimide (PI 2610) was spun onto a BF33 glass wafer. As a reference, the absorption and transmission of these two types of wafers were measured, to establish a baseline for the absorption and transmission of the glass. The UV-VIS device saves the transmission data points of the measurements over the wavelength range of 300–800 nm in an Excel spreadsheet. With the use of MATLAB, this spreadsheet can be used to plot the data points over the wavelength spectrum. To calculate the absorption values of the polymers over the wavelength, the following formula was used:

$$T\% = 10^{(2-A)} \tag{5.2}$$

The *'A'* represents the absorption coefficient, which can be used to calculate transmission in percentages. The absorption value shows us how much of the light exposed on the sample will be absorbed by the polymer; these results can be found in the next section.

Figure 5.15: The UV-VIS device used during the measurements [32].

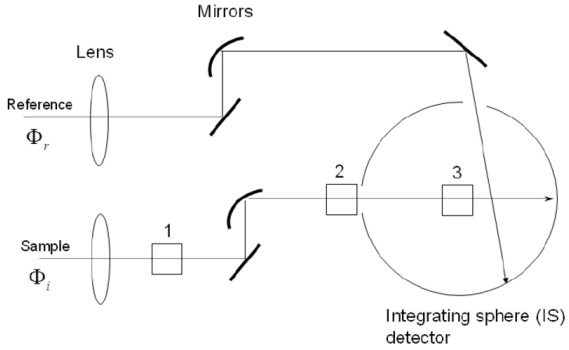

Figure 5.16: Schematic light emitted and following two paths at the same time. One bundle being the reference and the other the sample [33].

5.5. Results

In this section, the results are presented for the fluorescence measurements in Section 5.5.1 and 5.5.2 and the absorption measurements in Section 5.5.3.

5.5.1. Microscopic results

In Figure 5.17 the results of the microscope shutter speed are presented, with polyimide (PI); parylene-C (PAR) and silicon (Si), as reference. The vertical axis represents the inverse of the shutter speed. Since the maximum value for the shutter speed is one second, a fluorescent polymer sample would have a value lower than one second, thus the inverse results in a higher value for the fluorescent samples. Meaning, a tall bar corresponds to a higher fluorescence.
Apart from the results of SU-8, the values of the samples are equal for the filters I3 and N2.1, as it reached the maximum shutter speed of one second. Thus the polymers TMMR, BCB, polyimide, parylene and perminex were barely to non-fluorescent.

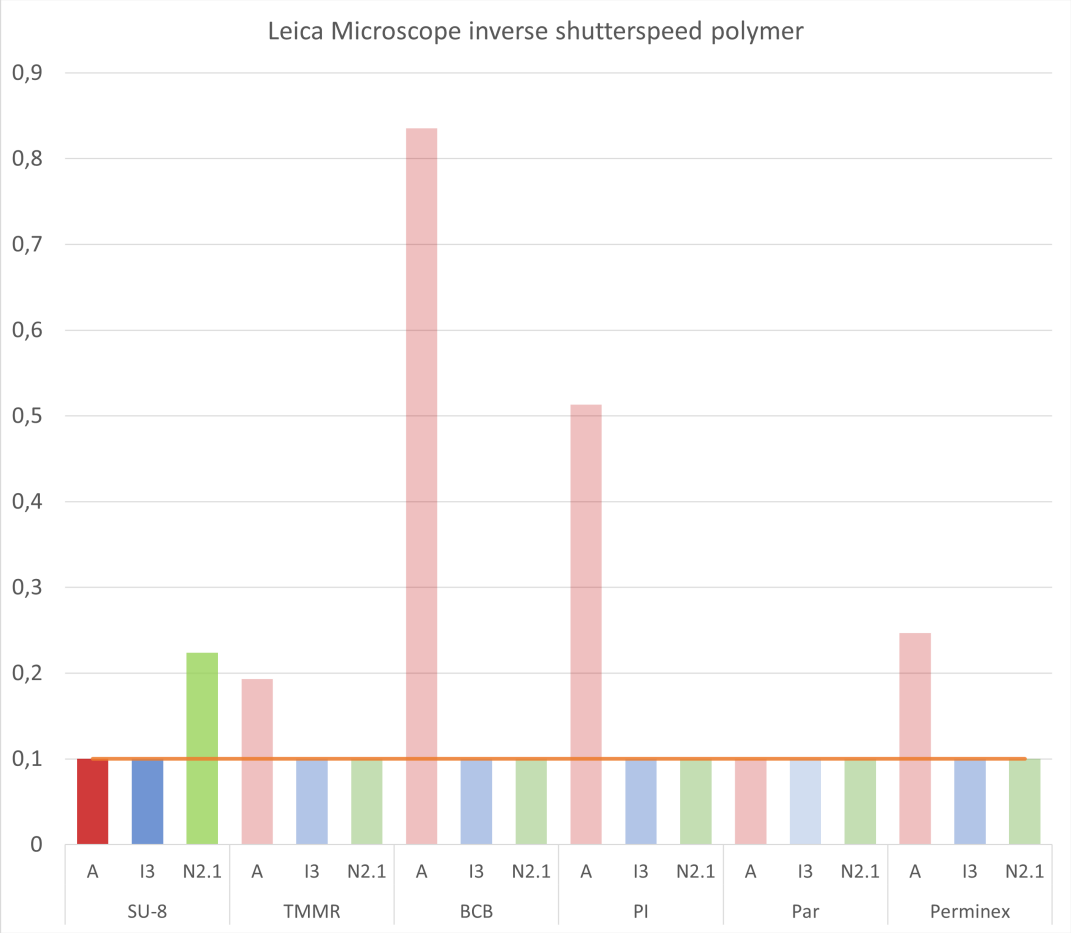

Figure 5.17: Inverse of the shutter speed measured with the Leica microscope on the polymer samples. (not normalized)

Filter	λ_{ex}[nm]	λ_{em}[nm]
A	340-380	400-425
I3	450-490	510-515
N2.1	515-550	580-590

Table 5.4: Microscope filters including excited and emitted wavelengths

5.5.2. Amersham Imager results

As the polymers differed in thickness, these values have to be normalized to compare their fluorescence level, this is only possible for the results on the imager as the maximum shutter speed of one second appeared too many times which made the results incomparable.
The thickness of the polymers were normalized to d=5 μm. This normalisation was also applied in the study of B.Lu et al. [20], for auto-fluorescence mentioned in the introduction of Section 5.2. Light absorption has an exponential decay with depth, as the attenuation of intensity can be written as follows:

$$I = I_0 e^{-\alpha d} \tag{5.3}$$

Meaning, the intensity is dependent of the initial intensity I_0 with an exponential decay, dependent of the attenuation coefficient (α) and thickness of the material (d). During these experiments the normalisation was taken proportional with the intensity of fluorescence since it is about thin film polymers in micrometers [20]. Formula 5.3 is used in studies with at least 50 μm. Thus, here it is assumed that the polymer thickness, used in these measurements, are proportional to the intensity. Table 5.5 present the wavelength that is excited and emitted by the filters of the imager .

Filter	**Colour**	λ_{ex} [nm]	λ_{em} [nm]
Cy2	Blue	460	505-545
Cy3	Green	520	565-645

Table 5.5: Amersham Imager filters including excited and emitted wavelengths

Polymers on silicon wafers

In the following figure (see Figure 5.18), there is an overview of all the polymers with known flowcharts of processing. As seen, there are two kinds of blank BCB wafers and two kinds of polyimide 2610 wafers. The difference between these two different wafers shows up in the process flow. With BCB, one of the wafers was made by curing it in the oven in the chemistry lab, just as the glass wafer was made with BCB. The other was processed as the first BCB would have been made, by baking it in the clean room. For polyimide, the question was whether the thin oxide layer (tox) influenced fluorescence. So here the thin oxide is between the silicon wafer and the polyimide 2610. In both, the polyimide is 3 micrometers. It can be seen from this that it primarily influences fluorescence in the green interval. Looking at the green striped interval, which is the range of wavelengths where we do not want fluorescence, the polymers parylene-C, SU-8, and BCB have the lowest intensities. In the blue wavelength interval, parylene-C and SU-8 continue to have the lowest fluorescent intensity, but perminex is now in the top three. Looking at the corrected and normalized values, it is visible that parylene-C, SU-8 perminex, and TMMR show low grey values for both blue and green fluorescence.

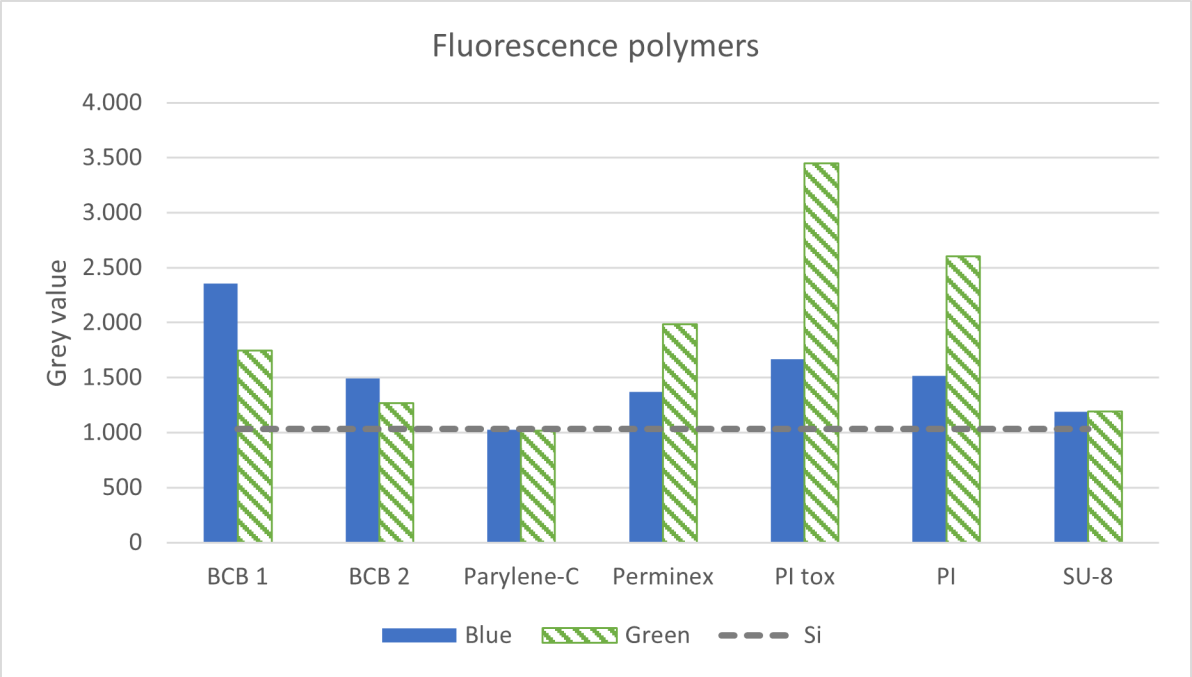

(a) Fluorescence of polymers with different thicknesses. TMMR excluded, value around 14.000 and 11.000.

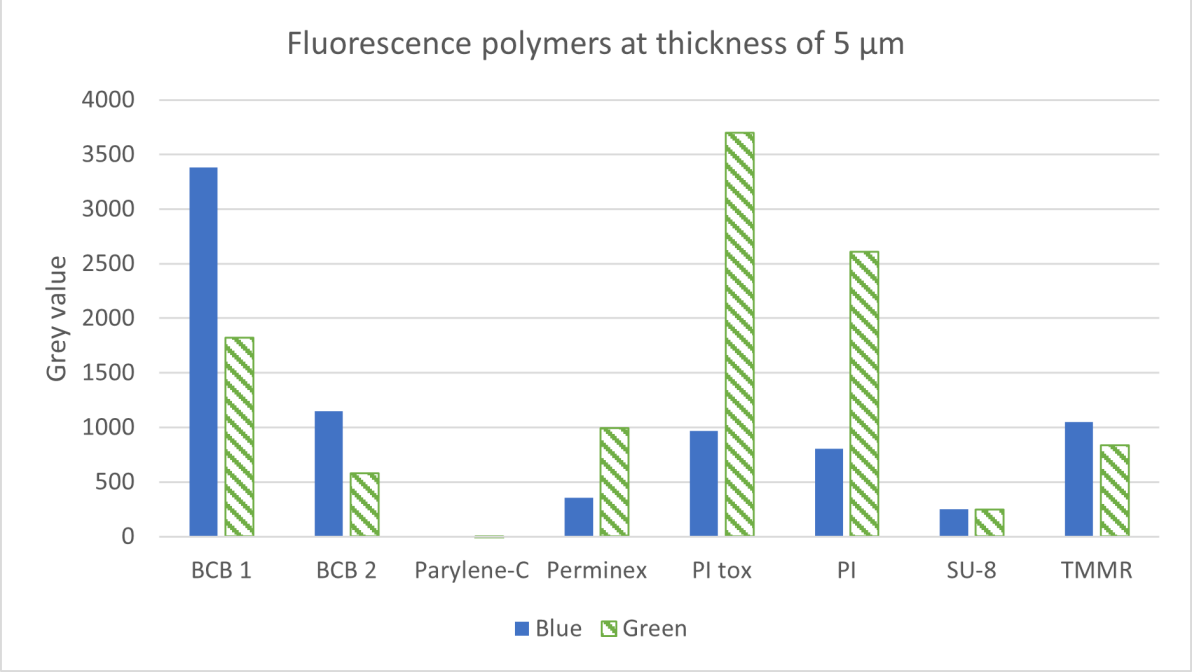

(b) Fluorescence of polymers (incl. TMMR) with correction for the background noise and normalized to 5 micrometers

Figure 5.18: Overview of the polymer fluorescence on silicon, with their probable application thickness versus thickness to 5 micrometers.

Polymers on glass wafers

When the polymers are not on a silicon wafer but on a glass wafer, it still seems that SU-8 and perminex show low values(see Figure 5.19). One should keep in mind that the polyimide was deposited on a different type of glass wafer, namely the BF33, whereas the other polymers were deposited on the AF45 type of glass wafer. However, both types of glass wafers did not show any levels of fluorescence. When normalized to a thickness of 5 µm, perminex and SU-8 show the least amount of fluorescence. Polyimide is acceptable with blue fluorescence but is unwanted with the required green fluorescence.

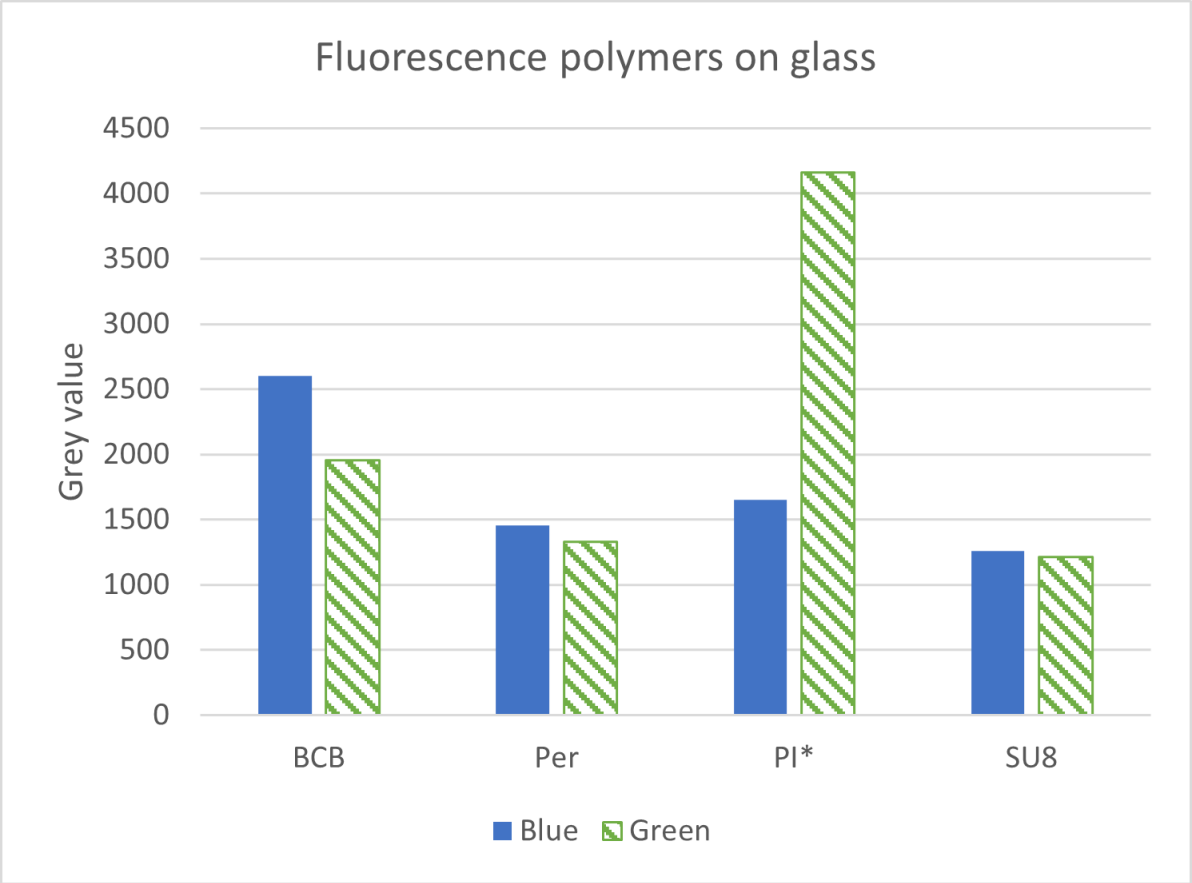

(a) Fluorescence of polymers on glass wafers. Polyimide on a BF33 glass wafer, the others on AF45 glass wafers.

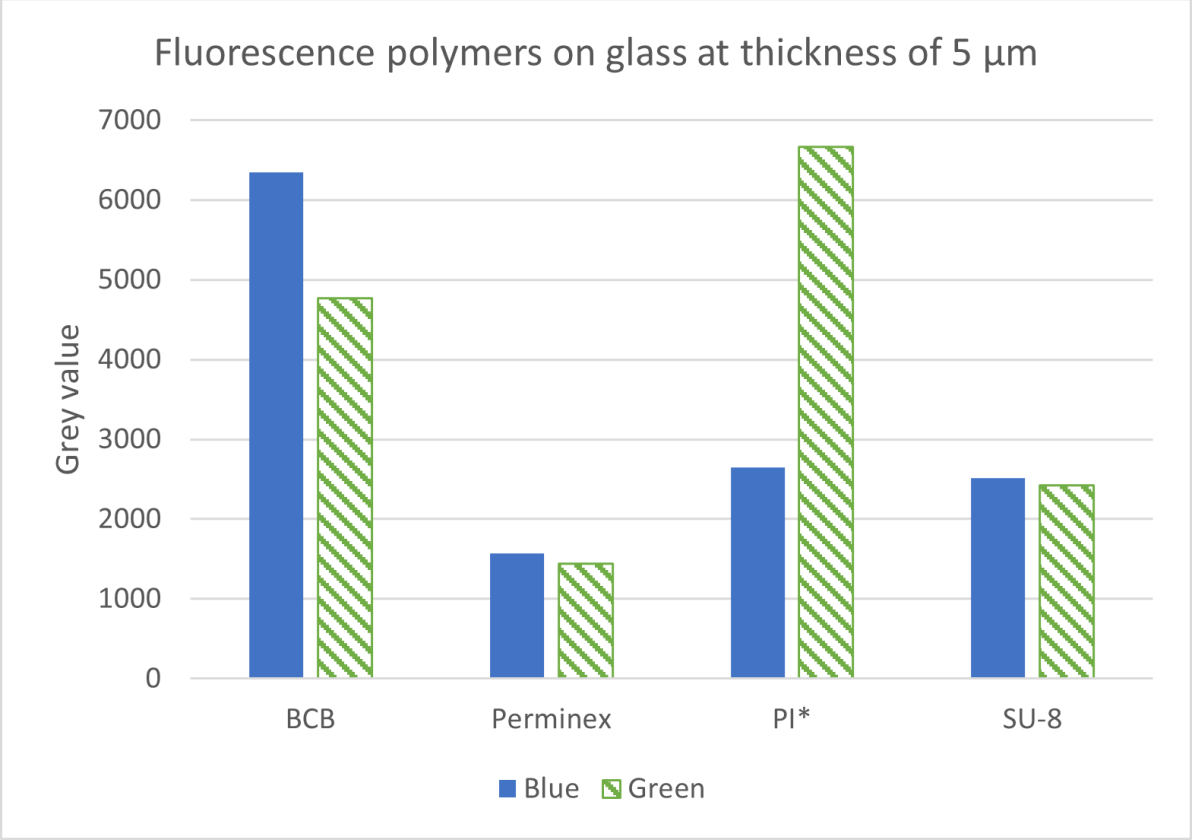

(b) Fluorescence of polymers with normalization to 5 micrometers

Figure 5.19: Polymer fluorescence on glass, with their probable application thickness versus thickness to 5 micrometers.

Polymers on one plate: cytotoxicity, hermeticity, glass
As a result of creating small samples for the absorption measurement and the hermeticity and cytotoxicity experiment, different polymers could fit on one plate. Before, this was not immediately possible as it was unknown how much of the samples was needed per experiment performed. When these experiments were finished, the leftover samples were used with the imager to read out the fluorescent intensity and compare the results. Since it was difficult to get parylene-C on glass, it was not included on the imager plate in both measurements of the hermeticity and glass substrate samples. For the cytotoxicity experiment, which will be discussed in Chapter 8.1, the wafers were broken into smaller pieces of one by one centimeter. For the absorption measurement, the glass wafers were also cut into smaller pieces, but without a specific area measurement. To distinguish the grey values of the polymers better, the photos were coloured with a small code created in MATLAB based on fluorescence intensity, resulting in Figure 5.21. The lighter the colors, the higher the grey value, and thus the more fluorescent the polymer is. The tables below the figures show, from top to bottom, the values of fluorescence intensity, from high to low values. The fluorescence of SU-8, BCB, and polyimide was the most intense among the cytotoxicity samples. Perminex, polyimide and BCB are the least fluorescent hermeticity samples, and SU-8 is the least fluorescent glass wafer. Remember that the exposure time of the hermeticity samples is different from that of the cytotoxicity samples and glass samples.

BCB fluorescence difference
Examining the different timings and types of processing BCB, one can observe the differences in fluorescence between the BCB samples. The first blank BCB wafer was broken into pieces BCB samples S1, S2, and S4 are the exact same sample. The S stands for session, meaning the sample of BCB used during that session. BCB S3 was part of the original old BCB wafer, but a different piece than the one used in sessions 1, 2, and 4. The polymer deposition of BCB happened at the same time for BCB N1 and N2. The difference between these two however is the curing. These BCB samples were made at the exact same time. So in this, time could not be a factor of influence, but mainly the method of curing.

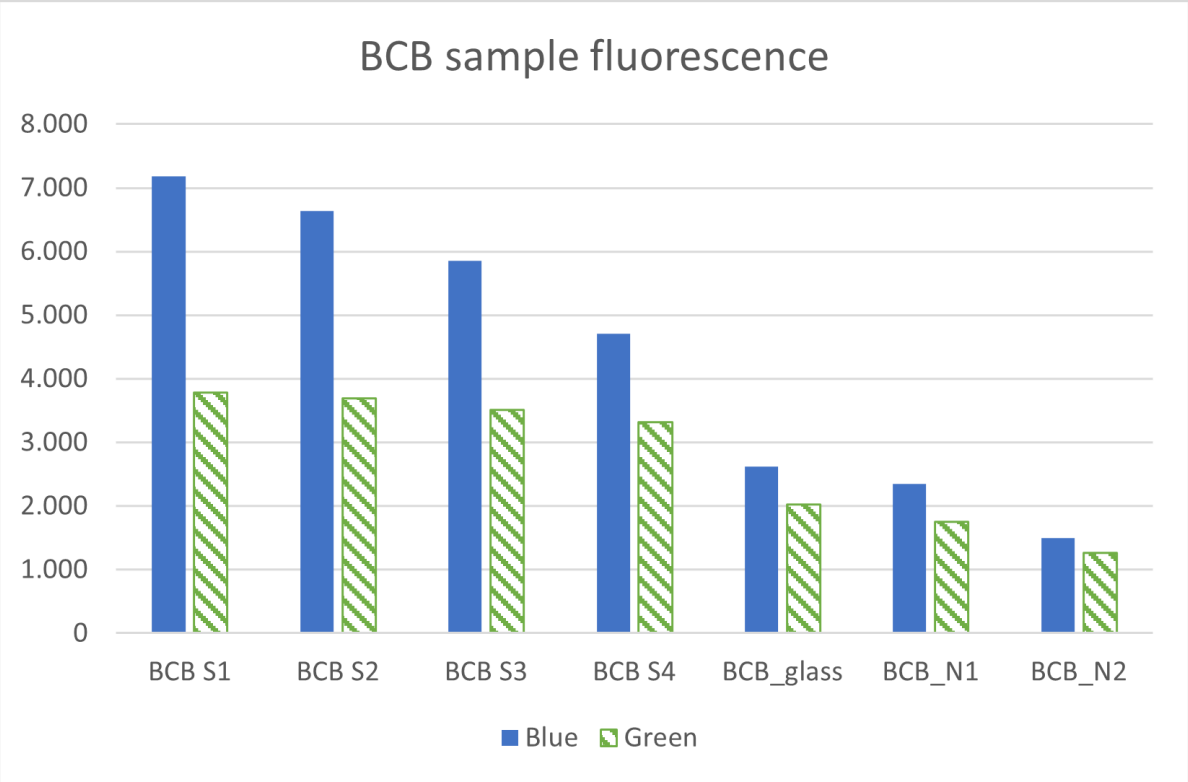

Figure 5.20: Overview of BCB samples processed per type but also over time, except for BCB N1 and N2.

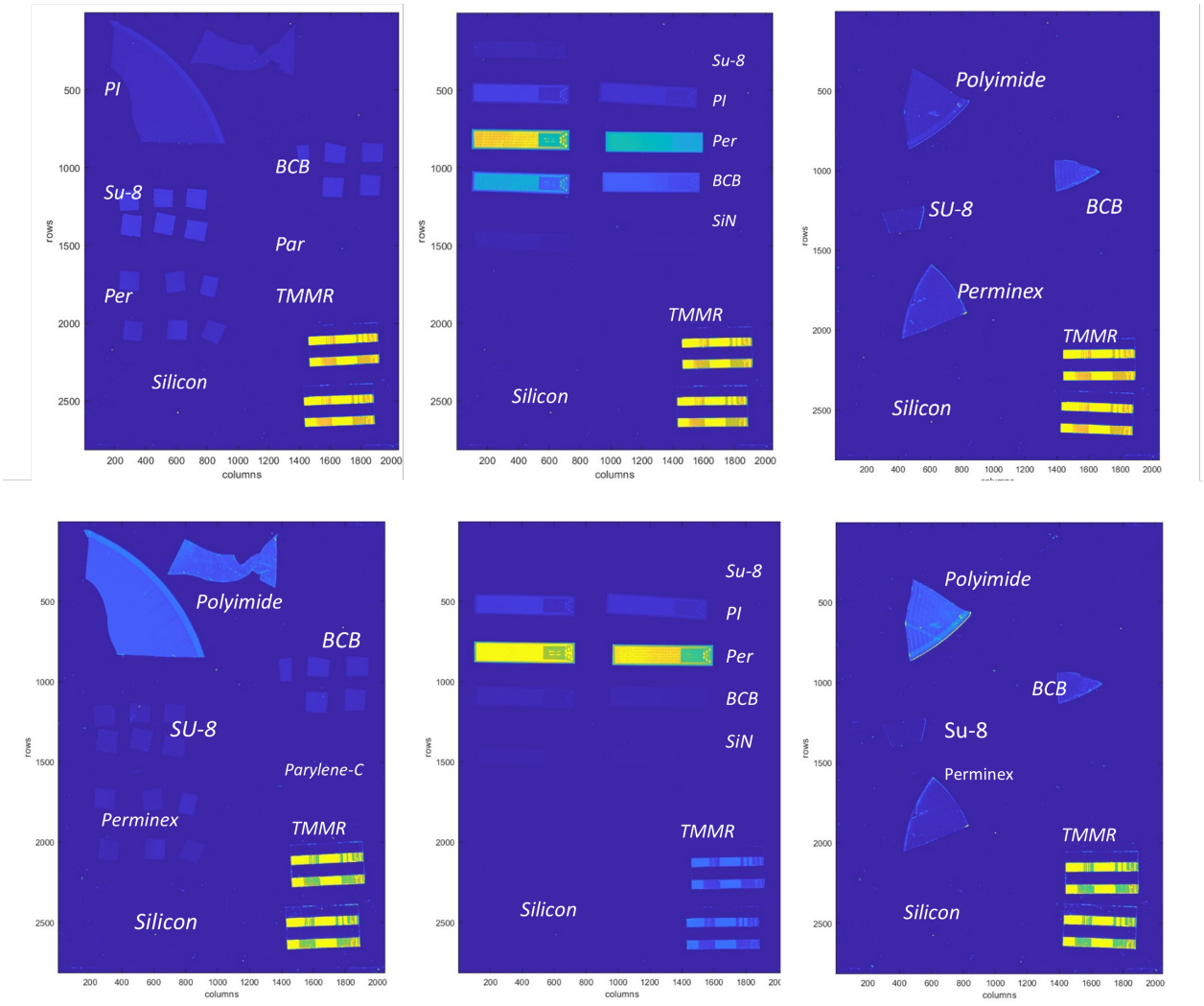

Blue	Green
SU8	PI
BCB	BCB
Perminex	Perminex
PI	SU-8
Parylene-C	*Parylene-C*

Cytotoxicity samples

Blue	Green	Red
Perminex	Perminex	Perminex
BCB	PI	PI
PI	BCB	BCB
SU8	*SiN*	Su8
SiN	SU8	*SiN*

Hermeticity samples

Blue	Green
BCB	PI
Perminex	BCB
PI	Perminex
SU-8	SU-8

Glass samples

Figure 5.21: Overview of the images, with table of highest to lowest fluorescence of all equal polymer samples on one plate.

Alignment

Based on the results of the previous sessions, there was a decrease in the fluorescence intensity of the TMMR and BCB samples, which had been used in all measurements. As the imager is normally not applied to measure the fluorescence of these types of samples, the position and exposure dependence of the samples were studied. The alignment was tested with the setup as seen in Figure 5.22a. The structures were rotated after 3 exposures on the same spot. Creating four different positions of the samples. After that, the samples were exposed with an exposure time calculated by the imager itself (automatic), which was longer. After that, we exposed it back on the manual exposure time and measured it three times. In Figure 5.22b, the fluorescence of one of the TMMR samples was graphed over time. The four locations are marked in the graph, one being the position bottom right to four being the position top right. In this graph, there are differences visible with the fluorescent intensity. Not only is the position on the plate influencing the intensity of the fluorescence but at each position, the fluorescence intensity decreases during the three consecutive measurements. This shows that the right

side of the plate can have a higher value than the left side of the plate. However, the analysis area is determined by hand and because the position of the sample to be observed changes, the area is not equal at the pixel level.

(a) From the top left, clockwise: BCB, Polyimide, TMMR, Silicon

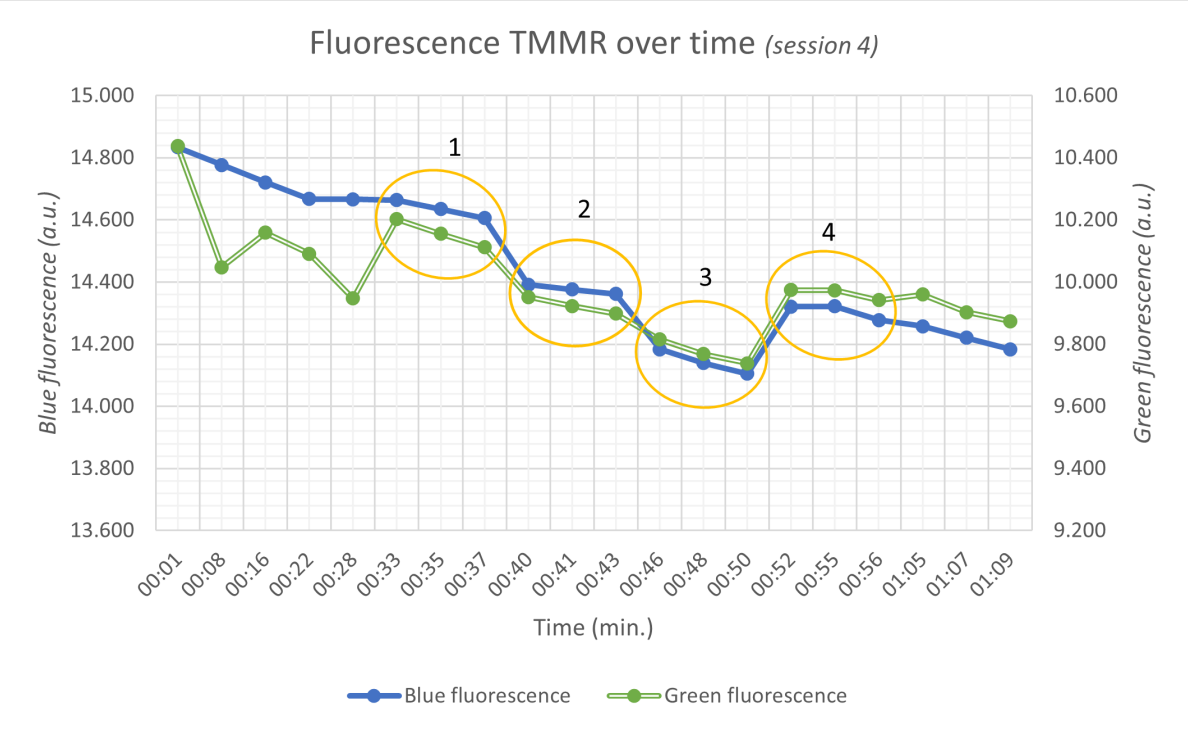

(b) TMMR over time

Figure 5.22: TMMR position and alignment during Session 4.

5.5.3. UV-VIS spectroscopy

As said in the section of methods, the UV-VIS spectroscopy measured the transmission of the light through the polymers on glass wafers. Apart from polyimide 2610 which was on a BF33 glass wafer, all the other polymers were deposited on a AF45 glass wafer. The black line, shows the transmission of the glass wafer. The polymers will cause reflections and therefore the fluctuating signal. As shown in the figure, polyimide 2610 has a lot of reflection. For SU-8, it is medium. Otherwise, it can be seen that the absorption of polyimide at wavelengths above 400 nm is high. At SU-8 this medium is from 350 nm and at BCB and perminex there is a low absorption at respectively 350 nm and 450 nm.

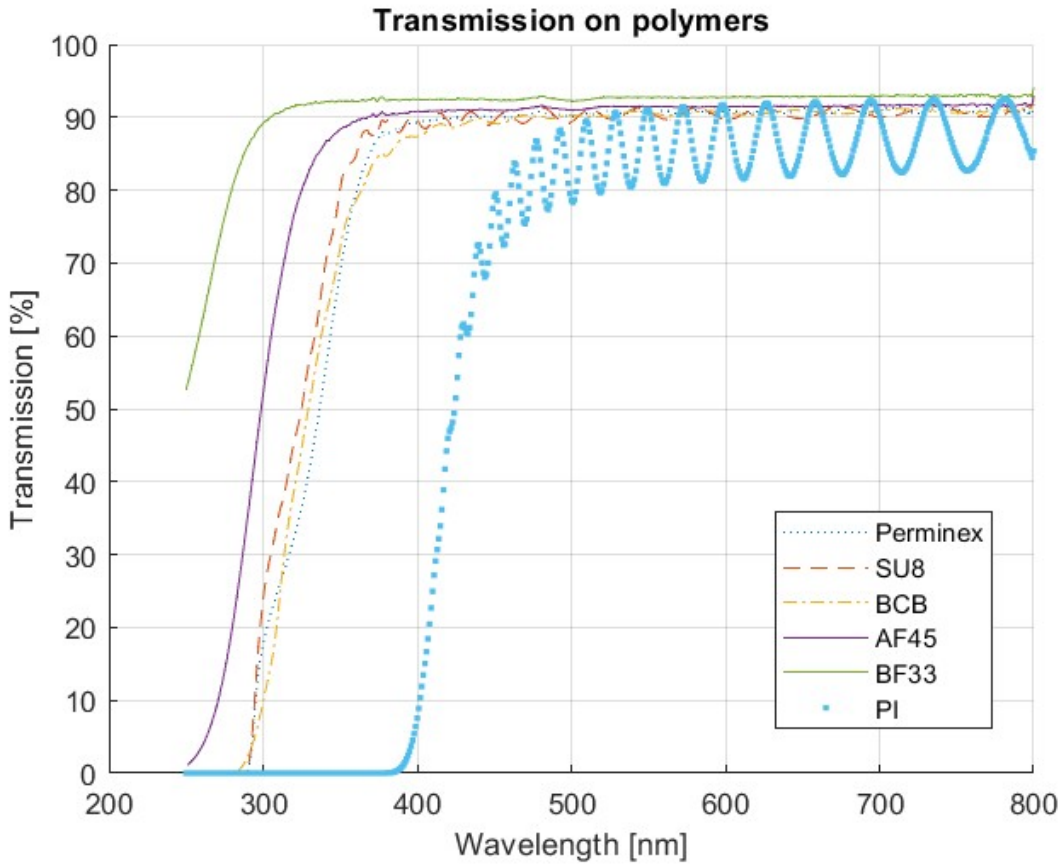

Figure 5.23: Transmission of polymers

5.6. Discussion and conclusion

The first setup indicated that the samples with TMMR and with SU-8 are fluorescent, but the other polymers were barely fluorescent. However looking at the second setup, more levels of fluorescence were visible. The imager showed that all polymers appeared to be fluorescent to a greater or lesser extent, except for parylene. The results of the microscope, that SU-8 and TMMR were the most fluorescent ones, match with the imager as its top three highest intensities are due to those two polymers. After normalization, the polymers SU-8, TMMR, and polyimide showed the highest intensities. For the blue wavelength, TMMR and polyimide produced the largest values. For the green wavelength, it is by far due to SU-8, followed by polyimide which intensity is almost three times less. In all the measurements it is clearly visible that polyimide had a higher intensity of green fluorescence compared to the other polymers. With the results from the last fluorescence measurement, on the amount of exposure, there is a drop in the fluorescence intensity. After the first three sessions, this was visible as the TMMR and BCB were used in multiple sessions and therefore endured more exposures created by the imager. This decrease in fluorescent intensity is called quenching of fluorescence. However, it is also visible that the position on the plate influences the fluorescent intensity. Creating the lowest fluorescent values at the top left and creating the highest value bottom right. A remarkable result is a difference between the fluorescence of the hermeticity samples compared to the cytotoxic samples. For the hermeticity samples, perminex caused a high intensity that the exposure time had to be adjusted due to overexposure. It was mentioned in the parylene-c literature section that the application influences the fluorescent intensity of the material. In this case, it could be due to the metal tracks underneath the perminex. Looking at the results from the absorption and transmission measurements, perminex had a fast and high percentage of transmission. This could mean that with the metal tracks underneath, its fluorescence could be reflected more compared to e.g. polyimide, which normally has a high fluorescence. However, polyimide has a lower transmission rate, especially around the Cy2 filter wavelengths.

Comparing results with literature

Comparing the results with the literature mentioned in Section 5.2, similarities are visible between the two sections. It was mentioned that SU-8 showed (more) fluorescence between 550 and 600 nm and none at lower values. Looking at the results of the imager this is indeed true, SU-8 is almost 10x more fluorescent within that waveband. Furthermore, the company that produces TMMR declared that its polymer has a higher fluorescence intensity between emission wavelengths 510-550 nm but decreases in fluorescence intensity with a wavelength above 575nm. This is also visible in our results of the microscope and imager. The study of Cen (2018), mentioned BCB to be (high) fluorescent at 535 ± 15 nm and low fluorescent at 650 nm. According to the imager, it is more fluorescent at the blue wavelength band and lowers at the green wavelength band, but compared to the others it is not highly fluorescent. Polyimide on the other hand was named to be low fluorescent due to its high charge transfer, although the results indicate that this polymer is respectively fluorescent compared to the others. According to the study of B.Lu et al. (2010)[20], polyimide is fluorescent at $\lambda_{em} =$ 515-555 nm and increased in intensity at $\lambda_{em} =$ 590-650 nm, this is also the case in the aforementioned results. In the study, they also compared its values with parylene-C. Comparing our parylene results with that of polyimide, displays that parylene fluorescence is in both cases lower than that of polyimide. In the study the wavelength of $\lambda_{em} =$ 515-555 nm show almost equal values for both of the polymers.

Limitations

For the fluorescence setup I, microscopic measurement, one should keep in mind that the shutter time is calculated with the amount of grey being 18% meaning, the calculation of the shutter speed with the software of the microscope is dependent on several factors: position of an object, focus, patterning, ambient light, and objective lens. To keep these factors as constant as possible, the amount of ambient light was constant, meaning the microscopic measurements were performed with the lights shut off and curtains closed. And all polymers were studied at several focal depths, keeping the objective lens constant during analyzing the results with other polymers.

Furthermore, the microscope should be focused on the surface layer of the sample as an unclear focus can result in a different shutter speed. Since it is not clear to assume it is focused on the surface layer of the wafer when there are no patterns, a scratch was made to get the correct depth of focus on the surface of the sample. Furthermore, as there are plentiful types of polymers, only five of them were investigated during this study. These were chosen, due to their availability at the company.

Alternative
Other than using a different polymer, there are more options to influence the fluorescence. There are studies on colored SU-8 to lower its fluorescence in a certain wavelength range, performing this or on other polymers can potentially be applied dependent on the fluorescent dye. Moreover, a different method of detection might be an option depending on the situation. Fluorescence detection is one option for optical detection, but electrical detection is also possible. Furthermore, it seems that there is fluorescence quenching, a principle that can also be applied to reduce the amount of fluorescence to ensure that it cannot interfere. But to what extent the quenching principle applies (exposure time) and whether it applies to all polymers may require further research.

5.6.1. Conclusion
Looking at the results of both setups, one can conclude that parylene has a low fluorescence in our wavelength band of interest. After normalization of the values and taking into account that SU-8 is the reference polymer, the polymers BCB and parylene show less fluorescence in all wavelength bands. The polymers TMMR and polyimide are less fluorescent between 565 and 645 nm, but are twice as high between 505-545 nm compared to SU-8. Nonetheless, one should keep in mind that these thicknesses fluorescent cannot be compared without thinking of the polymers thickness, as some polymers have a larger film thickness than others. In short, the type of polymer to choose is dependent on the required characteristics of its application, but BCB and parylene showed the lowest amount of fluorescence if the thickness is insignificant.

5.7. Summarized
- **SU-8** has a decent amount of fluorescence
- **Parylene-C** is almost non-fluorescent in the measured wavelengths.
- **perminex** after normalization the Perminex has a decent to low fluorescence.
- **TMMR** is very fluorescent, but due to a stop in production by the manufacturer, this polymer is no longer of importance.
- **BCB and Polyimide** are quite fluorescent. BCB has a high fluorescence in both wavelength ranges, especially compared to SU-8. Polyimide is even more unwanted, as it has the highest green fluorescence of all the polymers when blank on a silicon surface. Polyimide has a lower blue fluorescence compared to SU-8, therefore it can be used when a low fluorescence is needed between emission wavelengths between 505 and 545nm.
- It is difficult to compare the results with the literature, but the aforementioned bullet points are broadly coherent with the literature.

6

Surface characteristics

6.1. Introduction

Polymers can be used for wafer bonding and the encapsulation of a device. For these applications, any leaching or permeability to water is undesirable as it could cause corrosion of the BioMEMS and infections when the device is used *in vivo*. This chapter will explain the hermeticity of the polymers to investigate their durability in moist environments over time. Hermetics create an airtight (or gas-tight) encapsulation to prevent permeability between the environment and the inside of the encapsulated device. According to Lofink, Kähler, and Reinert [34], a hermetic package has to ensure environmental stability for at least ten years. This chapter starts with a short literature study, followed by materials and methods applied to perform a hermeticity test and the final results of the experiment. Next, this chapter will include contact angle measurements that give information about the wettability and therefore the characteristics of the surface. There is a relationship between wettability and biocompatibility, a higher wettability would also mean a higher compatibility. But the adhesion of particular cells or proteins is also dependent on the wettability. As mentioned in Chapter 2, the surface of a material affects its biocompatibility. This chapter will investigate the surface characteristics of polymers based on hermeticity and wettability. Section 6.3 will explain the methods used to perform these tests. The results are shown in Section 6.4, followed by the intermediate discussion on the surface characteristics of polymers in Section 6.5.

6.2. Literature

The literature on the hermeticity of the BioMEMS polymers will be built up, starting with the literature found on the polymers' characteristics related to hermeticity, followed by hermetic testing methods.

6.2.1. Polymer hermeticity

The polymers of interest have been mentioned before: SU-8, perminex, polyimide, parylene, and BCB. This section will review the studies on the hermeticity of these polymers. However, perminex has the same problem as before, and there has not been an extensive amount of research performed on perminex. Therefore, it is unknown if this polymer will be hermetic. Among the other polymers, parylene-C is a type that is known to be hermetic and has been tested extensively [35].

6.2.2. Methods for hermetic testing

In this section, the different ways of testing hermeticity will be briefly explained. A leak rate test is a common method for determining hermeticity. A distinction is made between the fine leak test and the gross leak test [36]. Furthermore, a standard and common corrosion test method used to evaluate the corrosion resistance of materials and surface coatings is the salt spray test (also known as the salt fog test). This method of testing is used to see if it can withstand corrosion. Since a setup has been used by a previous student for a similar test, it will also be taken into account.

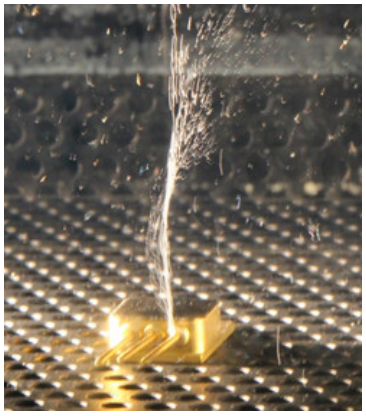

Figure 6.1: Image showing the leak of bubbles created by non-hermetic sealing

Leak tests
Gross leak test: This type of testing is performed in a chamber filled with a liquid at a high temperature. When there's a leak in the sealing, it will create bubbles from those leakage spots. The type of fluid is dependent on the test objects.
Fine leak tests: One of the most known types of leak tests is the fine leak test. This type involves high pressure in a package with tracer gas. During the curing process, it does not involve any catalysts, which increases the quality of bonding since no out-gassing takes place [37].

Saline solution soaking test
The saline solution tests are performed to investigate the resistance of a device against corrosion, namely testing the surface materials of the device (coatings). This can be performed with a salt spray (fog) test or a saline soaking test [38]. During this project, the saline soaking test is performed to test if the samples are hermetically sealed and if it prevents the sample from corrosion. The method to test this and the explanation of the samples are discussed in Section 6.3.

Setup previous student
Due to the accessibility of this setup versus the devices mentioned before, the setup of the previous student will be used. A previous MSc student worked on the hermeticity of polyimide and its interaction with silicon carbide (SiC) and silicon dioxide (SiO_2), comparing the effect of a metal layer sandwiched with polyimide and the effect of adding a ceramic layer [39]. Now, it is not of interest to investigate the interaction between different layers, only to test if the polymer can prevent corrosion in a saline solution and the metal tracks on a device.

6.2.3. Contact angles
Biomaterials require the characteristic of wettability in order to provide the desired biological reaction. Wettability tests are an essential part of the scientific analysis of the properties of biomaterials. The most popular technique for assessing the wettability of polymeric biomaterial surfaces is contact angle measurements. Surfaces that have a low contact angle are described as hydrophilic, whereas those that have a contact angle of around 90 degrees or more are described as hydrophobic. Hydrophilicity plays a critical role in cell adhesion and proliferation. The adhesion between functional groups on the surface and cells is stronger when a material is moderately hydrophilic. Cellular responses can also be impacted by hydrophilicity. Contrarily, large amounts of matrix protein adsorption are linked to hydrophobicity, which changes the cell's adhesion and lowers bioactivity.
The studies on the contact angles of the polymers were conducted with the aim of investigating surface treatments on the wettability of the polymers. With SU-8 it turns out that unmodified SU-8 has a contact angle of around 95.36 °, whereas a polyethylene glycol (PEG) modified surface will create a contact angle of almost 59 ° [40]. Currently, the focus will be on unmodified polymer surfaces. However, the fact that surfaces can be modified to obtain the desired wettability will be taken into consideration for future studies. Further literature studies show that polyimide has a contact angle of about 67 ° [41], parylene-C has an angle of 90 ° [42], and BCB has an angle of 100 ° [43].

6.3. Method

To perform the hermeticity test, there are two different samples per encapsulation layer, as listed in Section 4.3. The encapsulation layers are BCB, perminex, polyimide 2610, silicon nitride, and SU-8. The metal tracks are made of aluminum/ copper, or gold/platinum. The reason to create tracks out of aluminum is due to its sensitivity to corrosion.

6.3.1. Materials hermeticity

In Chapter 4.1, the process of creating the hermeticity samples was explained. After this stage, ten diced wafers were the result. From these ten wafers, it was clearly visible that the adhesion of SU-8 primarily on gold had failed. SU-8 on aluminum tracks still covered a majority of the tracks in Figure 6.2b. Even though it had little or no SU-8 on it, it was also included in the study. In addition to the samples, PBS was needed and a heating device. The phosphate-buffered saline (PBS) was used to soak the samples. It has a pH of 7.4 and is widely used as an indication of a biocompatible dialysis fluid, as it has the same ionic concentrations and osmolarity as the human body. To soak the samples at an elevated temperature, a box filled with water functioning as a waterbath. The bath consisted of a plastic container with a styrofoam box containing a plastic bag where the water could be placed. Because of the styrofoam, the heat will not dissipate as quickly and will stay at a better temperature. The plastic bag was intended to prevent leaks. The water bath also has a heating pump (Julabo model HL) that circulates the water and maintains an elevated temperature (see Figure 6.2a).

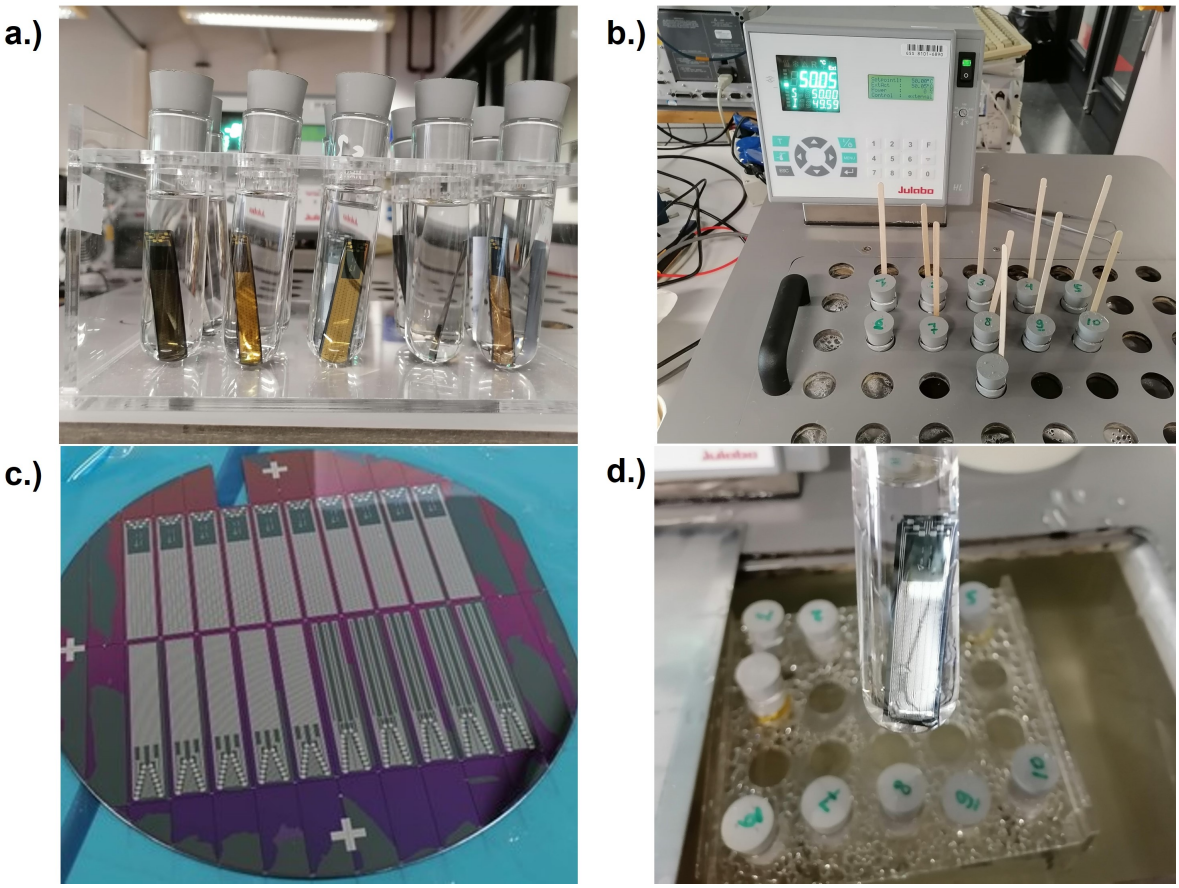

Figure 6.2: Hermeticity setup device and wafer: a.) Set-up of the pump in a box, with a cap. b.) SU-8 aluminum tracks wafer, after dicing. c.) Sample check on corrosion. d.) Aluminum samples in a tube with PBS.

6.3.2. Procedure of hermeticity test

To investigate the lifetime of the polymers, a saline soaking test is performed. The saline soaking test consists of putting a sample in a saline solution and examining the samples for corrosion. When cracks or breaks appeared in the polymer, it would not be hermetically sealed and should cause corrosion on the metal tracks since the metal tracks would be in direct contact with the saline solution. The samples were put into a tube with 20 ml of PBS, covering the whole sample. As the temperature influences the lifetime of a device, the temperature will be increased to accelerate the test. The temperature of the saline solution was kept on temperature, with a water bath. This sets the temperature of the water containing the tubes with the samples. The initial temperature was 50 °C, which was maintained for 1.5 weeks. The temperature was then raised to 60°C for one week. Followed by a continuous final temperature of 70 °C. During these experiments, the temperature was increased up to 70 °C, meaning that an accelerated lifetime test was performed. Examining the Arrhenius equation (Equation 6.1) and the dependence of *'k'* (Equation 6.2), this can be explained. The *'k'* stands for reaction rate constant, which is dependent on characteristic values of the material. An increase in temperature (T_2) during the test will result in an increase in *'k'*, reducing the aging time (t) [44]. With an increase of 10 °C compared to the temperature of the object in normal conditions, means a doubling of the reaction rate. In other words, if we would assume a device should work at a temperature of 37 °C, the number of days in lifetime expectancy would be double at 50°C. In total this would mean that these tests are performed equivalent to approximately 272 days at a temperature of 37 °C.

$$k = Ae^{-E_a/RT} \tag{6.1}$$

$$k = -\ln[\frac{P}{P_0}]/t \tag{6.2}$$

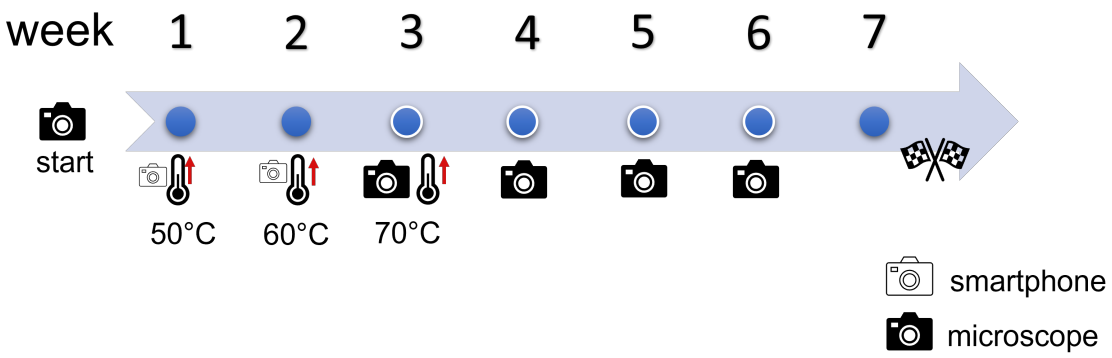

Figure 6.3: Timeline of the hermeticity samples in the waterbath

6.3.3. Contact angle measurement

The contact angles are measured to get an indication of their wettability and are one of the first tests performed when biocompatibility is mentioned. According to the various studies on the correlation between wettability and compatibility, it appears that higher wettability leads to higher compatibility. This implies that a low contact angle has improved compatibility. The syringe drop method is one of the commonly used methods where a syringe of liquid is dropped. By measuring the x and y displacements, the angle can be calculated. It can also be calculated by looking through the microscopic tunnel, but that is less exact. This type of measurement setup does have two disadvantages, one being evaporation; the measurement should be performed in a short time interval, or the droplet can evaporate. two, dehydration of the solid surface. At the surface, polymers may adjust their orientation in relation to the surroundings. If the polymer is left in a dry environment (e.g. air), the hydrophobic groups in the polymer will reorient themselves to the material's surface, which will reduce the material's wettability.

6.4. Results

The results consist of photos made with a smartphone for the first two weeks. Then the photos were taken with a macro lens on a Leica microscope. This allowed a more precise examination of whether differences were present throughout the weeks. For the first two weeks, the samples were not removed from the PBS. To view them under the microscope, the process with PBS had to be interrupted. For this purpose, the samples were removed from the solution every week, rinsed with demineralized water, and then dried to examine them. With the macro lens, each sample could be taken with three photos stitched back to back (see an example in Figure 6.4). One of the three images had an adjustment of brightness to make the potential damage on the sample visible. This section will discuss the observations for each polymer, with photos where necessary. The photos can be found in the appendix. Some samples were further examined with a scanning electron microscope (SEM), the results of which are discussed in Section 6.4.2.

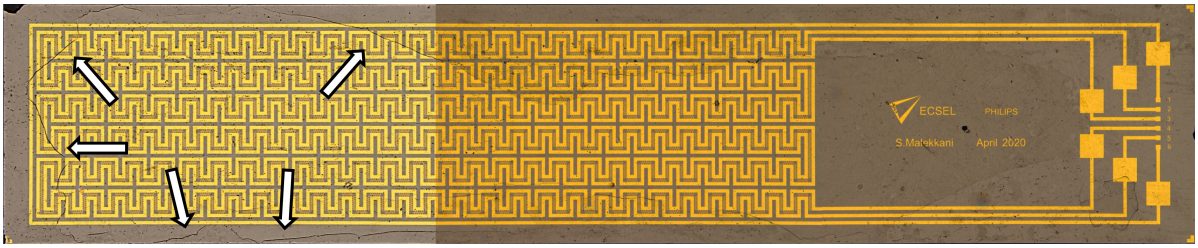

Figure 6.4: BCB hermeticity at week 6

6.4.1. Microscope photos

This section provides the microscope results on the development of the samples in the saline soaking test (hermeticity test). The focus at this point will be on the changes in the samples over the weeks. The Appendix includes the macroscopic images of each sample over the weeks. Not every polymer and/or not every week there was a noticeable change, but that will not be discussed. The microscope images consist of both macroscopic photos of the samples and zoomed-in sections.

SU-8

The wafer with gold tracks covered with SU-8 did not have a sufficient amount of SU-8 left, after dicing. Therefore, only the wafer with the aluminum tracks contained SU-8. The sample that was used was not completely covered with SU–8, parts of the aluminum tracks were in direct contact with the saline solution. This resulted in aluminum tracks that were tarnished. However, it was not a starting point to reduce the adhesion of the polymer layer in such a way that the SU-8 would detach. Some newton rings could be seen in week five but two weeks later this amount had not visibly increased either.

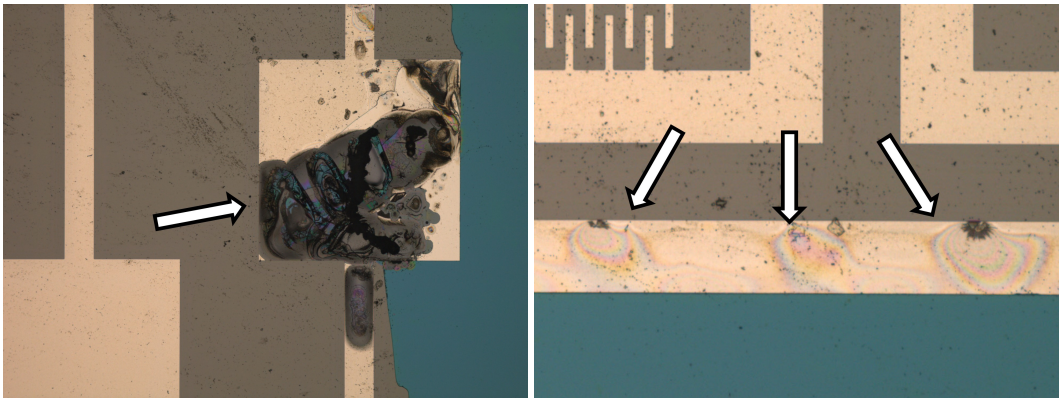

(a) Week 5: uncovered aluminum corroded. **(b)** Week 5: newton rings indicating height differences.

Figure 6.5: Hermeticity sample of SU-8 on aluminum in week 5

BCB

The samples with a BCB layer had different results. The sample containing gold tracks had a potential fracture in the top layer that was visible in the second week, see Figure 6.6a. In Figure 6.4 this potential fracture in the BCB layer is indicated with the arrows. This will be investigated further, to verify whether it is a crack. The sample was rinsed and dried multiple times with demineralized water for five more weeks to observe the changes in the sample by using a microscope. This rinsing and drying did not influence the crack in any way (see Figure 6.6b).

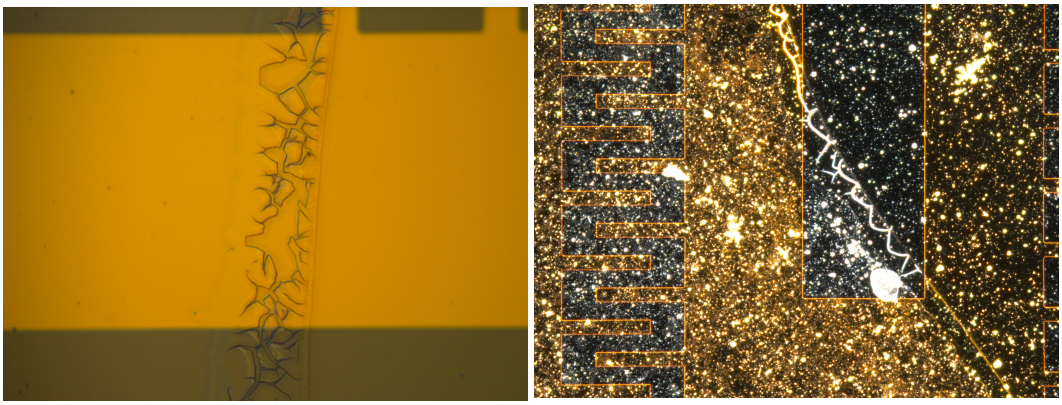

(a) Week 2: Possible damage on BCB layer **(b)** Week 6: BCB damage with interference contrast

Figure 6.6: BCB on gold tracks three and six weeks of soaking in PBS.

Perminex

At perminex, changes were visible over the weeks. Both in the sample with aluminum and in those with gold, delamination from the sides occurred. Especially with aluminum, the perminex was loosening more from the wafer each week. This means that the perminex at the interface with the SiO_2 is not adhering strongly. On the surface with gold, you mainly saw an increase in spots on the polymer. To determine with certainty whether this is on or in the polymer layer, will require more investigation.

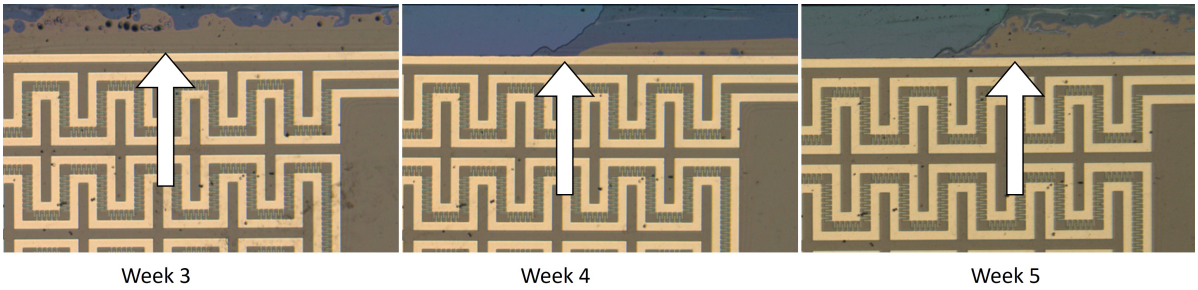

Figure 6.7: Perminex progression over the weeks.

Polyimide

With polyimide, not much happened either. There are no pinholes or corrosion. Only some remarkable stripe patterns are visible as shown in Figure 6.8. This could imply that there were contaminants that entered the tubes.

Figure 6.8: Polyimide on gold tracks after six weeks of soaking in PBS.

Silicon nitride
With silicon nitride, nothing remarkable happened; both the samples with aluminum and gold tracks remained intact.

6.4.2. SEM check

When the samples were removed from the saline solution, some of the samples were investigated further with a scanning electron microscope (SEM). With the SEM, the sample is bombarded with electrons (primary electrons). Then, secondary electrons are captured reflecting from the sample to the collector. This creates a visually zoomed-in picture up to 120.000x, which is about 12 μm. Because we are dealing with polymers in this situation, if the polymers are bombarded with electrons, a good visual representation will not be possible because the electrons are not captured. Therefore, a layer of platinum palladium is first sputtered. The result of adding a small metal layer can be seen in Figure 6.9. The SEM was used to investigate the following samples: SU-8 aluminum, perminex aluminum, perminex gold, BCB gold, and Si_3N_4 aluminum.

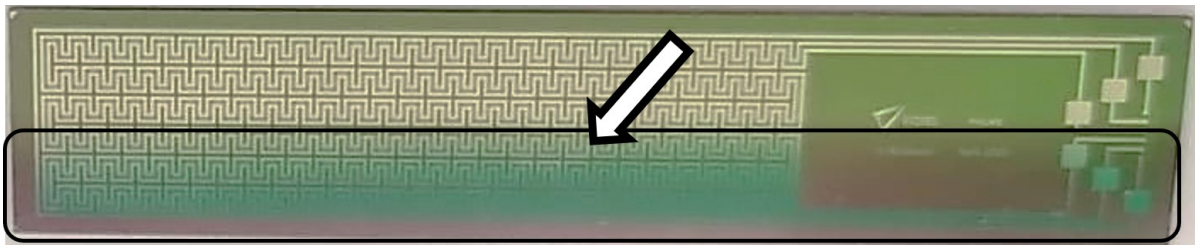

Figure 6.9: Samples after used with SEM with silicon nitride.

SU-8 aluminum
Figure 6.10 shows the results, where part of the aluminum tracks was not covered with SU-8. This resulted in corrosion. However, it is also visible that the SU-8 layer is also lifted in Figure 6.10b.

BCB gold
The sample with BCB on gold showed a possible tear in the polymer layer. However, it did not rinse away over the weeks. With the SEM, a significant amount of unidentified compounds were present on the surface of the BCB. This is visible in Figure 6.11 .

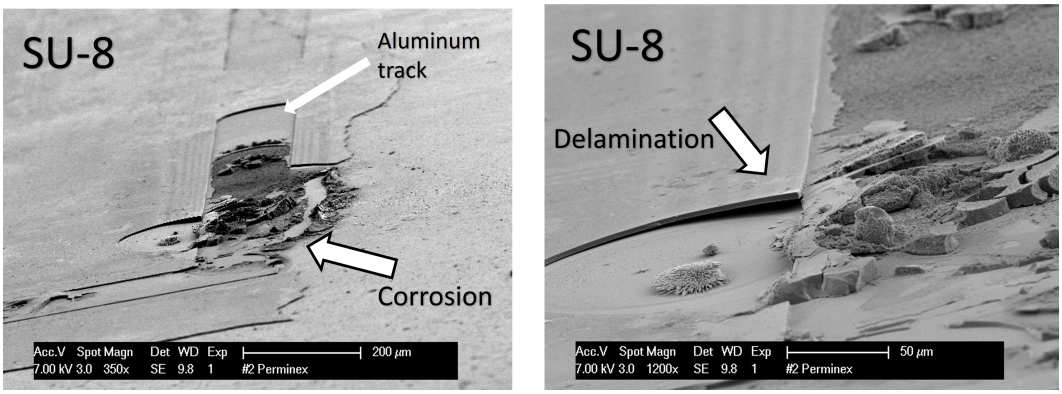

(a) Corrosion on the aluminum track visible.

(b) The SU-8 layer is loosening from the Silicon.

Figure 6.10: SEM images of the SU-8 on aluminum tracks after weeks of bathing in PBS.

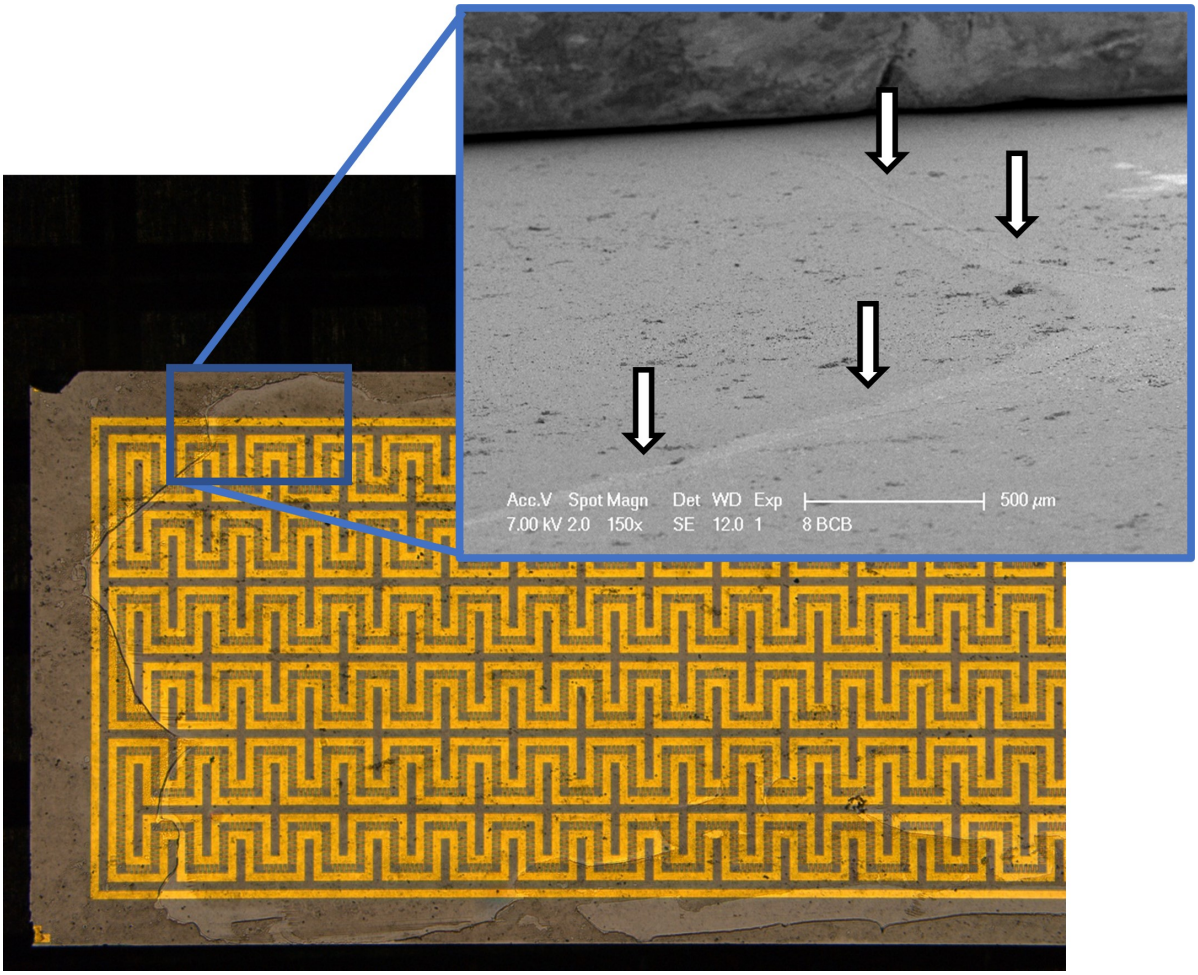

Figure 6.11: BCB zoom comparison with the fracture.

Perminex gold and aluminum

Figure 6.12 shows photos made with the SEM on the sample with aluminum tracks and the last one is a crystalline structure on the perminex gold sample.

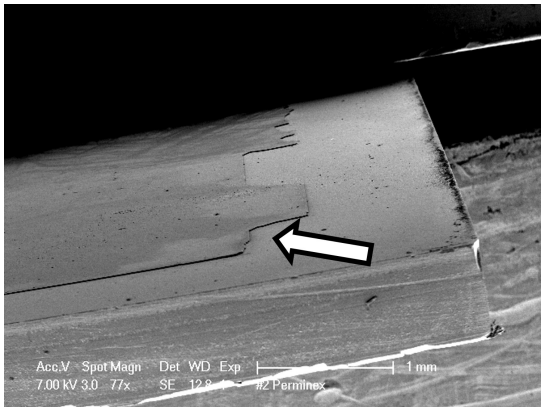

(a) Aluminum perminex sample with height difference angle from the corner.

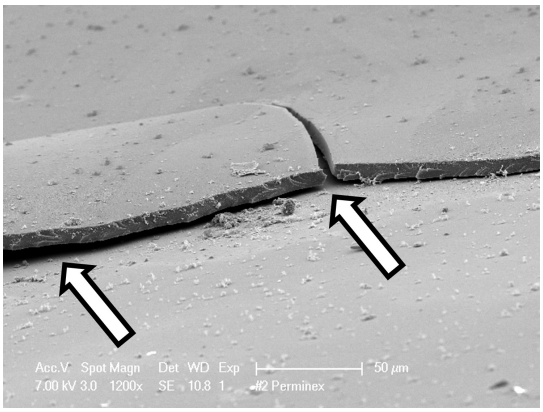

(b) Perminex broke and detached from the substrate layer.

Figure 6.12: Perminex SEM

Silicon nitride aluminum

This sample has been investigated to check its effect. Si_3N_4 is not a polymer and has a very thin layer, namely 0.5 μm, but it does prevent the metal tracks from corrosion.

6.5. Contact Angles

The hydrophobicity or wettability can be explained by investigating the surface of the polymers. In this section, the focus will be on the contact angles of the polymers. Contact angles were measured by the drip method. When the surface is hydrophobic, a droplet of water will create an angle larger than 90 °. And an angle smaller than 90° means the surface is hydrophilic. It is unknown what an angle of 90 degrees would mean. The wettability test, resulted in at least four measurements with a droplet method, performed in the cleanroom. This involved depositing water on the surface of the wafer through a syringe placed at a 90 °C angle on the wafer. Next, the height of the droplet and the total width are measured. These measurements can subsequently be used to calculate the angle. The results of the measurements are shown in Figure 6.13. After an oxygen plasma treatment, the angle on the polymer surfaces was immeasurable see Figure 6.14. This means that with an oxygen plasma treatment, the surface of the polymers is around 0°.

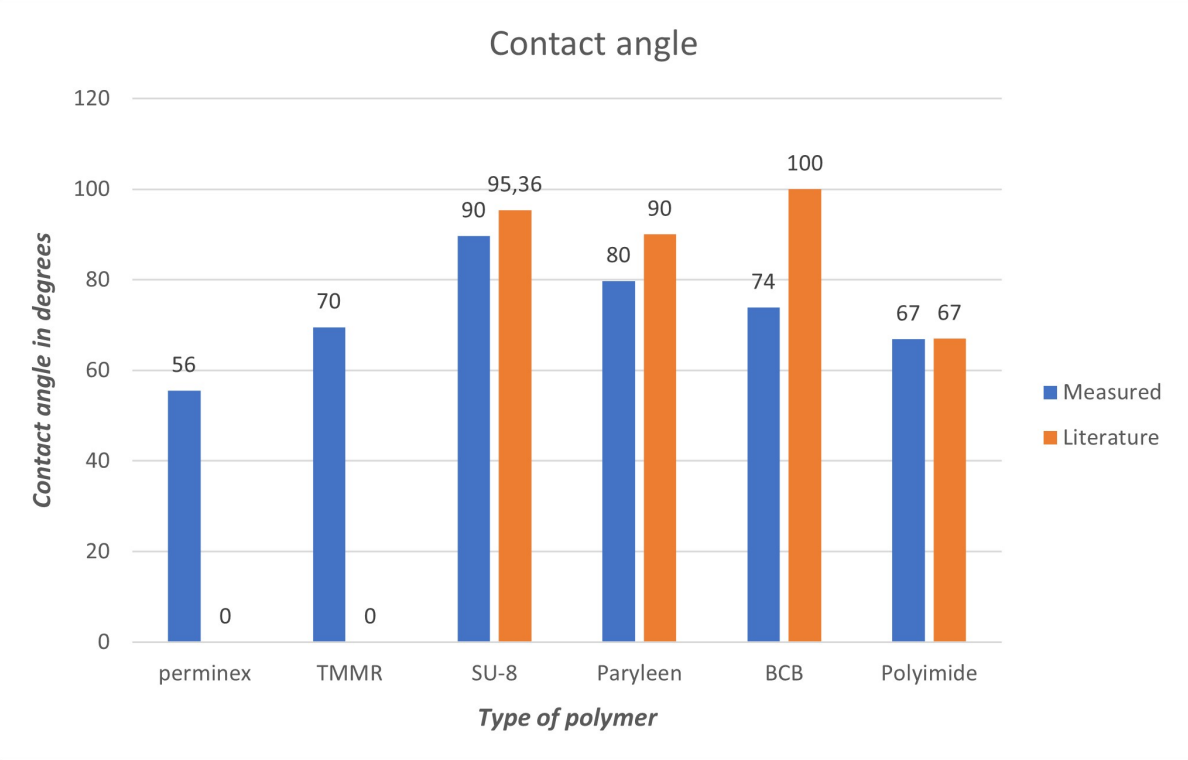

Figure 6.13: Overview of the contact angles measured versus what has been found in the literature studies.

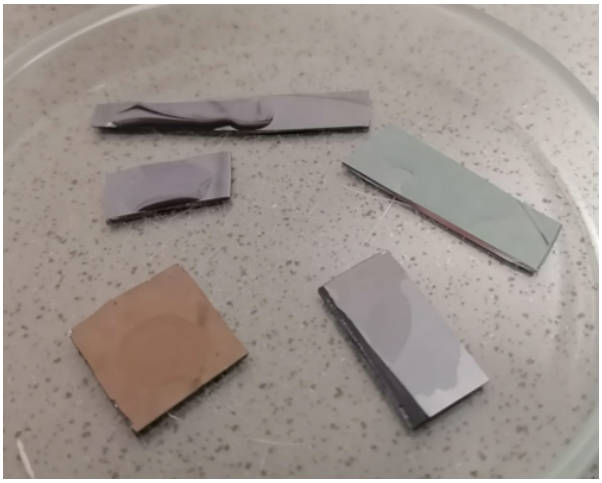

Figure 6.14: Result of droplets of water after the plasma treatment (barrel).

6.6. Discussion and conclusion

The purpose of this chapter was to examine surface characteristics, specifically studying hermeticity and wettabillity. This is relevant since liquid permeability can lead to the dysfunction of a BioMEMS device. Wettability reportedly had a relationship to biocompatibility, where a hydrophilic surface would mean it was more compatible.

Results

The first thing to notice about the results of the hermeticity tests is that the polymers seem to react differently based on the layer underneath it, as the polymers are still attached to the silicon wafer at the sides they should not react differently based on different metal tracks. Even if the adhesion at the metal tracks is worse on gold compared to aluminum, the polymer still attaches for a majority on the silicon dioxide layer of the wafer. Furthermore, it should be mentioned that corrosion on gold was not what was expected. For that reason, aluminum was chosen as this is a sensitive metal to corrode. Another interesting result was that the aluminum did not corrode immediately on some parts of the tracks.
It was evident that none of the samples suffered from pinholes. However, a difference in reactions was noticeable between the polymers. With perminex, for example, there was evidence of detachment of the polymer on the silicon oxide layer in both gold and aluminum samples. In the process, fragments of perminex disappeared from the sample. With BCB, there was a fracture in the polymer layer, however, it persisted until the end of the experiment. In summary, most polymers lasted in the PBS soaking test and no corrosion occurred on the metal tracks.
Contact angle measurements were performed on blank polymer layers without any modifications. Except for BCB, the contact angles of the polymers were consistent with what was reported in the literature. The only cases where this was unknown were for TMMR and perminex. The measurements showed that for unmodified polymer surfaces, perminex and polyimide exhibited the most hydrophilic character. After the blank samples had been in the oxygen plasma of the barrel, the contact angles on all polymers were reduced to the point where they were not measureable.

Limitations

Given the limited time and number of wafers to use, not all polymers were included. TMMR was eliminated, and in the case of parylene-C it was decided based on literature suggested it would be of little value with this polymer as it is often used as a coating. In conducting the experiment, other options were not considered in more detail because a previous student's setup still existed. Thus, the goal was to use the same setup.

Future works

The hermeticity tests could also be performed in other ways. Since there were contaminating components on the samples, condensed matter probably entered the tube when the rubber corks popped off. Furthermore, it would also be valuable to study the samples soaked in multiple solutions. For instance, a piece of aluminum wafer was placed in demineralizing water, tap water and PBS. These were examined for corrosion at room temperature and 70 °C. Thereby, the aluminum decayed most rapidly with tap water, followed by PBS and then demineralized water. At 70 °C it decayed first in tap water, then demineralized water, and in PBS it remained intact.
Multiple surface modifications related to the contact angles were not attempted, as this was outside of the scope of this project. However, this could be investigated further, to enhance the biocompatibility.

7

Adhesion and etching

7.1. Introduction

In this chapter, the adhesion, chemical resistance and etching of the polymers will be discussed. During this study of the characteristics of BioMEMS, a number of questions arose regarding the adhesion (and resistance) of the polymers against chemicals. As mentioned at the beginning of this report, etching is a method of removing layers from the substrate. Here, certain etching methods are applied to test the adhesion of the polymers on the substrate. For the cytotoxicity study, it was vital to know whether all polymers could withstand ethanol, as this will be used to sterilize the samples. Pieces of blank polymers on wafers were dipped into ethanol for a period of time. Since it can be interesting for the cleanroom whether the polymers are also resistant to different types of chemicals applied for wet processing, such as PES, KOH, PGMEA, BOE, and ethanol, these have also been included in the chemical resistance tests. The method mentioned above is a method of wet etching. In the next section, a dry etching method is applied. Therefore, a barrel plasma etch will be used to etch layers from the samples that were also made for the hermeticity tests.

7.2. Literature

This section is a brief literature review of polymer adhesion and chemical resistance. Since the tests applied here are not standard tests, only information related to adhesion or chemical resistance will be discussed.

SU-8

SU-8 has a lower adhesion to gold, compared to other substrates [45]. There are multiple studies on improving the adhesion of SU-8 on gold. Figure 7.1 shows that the attachment of SU-8 to each substrate varies. Here, a clear difference is noticeable between the adhesion of SU-8 to gold compared to an aluminum or silicon. During the production of the hermeticity samples with SU-8 (Chapter 4), a primer was used. The applied primer did not influence the adhesion of the SU-8 to the substrate layer. In a study of the adhesion of SU-8 it was said there is no significant difference in adhesion with or without primer, whether HMDS or TCPS as a primer[45].

TMMR

Since part of the adhesion test was conducted before it was known that the production of TMMR would cease, it was still included in the chemical resistance test. TMMR has information on resistance to some of the chemicals [9]. According to the manufacturer, TMMR can withstand 10% KOH and 2.38% TMAH for 10 minutes at a temperature of 40 °C without changing. It's also resistant to PGMEA for 15 minutes at a temperature of 23 °C.

Polyimide

Polyimide needs a primer to adhere to the silicon wafer. The best adhesion will be obtained with a thoroughly hydrolyzed silicon oxide surface because the primer interacts with OH groups on the wafer's surface. The adhesion of polyimide on silicon is dependent on the way it is processed [47].

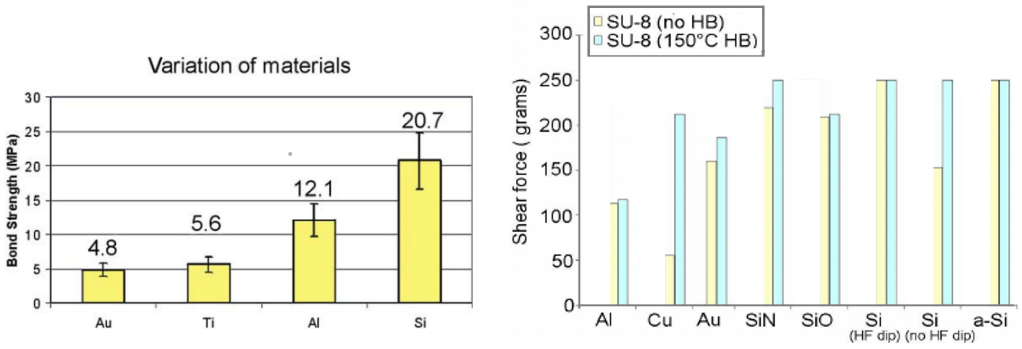

(a) The adhesion of SU-8 on different gold, titanium, aluminum and silicon [46].

(b) SU-8 adhesion with and without hardbake (HB) on different substrate layers.[45].

Figure 7.1: Adhesion of SU-8 on variety of substrate layers

Parylene-C
Also because parylene is deposited in a different way, it has better adhesion because it depositis very conformly. However, because parylene is deposited in a different way, it mainly adheres to itself. As a result, parylene may have more difficulty in adhesion on smooth surfaces because it cannot hold onto anything. This therefore also applies to substrate layers of gold and silver.

Perminex
For perminex, at the moment there is no literature regarding the adhesion characteristics of this polymer.

7.3. Methods

In this section, the methods of both tests will be explained. Starting with an explanation of the chemicals and why these are important. This is followed by experiments to remove the polymer from the samples.

7.3.1. Chemical resistance

Etchants are chemical compounds which chemically react selectively with the layer to be removed. Various processes are used during the production of a BioMEMS, including the wet etching method. When a photoresist is used, a patterned mask will create a structure that is not covered. When the wafer with the photoresist is placed in a bath with the etchant, the unexposed material will be etched. During these tests, the following chemicals are used to examine the resistance of the polymers:

- Ethanol: this is not used for wet etching, but it is important to investigate its resistance as the materials will be cleaned with ethanol during the cytotoxicity experiment.
- PES: PES etch consists mainly of phosphoric acid. It is a metal etchant thus used for etching aluminum.
- KOH: potassium hydroxide. This chemical is used for bulk etching silicon, to create cavities. For this test, warm 10% KOH was used.
- BOE: also known as buffered oxide etch or BHF. HF, hydrofluoric acid, is used to etch silicon dioxide, titanium. Thus BOE can be used to etch SiO_2,Si_3N_4, titanium, glass and aluminum. During the test, a solution of 7:1 BOE was used (HF : NH_4F = 12.5 : 87.5%).
- PGMEA: is used as a photoresist solvent, primarily for coating silicon wafers with primers such as HMDS. It has also been used in developing fluidic channels in a PDMS microfluidic device.

The chemical tests were performed on the following polymers: BCB, parylene-C, perminex, polyimide, SU-8 and TMMR. These tests are performed with the first batch of polymer samples. The exact process flow of BCB and polyimide is unknown.

7.3.2. Polymer etching

As a preparation for a further study on the hermeticity samples, open bondpads were necessary to attach the samples on a (printed circuit board) PCB. The files to get this PCB was already there due to the work of a previous student [39]. However, since that was only with polyimide, the mask was

not usable since it had the wrong polarity. Instead of ordering a reverse polarity mask, we wanted to see if it was possible to remove the polymer from the bondpads, as it wasn't necessary to cover the parts around the bondpads with the polymers. In short, this initiated another study on the removal of the polymers around the bondpads but also gave an indication of the adhesion to the previous layers. As explained in the chapter on the production of the hermeticity samples, there are samples with gold tracks and those with aluminium tracks covered with an encapsulation layer. This encapsulation layer consists of BCB, perminex, polyimide, SU-8, or Si_3N_4. To see if the sheath layer had been removed, a probe station was used to measure conductivity. When the two needles are on one bond pad, there should be conduction when the needles touch the metal layer. If this was not the case, the samples were placed back into the barrel and the experiment was continued. To protect the interdigitated test structures the samples were partly covered with a layer of aluminium. The BCB and Si_3N_4 layers were removed using CH_4, and the remaining layers were removed using O_2. The SU-8, perminex, and polyimide samples had initially been in the barrel for an equal time and temperature. However, because etching rates were different for each polymer, variations in barrel times occurred thereafter.

7.4. Results

There were two different kind of tests, one to test the chemical resistance test and the other to with each a different type of sample containing the polymers. In the Section 7.4.1, the first batch of unpatterned] wafers was used. This batch consisted of unpatterned silicon wafers with a layer of polymer. The second test of removing part of the polymer layer was performed with the samples made for the hermeticity test. As one wafer consists of 10 meandering beam samples, 5 interface samples, and 5 dummy samples, could be used for the etching experiments.

7.4.1. Chemical resistance

As mentioned in the previous section, the samples were all simultaneously placed in a bath with the chemical to be tested for 70 or 95 hours. Especially in the beginning the samples were regularly checked. The table in Figure 7.2, lists the changes in polymer samples caused by the chemicals over time. The chemicals causing the most damage to the samples are: PES, KOH and BOE.

Time interval	Chemical	Type of change
30 min	PES	Perminex discolored
	KOH	TMMR detaches from surface
	BOE	Bubbles on the interface of other polymers
1 h	BOE	More bubbles at BCB
2 h	KOH	Multiple samples move due to bubbles. TMMR and polyimide are detached
3 h	PES	BCB discoloring spot
	KOH	Process of interface attach continued
	BOE	More bubbles at polymers
4 h	PES	More discoloration of BCB and TMMR partly loose
	BOE	Bubbles
22.5 h	PES	TMMR detaches at interface. Small discoloration of parylene-C; Full discoloration BCB
	BOE	Polyimide detaches; SU8 is partly loose, lot of bubbles
	KOH	SU8 detached. Probably also polyimide & BCB detached
95 h	BOE	Perminex and parylene-C semi detached, SU8 detached; TMMR and BCB more bubbles

Figure 7.2: The table shows the changes that were visible when comparing the photo's of the time intervals. No changes between time intervals were not mentioned.

In the following table (Table 7.1), the chemicals are mentioned with the effect at the end of time period versus the start.

Polymer	Ethanol	PES	KOH	BOE	PGMEA 72h
BCB	✓	✓	✗	✗	✓
Parylene-C	✓	✓	✓	✗	✓
Perminex	✓	✓	✗	✗	✓
Polyimide	✻	✻	✓	✗	✻
SU-8	✓	✓	✓	✗	✓
TMMR	✓	✗	✗	✗	✓

Table 7.1: Overview of the chemical resistance versus the polymers. Even though, the polymers were not dissolved, the ✗shows when the polymers were delaminating at the interface and the ✻shows when they were partially delaminating at the interface

7.4.2. Polymer etching

As the whole layer of SU-8 on gold tracks had already deleminated after dicing the wafer, this variant could not investigate in these tests. Therefore, only the removal of the BCB, perminex, polyimide, and SiN were performed with gold or aluminum tracks, and the SU-8 layer removal test could only be performed with the aluminum tracks. The etching experiments were performed with the following steps: etch for a certain time in the barrel, check with the microscope, and measure conduction with probe station. This process was repeated until the bond pads were conductive. The experiments showed that it matters which metal track is underneath before the polymer layer is etched and that it also depends on the surface area to be removed. With the interface samples, there are more bondpads, and the area that needs to be polymer-free is more than twice as large. As far as can be seen, this has no proportional relationship to etch time in the barrel to remove the layer. An overview of the etch time in the barrel, temperature, and result of the samples can be found in the appendix D. The SU-8, perminex and polyimide samples started with a oxygen plasma time for a total of 48 minutes in five intervals at a power of 385 W.

Polyimide

Figure 7.3 shows how the polyimide is gradually removed from the bondpads. The time is the accumulated time. By limiting the time in the barrel, the temperature does not rise continuously.

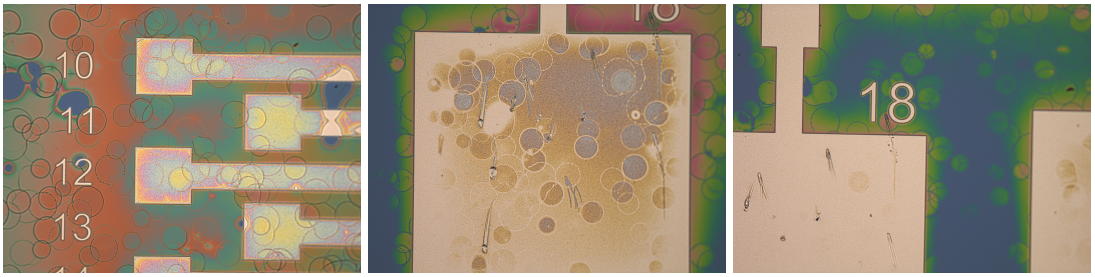

(a) After 159 min. **(b)** After 169 min. **(c)** After 184 min.

Figure 7.3: This figure shows the difference between steps in the barrel of a polyimide sample on aluminum tracks. It shows the result of an oxygen plasma (in time intervals of max 20min) after (Figure 7.3a) 159 min., (Figure 7.3b) 169 min. and (Figure 7.3c) 184 min.

Etching sequence in the barrel until the polyimide was completely removed

- Etching: PO_2 = 385 W for 48 minutes (including intervals).
- Pre-heat:PN_2 = 370 W for 2 minutes.
- Etching: PO_2 = 385W for 20 minutes.
- Pre-heat: PN_2 = 370 W for 1 minute.
- Etching: PO_2 = 385W for 101 minutes (see Figure 7.3).
- Etching aluminum sample : PO_2 = 385 W for 15 minutes (see Figure 7.4a).

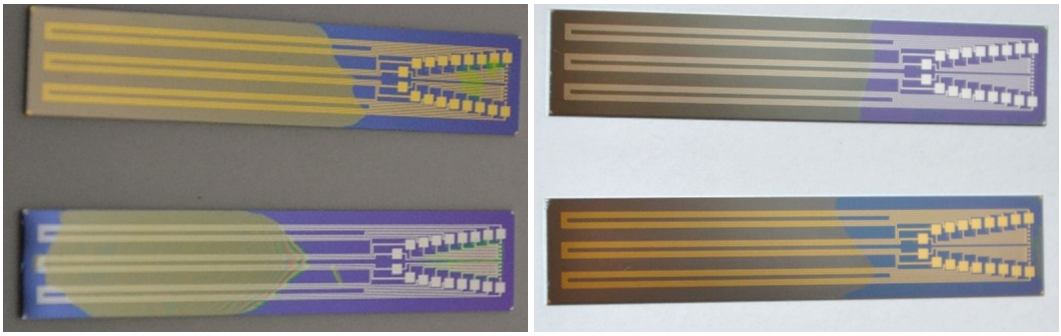

(a) Polyimide after oxygen barrel etch for a total of 179 minutes for gold and 184 minutes for aluminum.

(b) Perminex samples after a 48 min. oxygen plasma and 20 min. extra.

Figure 7.4: Results after removing the polymer layers.

Perminex

The perminex samples were etched with the following barrel sequence. After etching the bondpads were opened, while the tracks were still covered.

- Etching: PO_2=385 W for 48 minutes (including intervals).
- Pre-heat:PN_2=370 W
- Etching: PO_2=385W for 20 minutes (see Figure 7.4b).

SU-8

Removing the layer of SU-8 could only be done with the samples with aluminum tracks. After a total etch time of 48 minutes in an oxygen plasme, the SU-8 layer was completely removed, see Figure7.5.

- Etching: PO_2=385 W for 48 minutes (including intervals) (see Figure 7.5b).

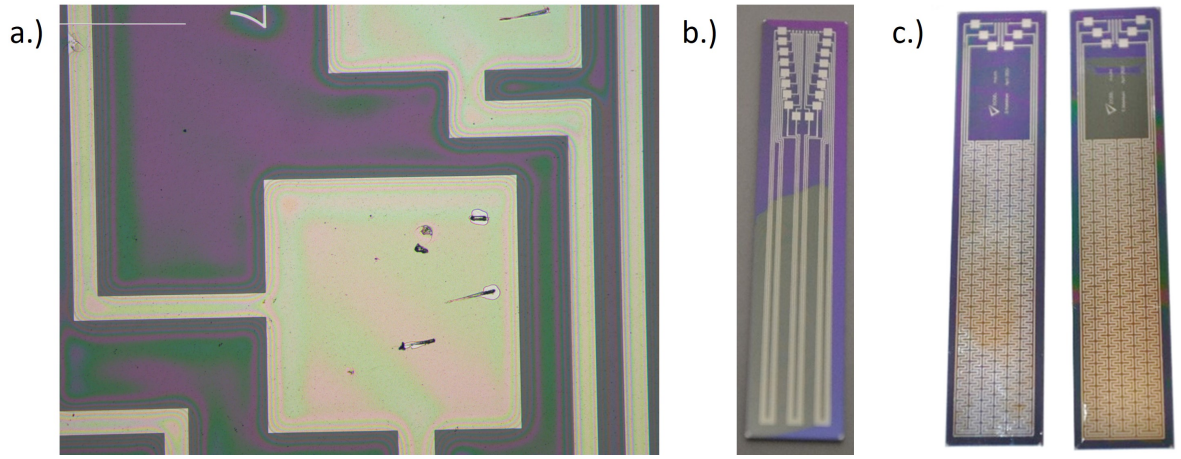

Figure 7.5: SU-8 results of layer removal tests. a.) SU-8 after an oxygen plasma etch time of 36 min. b.) SU-8 results after an oxygen plasma etch time of 48 min. c.) SU-8 results of cover test.

Silicon Nitride

The samples with a Si_3N_4 layer were etched in 24 seconds in a CF_4 plasma and compared with etching in BOE 5:1.

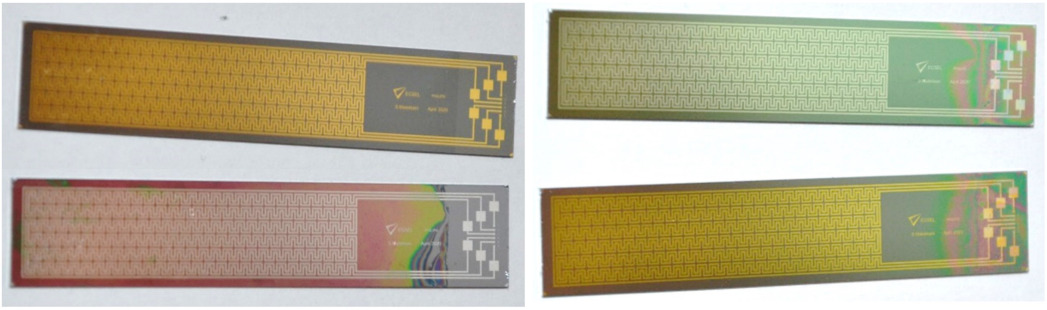

(a) Result of etching Si_3N_4 with BOE 5:1. **(b)** Result of etching Si_3N_4 for 24 seconds in the barrel.

Figure 7.6: Silicon Nitride etching of BOE compared to barrel.

7.5. Conclusions and discussion

In this chapter the chemical resistance of polyimide, BCB, SU-8, TMMR and parylene was tested for some of the most commonly used chemicals in microfabrication: Ethanol, PES, KOH, BOE 5:1 and PGMEA. Test samples were immersed in the chemical for a total of 70 to 95 hours and regularly inspected. All polymers were very resistent to ethanol, PES and PGMEA. BCB, Perminex and TMMR showed bubbles and delamination in KOH. None of the layers was long term resistant to BOE 5:1. After prolonged exposure, bubbles were observed in the layers, while perminex, parylene and SU-8 delaminated.

To be able to electrically test the samples for the hermiticity test, it was necessary to remove the polymer layers from the bondpads. To open these bondpads selectively, and because no suitable mask was available, the part of the sample containing the interdigitated tracks was covered with aluminum foil. In all cases the polymer could be etched in a barrel etcher using and oxygen plasma. Large differences in etching times were found. Surprisingly, it was found that there was a significant difference in etching behaviour if the polymer was deposited on aluminum or gold tracks. Also the surface area of the metal underneath the polymer appeared to influence the etch time. Interrupting the etching process in the barrel might result in a longer total etch time as compared to samples that are etched in one single run. This is caused by the differences in etching temperature when the etching process is interrupted. Although the results in this chapter give a first indication, to determine the optimum etching time, the experiments should be repeated with samples that are etched in a single run.

8

Cytotoxicity

8.1. Introduction

To test if the polymers are biocompatible and non-toxic, they need to be tested with a cell culture test. This chapter will begin by explaining the basic background knowledge of the cell lines for cytotoxocity studies and how these assays are performed. Furthermore, as in previous chapters, studies on the cytotoxicity of polymers will be called out, as they give us information on what we could expect from the experiments and results. Before the experiment started at TU Eindhoven (TU/e), a basic training on cell culturing was performed at TU Delft, which included practicing with pipets, prevention of contamination, and the basic cell culturing procedure. Followed by the execution of the experiment at TU/e. The protocol of the experiment will be explained in the method section of the chapter, along with the method of analysis.

8.2. Literature

In this section, an overview of the cytotoxicity protocols and the studies on the cytotoxicity of the polymers will be given. Since the cell line and the method of the assay are different from those prescribed in the ISO standard, information on this alternative method and cell line will also be provided. These are additional studies on the differences between this approach and the ISO standard.

8.2.1. Cytotoxicity protocol

During the cytotoxicity tests, ISO 10993-5 and ISO 10993-12 will be used. The conditions of dimensions to test polymers are specified in ISO standard 12, where it is stated that a material with a thickness of less than 0.5 mm requires an area of 6 cm2. This is because the thickness is thin enough to be extracted from the material. If the thickness of the material is more than 0.5 mm, it cannot be properly extracted. Another important ISO standard is ISO standard 10993-5, which defines the procedure for cytotoxicity testing. ISO Norm 5 is followed in the cytotoxicity testing procedure. According to ISO 10993, there are four types of protocols that qualify for an ISO biocompatibility test. To investigate cell viability, the so-called MTT procedure is applied, which works with cells called L929. The MTT procedure measures the metabolic activity of the cells and indicates their viability. However, in this project, a different substance than MTT will be used, as well as different types of cells, but the same test flow will be used as in the MTT assay according to the ISO standard. As stated in the introduction, MG63 cells were used; these are fibroblastic cells derived from human bone tissue. L929 cells, which are mouse fibroblasts, should be used to test for cytotoxicity, according to the protocol. The MG63 cell line is used to test the safety of acrylic bone cement extracts, mainly testing bone tissue-related innovations on cytotoxicity. Thus, since MG63 cells are also used for cytotoxicity tests on bone extracts, they can also be used in this case. In the next paragraph, the two types of cells and their differences will be discussed further.

Grade of severity
Cytotoxicity grade is distinguished by the amount of death over living cells. Qualitative analysis is performed when the morphology of the cells is investigated with the table as shown in Figure 8.1. This grading system will also be used to grade the cytotoxic severity of the polymers. A quantitative method is performed when there is a measurable parameter, for example, the number of cells before and after extracts. A material is called cytotoxic, when there is less than 30% cell viability.

Grade	Reactivity	Conditions and responses of all cell cultures
0	None	Discrete intracytoplasmatic granules, no cell lysis, no reduction of cell growth
1	Slight	Not more than 20% of the cells are round, loosely attached and without intracytoplasmatic granules, or show changes in morphology; occasional lysed cells are present; only slight growth inhibition observable.
2	Mild	Not more than 50 % of the cells are round, devoid of intracytoplasmatic granules, no extensive cell lysis, not more than 50 % growth inhibition observable.
3	Moderate	Not more than 70 % of the cell layers contain rounded cells or are lysed; cell layers not completely destroyed, but more than 50 % growth inhibition observable.
4	Severe	Nearly complete or complete destruction of the cell layers.

Figure 8.1: Grading cytotoxicity based on morphology.

MG 63 cell lines
During the experiment, an MG63 cell line will be used. In the previous subsection, it was mentioned that, according to protocol, an L929 cell line should be used. A different cell line, MG63, was employed instead because due to availability and experience at TU/e. This cell line is also used in cytotoxic experiments regarding implants that replace or interfere with bone tissues. However, there are quite a few differences between the L929 and the MG63 cells. The L929 cell lines are besides ISO norm cytotoxicity tests, also used in anti-cancer research. In the article of Ferreira et al. (2021) both cell lines, L929 and MG63, were used to investigate the cell viability [48]. From this, differences in results emerged as the concentration of their studied material increased. It was possible to arrive at a conclusion about cell viability despite these differences. It can therefore be said that using the MG63 cell does not provide the same results as the L929, but it could be comparable.

PrestoBlue Studies
The Prestoblue reagent has been compared with the MTT procedure, according to Invitrogen. During the comparison tests, one group of cells was loaded with Prestoblue for 10 minutes and the other group was loaded with MTT for 4 hours and a 16-hour solubilization step before readout. The conclusion was that both tests obtained a comparable EC_{50} value. EC_{50} stands for half maximal effective concentration, which measures the halfway response from baseline to maximum after an exposure time of the reagent. The benefit of the PrestoBlue however is the fact that the cells can be cultured again after the viability assay as it is a live cell assay and the MTT requires breaking down the membrane of the cell (cell lysis). It will not be discussed thoroughly how a cell's viability can be investigated without breaking them down. In short, PrestoBlue is a cell viability test that takes advantage of the property that cells reduce their environment in the cytosol to remain viable. The reduced power of the living cells can then be used to convert the blue-colored, non-fluorescent resazurin into the red-colored, fluorescent resorufin.

8.2.2. Cytotoxicity of polymer

SU-8
SU-8 has already been widely used in studies of biocompatibility. SU-8 can be called biocompatible and is already used for those applications. However, the application and processing of SU-8 can influence potential leaking effects. When the SU-8 has leakages it can cause toxic effects [49]. However, other studies say it may inhibit cell growth, but it will not be cytotoxic.

Polyimide
There are several types of polyimides that have also been studied for cytotoxicity. The PI2611 does not seem to have good viability for L929 fibroblasts on the surface of the PI film compared to another polyimide film, for example, KaptonHN [50] [51]. However, there is no proof of cytotoxicity.

Parylene-C
During a study of the biocompatibility of IDE chips, the cytotoxicity of the IDE chips was also examined [52]. Here, an extract was taken from the IDE chips containing both parylene-C and polyimide. To study cytotoxicity, the cell line L929 was used, using the gradation specifications of Table 8.1. In short, there is little information regarding the cytotoxicity of the polymers of interest for the cell line MG63. But with the L929 cell line, the following polymers are non-cytotoxic: SU-8, polyimide, and parylene-C. Thus, the only ones that have not been tested for cytotoxicity in literature studies are BCB and perminex.

BCB
There are no studies of BCB and its cytotoxicity test with the L929 cells as prescribed by the ISO standard. Photosensitive BCB has been tested for cytotoxicity and cell adhesion, however this was performed with Cyclotene 4026. In doing so, it was found that when deposited on silicon wafers, it had no negative effects on the cells 3T3 fibroblasts and t98-G glial cells in vitro. Furthermore, they were also not adherent to these cells [53].

In short, there is little information regarding the cytotoxicity of the polymers of interest for the cell line MG63. But with the L929 cell line, the following polymers are non-cytotoxic: SU-8, polyimide, and parylene-C. Thus, the only ones that have not been tested for cytotoxicity in literature studies are BCB and perminex.

8.3. Cell culturing training

To perform the cytotoxicity tests, training on the basic principles of cell culture was necessary. This was a 4-day training consisting of pipetting and the cell culture procedure taught by PhD student Maria Klimopoulou for the TU Delft 3ME. The taught cell culture procedure is similar to Day 2 and 3 of the protocol found in appendix E.

8.4. Experiments at TU/e

The cytotoxicity tests were performed at TU/e in collaboration with Ph.D. student Roel Kooi. Figure 8.2 shows a schematic representation of the experiment. Earlier it was mentioned that the ISO norm biocompatibility tests are performed with an MTT procedure, however, the TU/e used a different procedure with a Prestoblue reagent. The reagent has been compared with the MTT procedure, according to Invitrogen. During the comparison tests, one group of cells was loaded with Prestoblue for 10 minutes and the other group was loaded with MTT for 4 hours and a 16-hour solubilization step before readout. The conclusion was that both tests obtained a comparable EC_{50} value. EC_{50} stands for half maximal effective concentration, which measures the halfway response from baseline to maximum after an exposure time of the reagent. The benefit of the Prestoblue however is the fact that the cells can be cultured again after the viability assay as it is a live cell assay and the MTT requires breaking down the membrane of the cell (cell lysis). Therefore, it is possible to study the cells further if needed with Prestoblue.

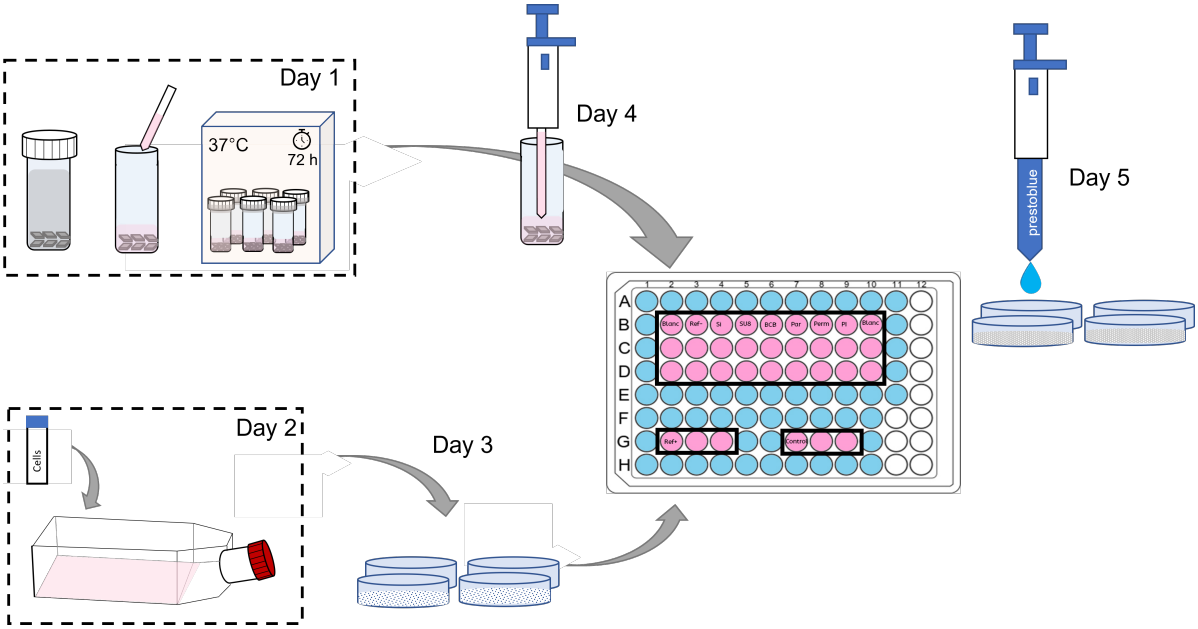

Figure 8.2: Schematic representation of the cytotoxicity test.

Day 1 is devoted to preparing the extracts. This involves breaking the samples into 1 by 1 cm squares and then sterilizing the tubes containing the samples. After that, the cell culture medium is then added, the lids are coated with parafilm, and the vials are put in the incubator for three days at 37 °C. On day 2, the cells were prepared for proliferation in a flask. This is done by removing them from the vial, rinsing them, and centrifuging them. Then the pallet of cells resulting from the centrifuge is mixed with fresh medium. This is mixed, and then the bottom plate of the flask is covered with the cells. After 24 hours, the cells have multiplied and, after being detached from the soil, can be distributed on a cell plate. This requires several thorough steps that can be seen in Appendix E. Here, however, mainly the calculation and cell count will be named. To obtain good results, the number of cells used is important. If the number of cells is too low, too many dead cells may appear, and the difference cannot be compared. When the number of cells is too high, the plate reader may no longer be able to read the values. The use of the plate reader can be read in Section 8.4.4.

8.4.1. Week 2

Given the fact that there were unreliable results, in which the reference materials had not obtained the required values relative to the blanks, the experiment was conducted a second time. In the second week the procedure was reproduced, but with some adjustments due to the result of the previous week (which will be mentioned in the next section **sec:Cytotox_results**. Since a UV with a wavelength of around 300 nm can break down particles, the UV sterilization step was skipped. When these particles are broken down, they would normally be washed away with ethanol, but since the suction tips were the same it could have influenced the results. Especially with the toxic reference. Thus, another adaption on day 1 was using different suction tips in each of the vials. Another adaption was on day 3 when more cells were used. Instead of 5.000 cells, 7.500 cells per cm^2 were used. When applying the steps to count the number of cells in the supernatant, it resulted in the following: $9.5 \cdot 10^4$ cells/mL, which were diluted and is in 3mL, therefore, the total amount is 285.000 cells per milliliter. This was then calculated to get around 7500 cells per well distributed over 33 wells.

Furthermore, the wells and their relevant materials were classified differently. For this reason, wells B2 until D9 and G2-4 and G8 were with cells. On day 4 100 µL of the extract was added and the materials in the wells were differently distributed compared to the first week (see figure E.2b). There was more room between the positive reference material and the sample materials to prevent the influence of evaporation. On day 5 the goal stayed the same, adding Prestoblue, incubating, and scanning with a plate reader. The difference is that a snake pipetting pattern was applied when adding the Prestoblue, to prevent contaminations from the sleeve onto the wells. In essence, this should not make any difference from potentially reading a higher value at short incubation times.

8.4.2. Week 3

In the third week, the cytotoxicity tests were performed by the supervising Ph.D. student due to time issues. Furthermore, there were changes regarding the sterilization of the samples once again. This time the vials and caps were sterilized with UV before usage for 15 minutes.

8.4.3. Plate reader information

The wells plate can be read out with a plate reader. The plate reader used during these tests is the synergy HTX (see figure 8.3), where the well plate is placed into the machine the same way as a Compact Disk (CD) into a CD player. After programming which wells, it must check the fluorescent intensity and absorption spectrum of each of the wells. The fluorescence is caused by the resazurin development. PrestoBlue works with resazurin, a blue reagent that is non-fluorescent and cell permeable. Living cells have a reduced environment for survival. When resazurin enters a cell, it is converted to resorufin, a red fluorescent substance. Thus, the viable cells will absorb the resazurin and create fluorescence. The fluorescence values of the plate reader show the cell viability. This does not indicate a toxicity value right away, for this, the photos must be studied and analyzed to see if the cells are evenly sown over all the wells. Figure 8.4 shows schematically how resazurin development proceeds. Three lines have been sketched, which represent possible different phases of a cell. In addition, it is undesirable if the entire resazurin has already been developed. That is why the time interval is important and it should not be too late, but should take place in the interval of interest. Hence the fluorescence examined after 15 and 30 minutes of incubation.

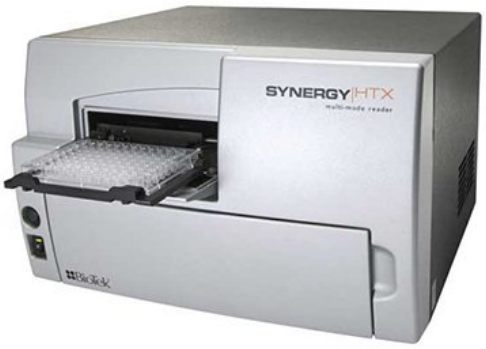

Figure 8.3: Plate reader [54].

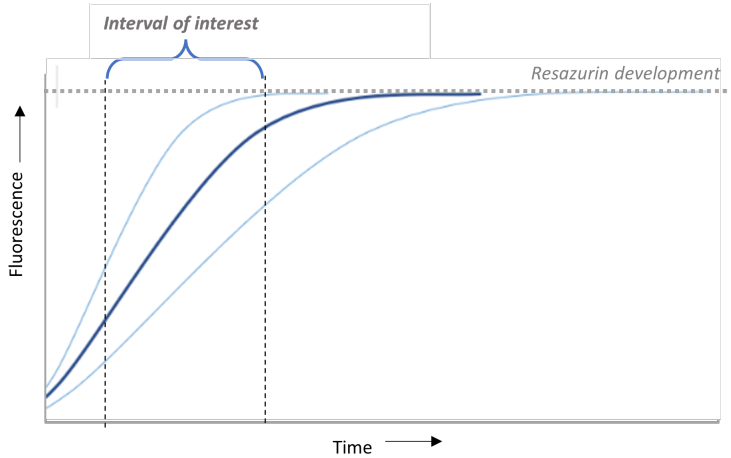

Figure 8.4: Schematic representation of resazurin development range for different cells.

8.4.4. Analyzing

To gain more insight into the viability of the plate reader results, these values must be analyzed with the number of cells per well before and after exposure to extraction. To get the number of cells, these cells must be counted manually. This was performed with a utility of ImageJ called a cell counter, see Figure 8.5. It allows us to click on each individual cell and count the cells that are clicked on, including the coordinates of each click. These coordinates were only used to check the spread of all the cells over the wells.

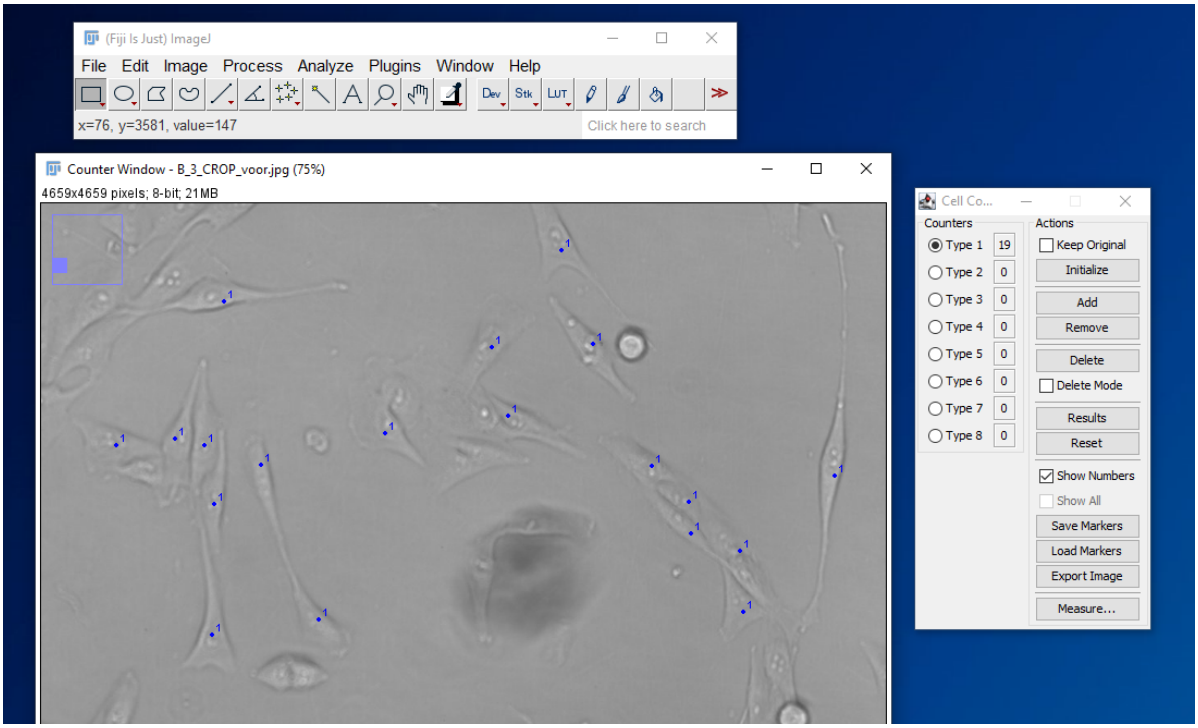

Figure 8.5: In the image one can see the markers on the living cells on parts of a well. These images are created with a phase contrast microscope.

8.5. Results

In this section, only the results of the third week will be discussed in detail since here the values of the reference materials were correct. The results of the previous two weeks are not considered in this section. The Prestoblue was incubated for 15 and 30 minutes, which are the time intervals to read the well plate with the plate reader. Figure 8.6 shows the tables with the fluorescent values of the wells in arbitrary units as received from the plate reader. However, fluorescence values indicate cell viability. Thus, this value also depends on the number of cells per well. Although efforts were made to keep the number of cells per well the same, it is inevitable that the amount of cells changes. This is because it does not have to be completely homogeneously distributed even though you mix them it is also because the cells continue to divide. At first glance, the values at SU-8 and parylene are quite low. For correct reference values, the positive reference must have a value of 70% less than the blanks. Furthermore, the differences between the blanks must differ by less than 15%.

	1	2	3	4	5	6	7	8	9	10	11	12	
A		**Blank**	**RM-**	**Si**	**SU8**	**BCB**	**Paryleen**	**Perminex**	**PI**	**Blank**			
B		156	132	140	67	110	59	125	100	149			
C		159	118	149	67	95	64	118	79	126			
D		146	120	143	62	104	59	117	85	152			
E	*average*	*153,667*	*123,333*	*144*	*65,3333*	*103*	*60,6667*	*120*	*88*	*142,333*			
F		**RM+**					**Cell control**						
G		27	26	25			165	175	174				
H	*average*	*26*					*171,333*						

15 min

(a) Results after 15minutes of incubation time.

	1	2	3	4	5	6	7	8	9	10	11	12	
A		**Blank**	**RM-**	**Si**	**SU8**	**BCB**	**Paryleen**	**Perminex**	**PI**	**Blank**			
B		391	335	348	150	258	132	304	234	351			
C		362	287	353	142	217	135	282	188	316			
D		345	294	349	139	240	123	277	194	332			
E	*average*	*366*	*305*	*350*	*144*	*238*	*130*	*288*	*205*	*333*			
F		**RM+**					**Cell control**						
G		42	43	42			386	406	406				
H	*average*	*42*					*399*						

30 min

(b) Results after 30 minutes of incubation time.

Figure 8.6: The tables above show the fluorescent values after an incubation time of 15min (a) and 30min (b). When the value is close to the values of the blanks, there is normal cell viability.

Images of the wells were made, with a phase contrast microscope, before the cells were exposed to the extracts of the material and 24h after the exposure. Figure 8.7a shows one of the blank wells. These blanks only consisted of cell medium also incubated for three days same time as all the other extracts. The cells have proliferated within those 24 hours. The other blank wells show similar cell proliferation patterns. When compared to the wells with other extracts, a differences in cell growth is apparent. If fewer cells are present compared to the blank extracts, there is inhibition of cell growth. If there is still a growth of cells compared to the blank wells, but more dead cells are present there is cytotoxicity. Looking at the wells containing the SU-8 Figure 8.8b and parylene-C Figure 8.8c extracts, there is a low amount of cells present compared to the wells of the blanks. So, in these extracts, there is an inhibition of cell growth, especially when compared to the other extracts. There the number of cells did increase visibly with BCB, perminex, and polyimide.

Resulting in the viability percentages seen in Table 8.2 According to the ISO standard, viabilities lower than 70% of the blanks are cytotoxic. Which are calculated with the formula:

$$Viability[\%] = \frac{100 * OD_{sample}}{OD_{blank}} \tag{8.1}$$

In the equation, OD stands for the mean measured optical density. Where the optical density of the samples were compared with the blanks. To study if it causes cytotoxicity, the number of cells per well must be counted manually. The assumption was that the number of cells in each well would be the same. But because cells continue to divide continuously, the number of cells may vary between

		Blank	RM-	Si	SU-8	BCB	Paryleen	Perminex	PI	Blank	RM+	ctrl
Alive	Before	666	623	619	692	813	672	684	737	697	729	798
	After	1795	1257	1569	664	1126	582	1287	1038	1531	663	1689
	Growth	1129	634	950	-28	313	-90	603	301	834	-66	1689
Dead	Before	79	93	97	74	91	77	72	89	83	106	107
	After	95	70	74	156	61	250	54	85	86	124	156
	Growth	16	-23	-23	82	-30	173	-18	-4	3	18	156

Table 8.1: Overview of the cells counted in a quarter of a well before and after extraction to the material. Per polymer there were three wells.

	Blank	RM-	Si	SU8	BCB	Paryleen	Perminex	PI	RM+	Cell control
Viability	100	79,13	83,38	44,61	86,05	38,15	82,27	70,91	18,94	126,69

Table 8.2: Overview of the viability of the materials relative to the blanks.

wells. Table 8.1 shows the number of cells counted in a quart well, from before and after exposure until the extraction of the materials. Here it can be seen that with SU-8, parylene, and the positive reference, there is a decrease in the number of live cells. However, the number of dead cells increased significantly in these extractions. This would imply that not only is cell growth stopped but also that it appears to have cytotoxic effects.

8.6. Conclusion and discussion

With the aim of performing cytotoxicity test to study the polymers response, it could be stated that two polymers currently appear to be positive for a cytotoxic response to MG63 cells and adverse effects. It is difficult to obtain an unambiguous conclusion from the cytotoxicity tests. Reproducing the test proved more difficult than expected. It was initially hypothesized that inexperience might be a factor for the variable and unexpected results in the first weeks. Partly for that reason and for reasons of time efficiency, the test was performed in the third week by the PhD student who was more experienced with the process. Although the results are slightly different, it is remarkable that polymers with adverse effects on cells are already widely adopted.

Normally it is customary to prepare an extract of the part to be tested. Since it was not possible to peel off the polymer for these thin layers, silicon was taken into account from the second week.

Results

The positive reference in the second week had a good value but was not in proportion to the other material results. This is mainly because the values of the blanks and the value of the negative reference relative to the blanks are too diverse. The blanks should have a maximum difference of 15% with respect to each other. Furthermore, we see that the number of cells in the cell control is much more than for the other cells, causing a higher value in fluorescence, thus more cell viability. The cause of these inconsistent results is not clear. Since the cells looked good overall until the addition of the extracts, it could be because they experienced problems with sterility. If there was a pipetting error or an error with the sterility of the pipette tips, it was noticeable using the pipette in subsequent wells. Since no pattern could be recognized in this, it is not clear what the cause could be. The number of cells differed per well, however, the cells that were counted were not from the entire well, with the accessible microscope it was difficult to take pictures and count them. However, it does involve the same area in and of a well. The negative reference and the blank should not differ more than 15%, in addition, these values should differ by 70% from the positive reference.

Limitations

- Different researcher in week 3;
- Experience in counting cells is different with a cell biologist, which could cause in-differences;
- Amount of cells in week 1 was counted with microscopic images, but due to unavailability of the phase-contrast microscope it was more difficult to count;
- Inhibition of cell growth visible, not known if this is also polymer process dependent;
- Results do not synchronize with the literature;
- Re-suspend and mixing the cells while pipetting them in the wells was unknown due to lack of lab experience.

Compared with literature

The literature mainly reported that these materials would not present cytotoxicity. With the exception of perminex, because there were no studies conducted on it regarding cytotoxicity. It was mentioned that there are possible leakages with SU-8 that could have toxic effects but this was not immediately apparent in the results. It was also found that SU-8 and parylene could cause possible inhibitions of growth. However, in the studies with the L929 cells, the results showed that these polymers would not have any negative effects. In this case, they did. A different cell line was used here, but it does seem to have adverse effects.

Future works

To investigate whether the polymers do in fact have adverse effects on cells, an alternative cell line can be used. Preferably the cell line recommended in the ISO standard. Furthermore, the use of Prestoblue is fairly new and the MTT test can also be used. It might be best to use the same extracts and perform tests in both of them, allowing at least a conclusion on that matter. Furthermore, a polymer on a silicon wafer has been used as samples.

There can also be a further analysis of growth inhibition. The blanks show what the normal growth is after 24 hours and even after 48 hours a formula can be drawn up. It can then be compared to the growth of the other materials, mainly SU-8 and parylene-C. With this approach one can visualize the potential growth inhibition of the polymers. Subsequently, the fluorescence value and thus the cell viability can be normalized.

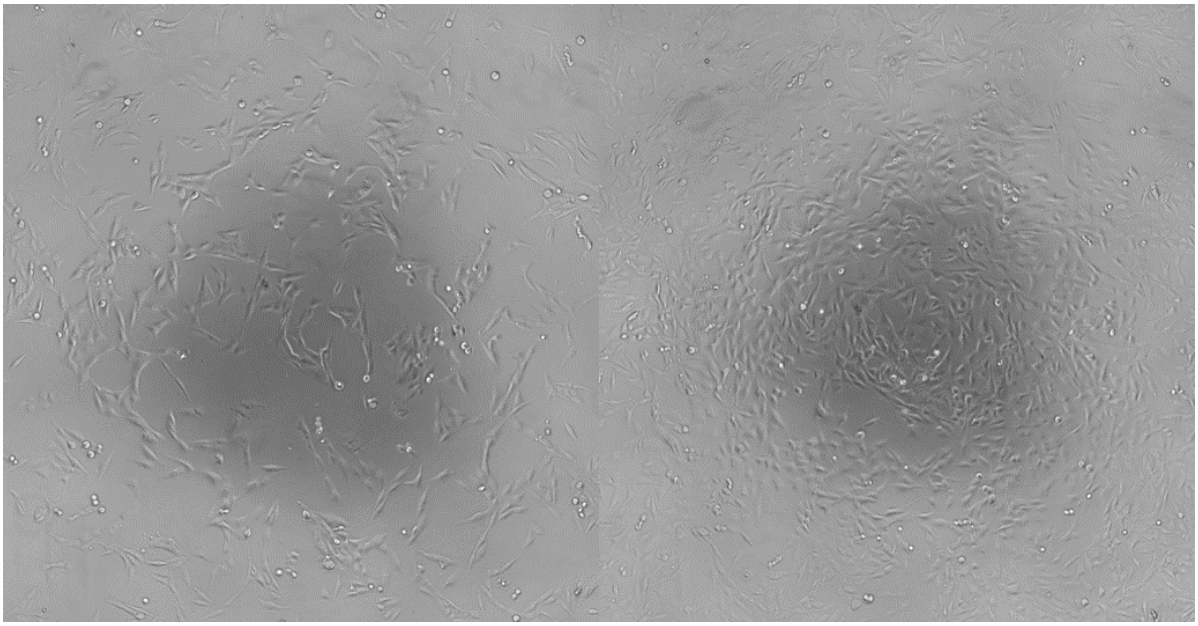

(a) Blank well (B2)

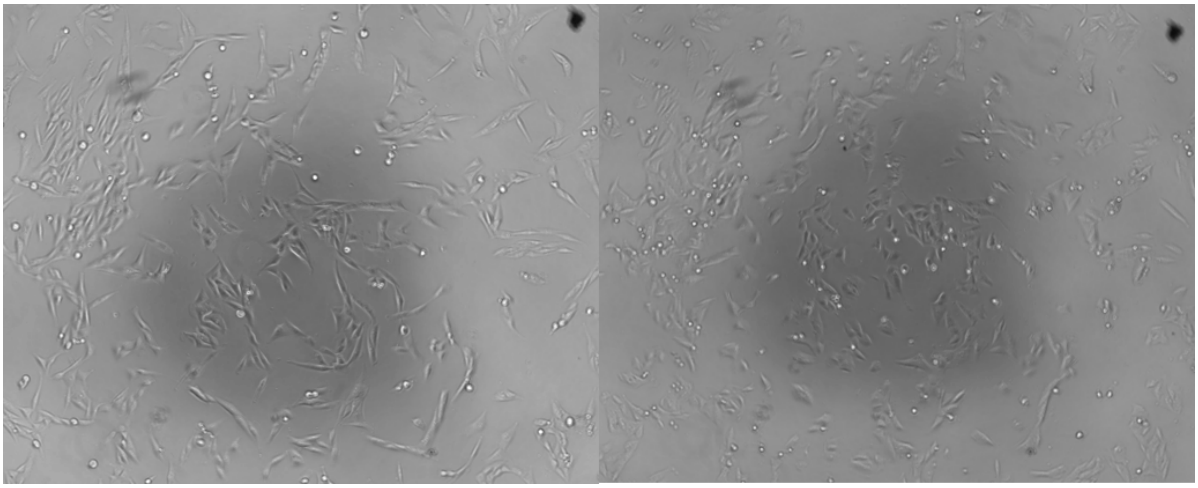

(b) SU-8 well (B5)

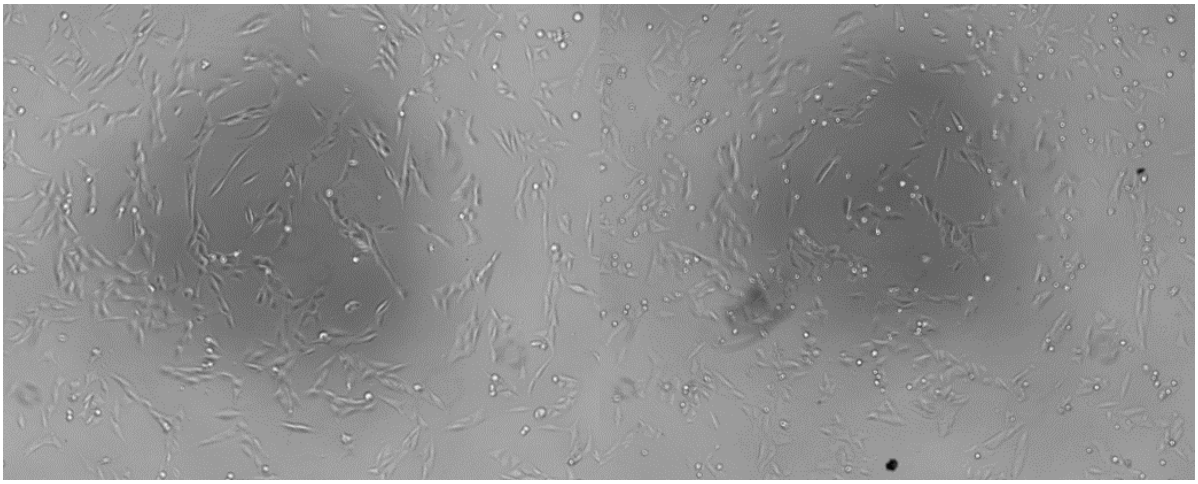

(c) Parylene-C well (B7)

Figure 8.7: Cells in a well, before and after the extract exposure.

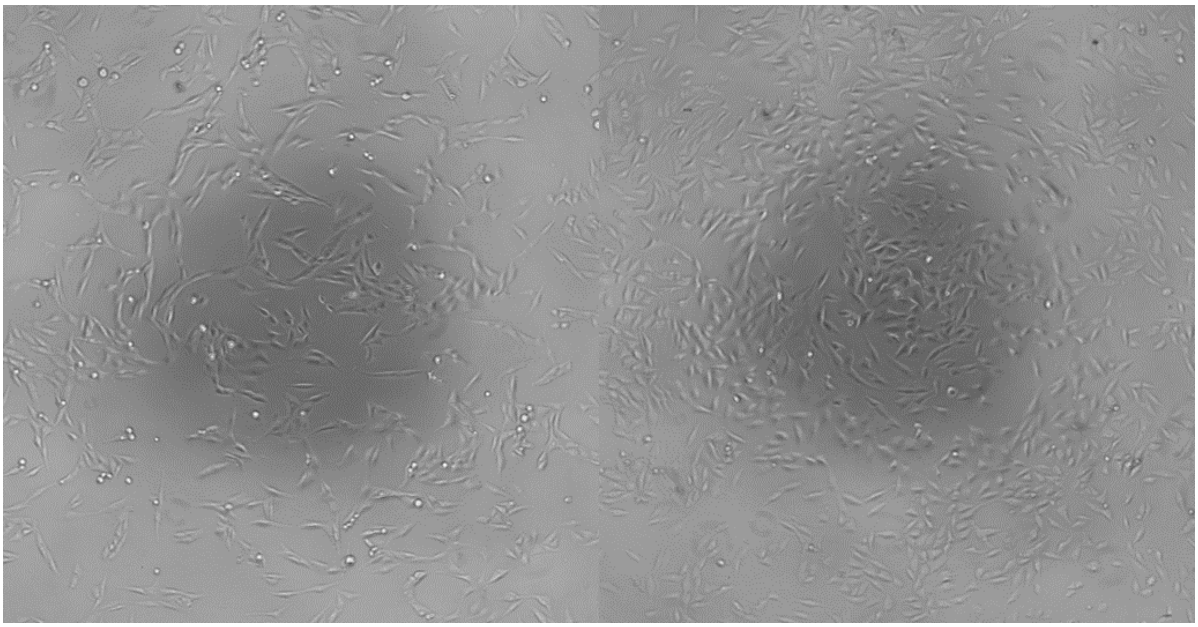

(a) BCB well (B6)

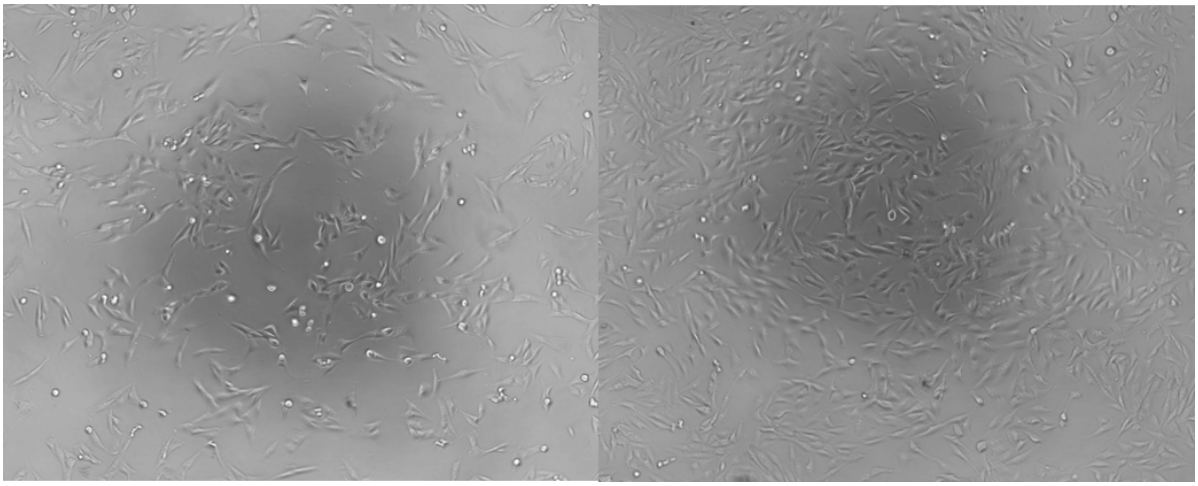

(b) Perminex well (B8)

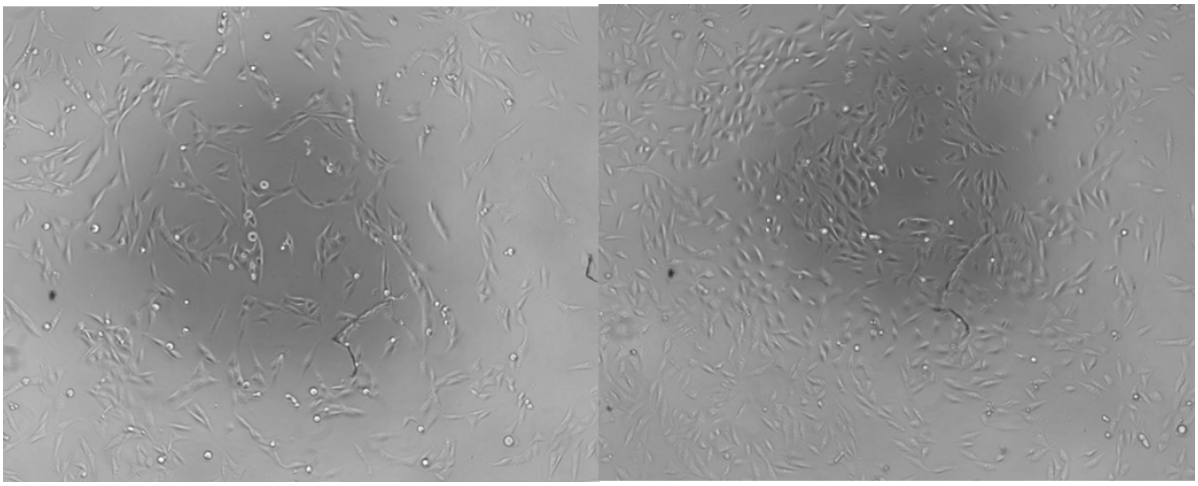

(c) Polyimide well (B9)

Figure 8.8: Cells in a well, before and after the extract exposure. These do not show a visible cell growth inhibition or cytotoxicity.

9

Discussion and conclusion

Throughout the report, there were intermediate discussions and conclusions covering a more in-depth discussion regarding the interpretation of the results, limitations, and possible other ways to investigate the specific topic further. This chapter will discuss the entire study with key findings, obstacles, and other discussion points.
It should be mentioned that some polymer characteristics can be modulated based on the production process that the polymers follow. In this case, only the processing steps that are currently used by the company and/or are recommended by the manufacturer were conducted. There are studies on creating enhanced biocompatibility with surface modifications, which can be used besides the results from this report to perform further studies on the desired polymer. In this research, the surface of the polymers has also been looked at, but no in-depth research has been performed on modulating the production process to improve biocompatibility. This was not possible due to the short time frame. Furthermore, a basic reference is needed to know the current status of the biocompatibility of polymers.

Summarized results
Based on the optical characteristics, the blank wafer with SU-8 and parylene is most suitable for low fluorescence. These low fluorescent values are in the desired range of wavelengths of 500 to 550 nm. Furthermore, a fast transmission would be an advantage. Polyimide has the least favorable transmissions, with a higher absorbance between 400 and 550 nm compared to BCB, SU-8, and perminex.
The surface characteristics showed that perminex has the most favorable contact angle and therefore has a hydrophilic surface, resulting in fewer biomolecules adhering. However, the hermeticity studies showed that perminex exhibited a less favorable reaction, with parts of the polymer degrading during saline soaking. BCB on gold also did not yield the best results, as a fracture was noticeable. However, when considering cytotoxicity, these polymers were favorable. Thereby, it was shown that SU-8 and parylene caused adverse effects in these experiments.

Future works
As there are results with inconclusive endings mentioned, there are opportunities towards follow-up research. A suggestion would be on a specific application. From multiple results, it was visible that the application has an influence on biocompatibility. Sure, there are many ways to enhance the biocompatibility and test the separate materials, but one should not forget that the cytotoxicity does not show a yes/no cytotoxic effect when used *in-vitro*.

Conclusion
To answer the question: ”How biocompatible are the polymers that can be used for BioMEMS processing at Philips MEMS foundry during an *in-vitro* situation compared to SU-8?”, it depends on the applications. But on optical-, surface- characteristics, cytotoxicity and adhesion there are polymers, which only require the basic processing steps to get a better or more desired result compared to the other polymers.

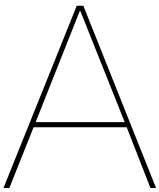

Wavelengths of proteins and dyes

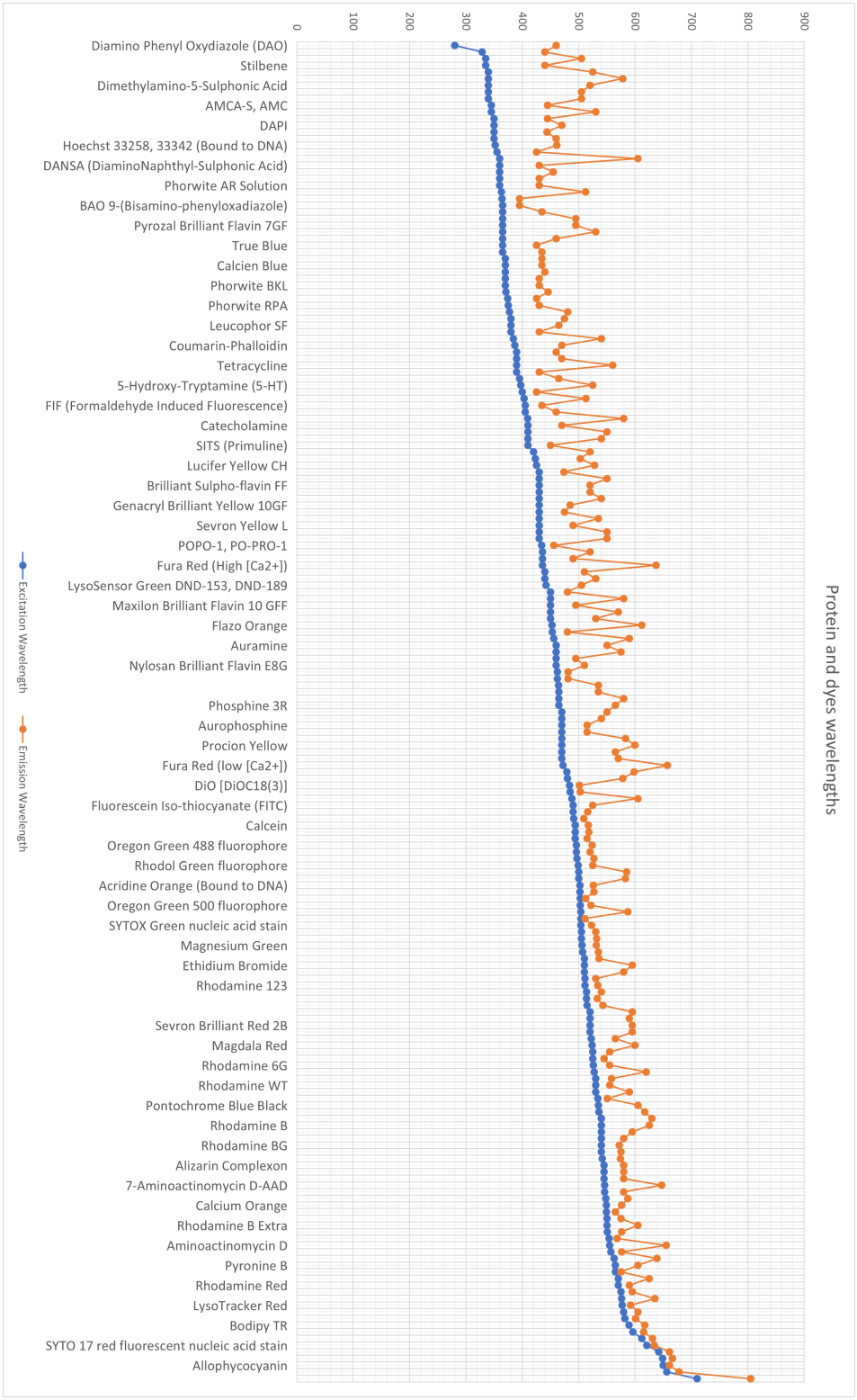

Figure A.1: Protein and Dyes excitation and emission levels in wavelength.

B

Polymer samples

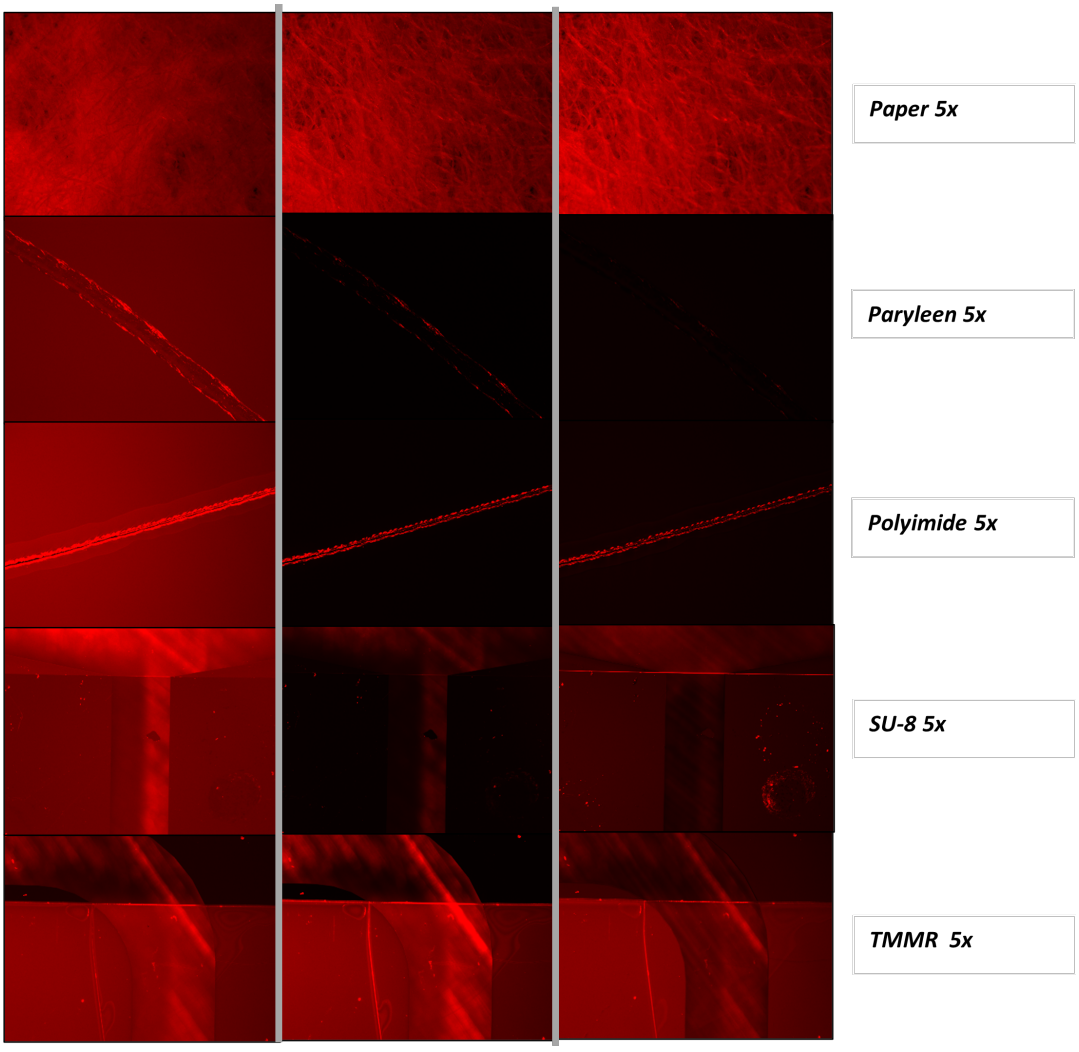

Photos of microscope with visibility on the fluorescent parts. From left to right column of images: λ_{em}=400nm, 510nm, 580nm

C

Hermeticity progression

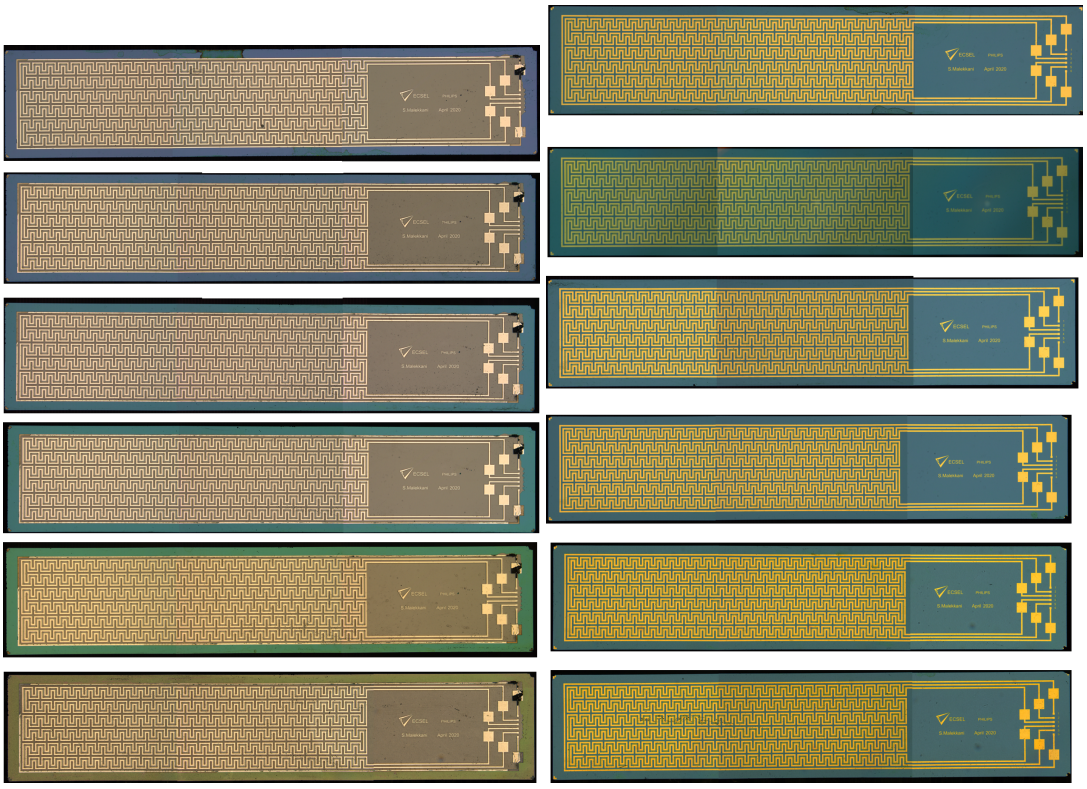

(a) SU-8 aluminum **(b)** SU-8 gold

Figure C.1: SU-8 progression over 6 weeks.

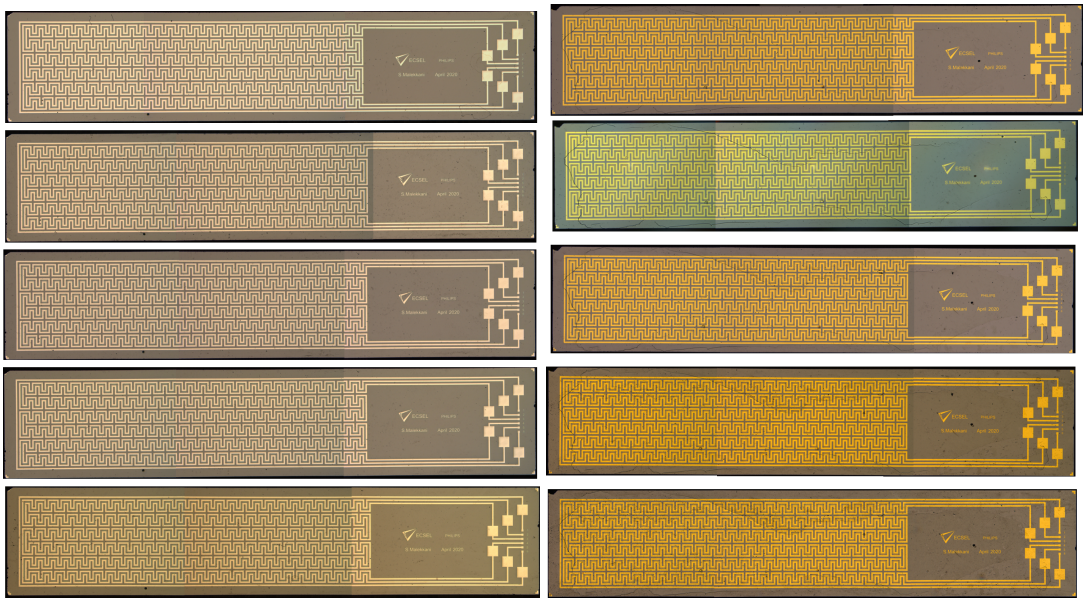

(a) BCB aluminum **(b)** BCB AU

Figure C.2: BCB progression over 6 weeks.

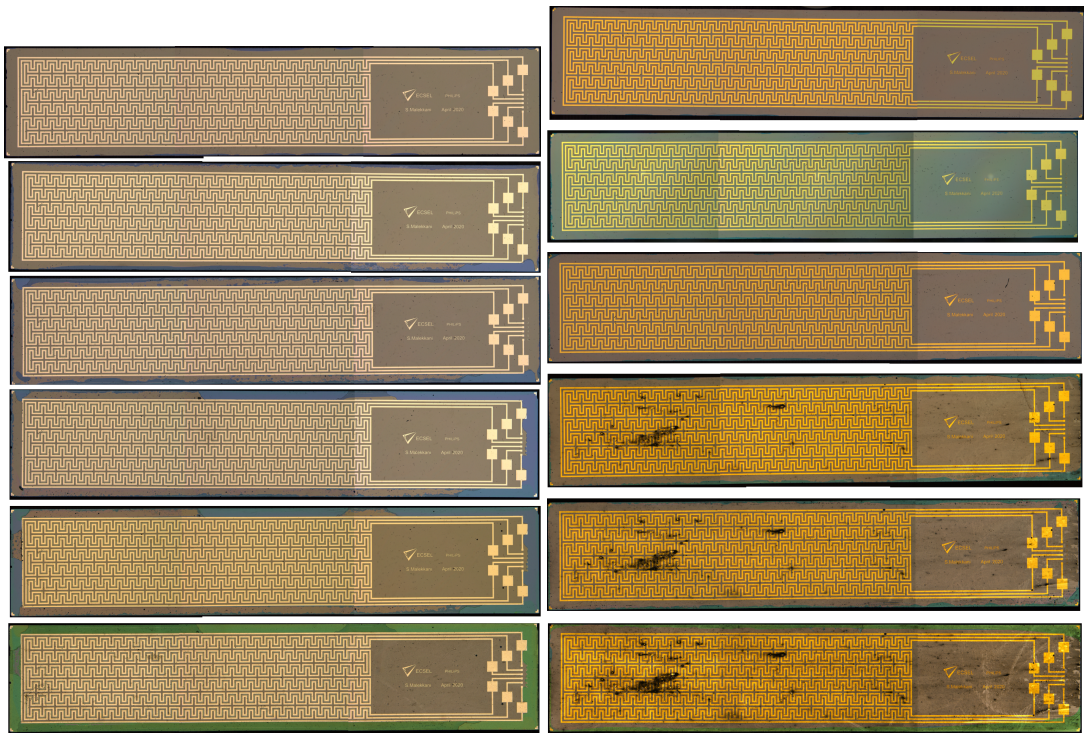

(a) Perminex aluminum **(b)** Perminex AU

Figure C.3: Perminex progression over 6 weeks.

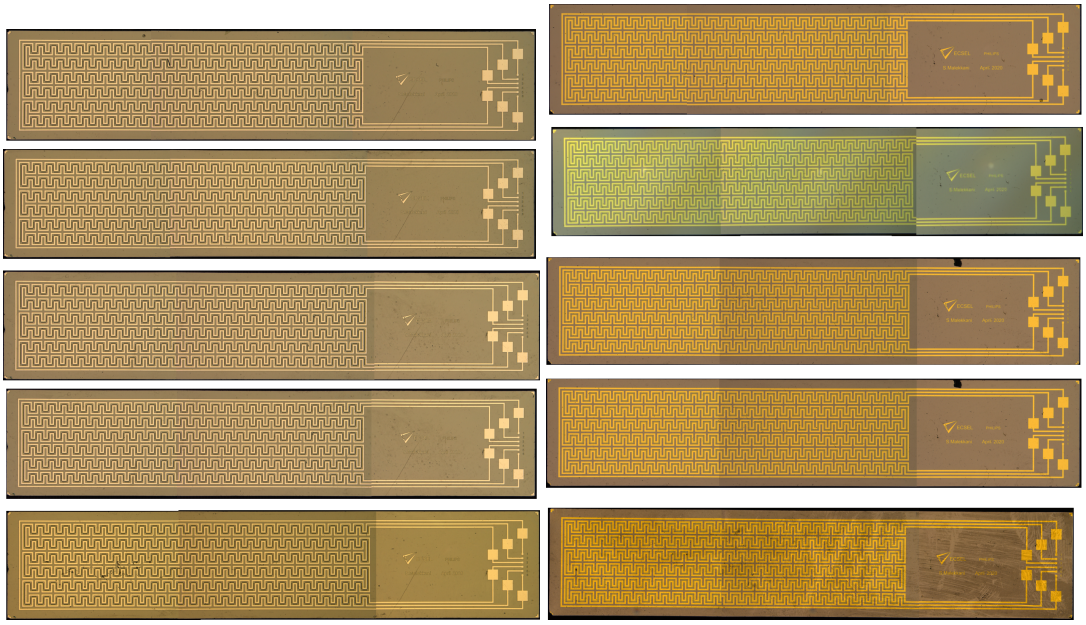

(a) PI aluminum

(b) PI AU

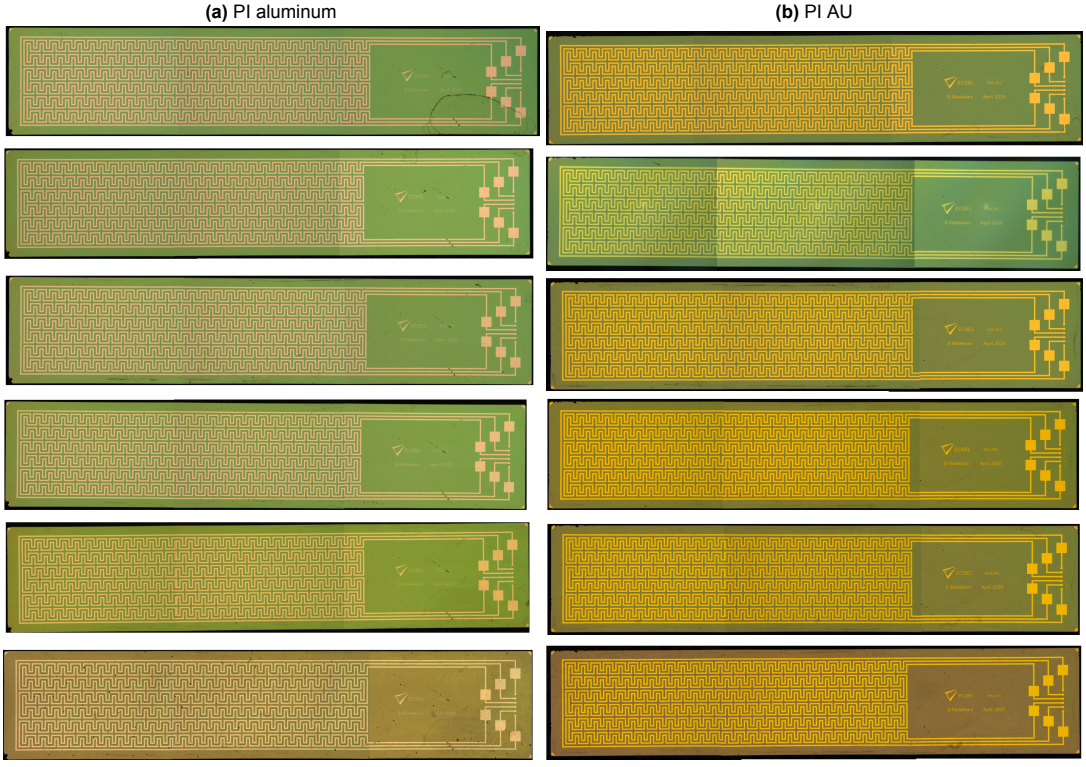

(c) SiN aluminum

(d) SiN AU

D

Layer etching sample results

Layer	Barrel settings	Result photo	Result
SiN	5min N2 2min CF4	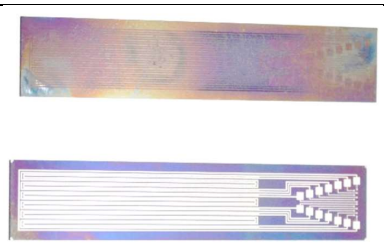	Layer completely removed. But with the gold tracks, there is more damaged; gold is gone
	5 min N2 30s CF4	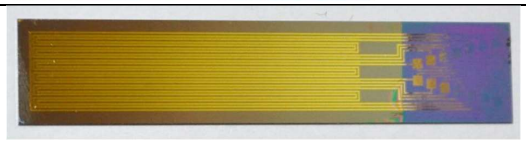	The heat after 5min of heating is still too warm, removing the gold.
	30s CF4		Not everywhere conduction
Si_3N_4	30s	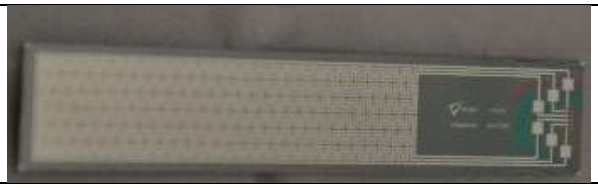	Conduction on aluminum bondpads

	4x 30s +1,5min +3min +6min	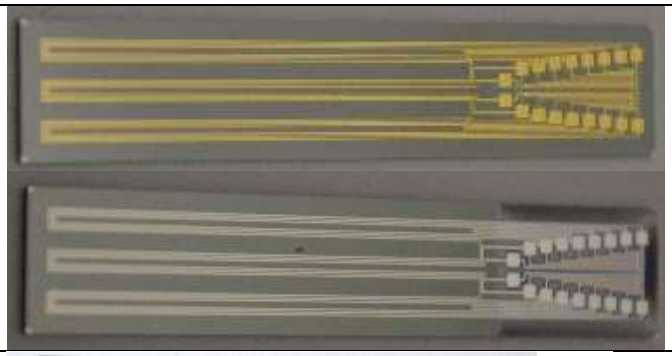	No conduction on gold tracks. Conduction on aluminum tracks.
	2min N_2 0.4 min CF_4	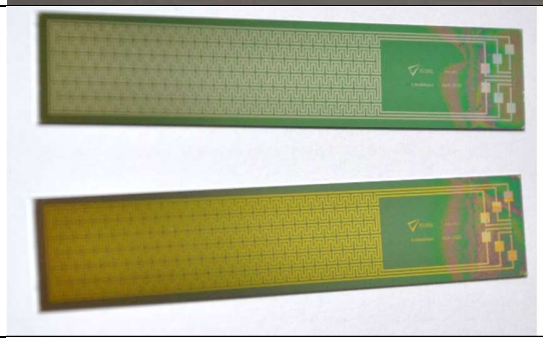	Conduction present. bondpads free from silicon nitride
BCB			The temperature of the barrel has a significant effect on the gold removal. As seen, the aluminum is still there while the gold bondpads are vanished.
	10+10+4+5.4+4+4 10+10+4+4+4+10		It is also dependent of the samples, how long it takes to remove the polymer from the bondpads.

SU8			For the SU-8 it was possible to remove the layer around the bondpads. But during this test, also the covering was tested. Surprisingly, Aluminum covering with polyimide tape, caused a worse result compared to only aluminum covering
SU-8	P O2= 385W T=10,6,6,10,14,12 min P N2=370W Heat time =5min till 102 P_O2 T=30min	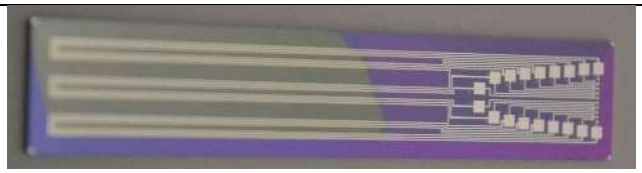	
Perminex	P O2= 385W T=10,6,6,10,14,12 min P N2=370W Time= 2min to T=70 P395W for t=20min	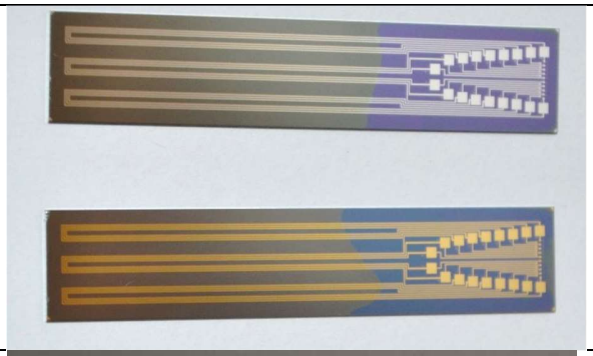	Still, most of the tracks are still covered with Perminex, and the bondpads are uncovered.
Polyimide	P O2= 385W T=10,6,6,10,14,12 min P N2=370W Time= 2min to T=70 P395W for t=20min T=15+20+20+20+18+8 AL=Tnew+10+5	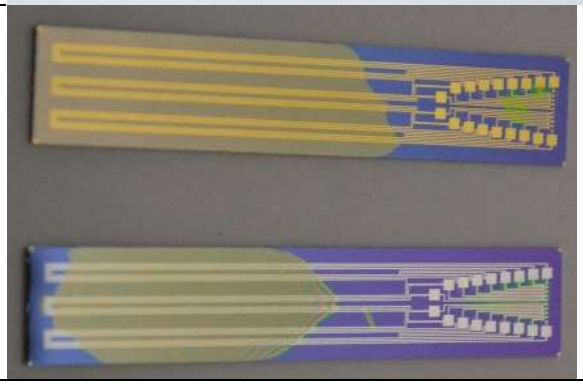	To remove the bondpads with the polyimide, also part of the tracks got uncovered. Even though this was covers with aluminum foil and PI tape

E

Cell culture procedure

Materials:

- Cells: cells of interest are in a vial or a flask.
- Trypsin: is an enzyme used to detach the cells from the bottom of the flask (re-suspend).
- Cell medium: to get the cells back in their surroundings.
- Tubes & vials
- Pipets: micropipettes and suction pipets.
- Microscope: to examine the cells.
- Centrifuge: spinning supernatant to get a compact suspension of cells at the bottom of a tube.
- PBS: Phosphate buffered saline to rinse the cells.
- 96-wells plate: a transparent case with wells to put the cells in and add the extracts.
- HTX plate reader: Device reading the fluorescence of the wells plate.
- Image J: software plugin to analyze the photos of the (phase-contrast) microscope.
- Phase-contrast microscope: Creates an image of one well, were it first takes 25 photos per well.

E.0.1. Protocol

Day 1: polymer extraction

- Total area of the samples is 6 cm^2/mL.
- Break them into even smaller pieces to fit into the tubes.
- Bring the samples into the glass tubes in the Bio cabinet (first clean with ethanol).
- UV light.
- Keep them in UV for 20min.
- Fill them with 1 mL ethanol, also to see if all polymers can fit in 1 mL for a later step.
- Leave them in the ethanol for at least 15 minutes to sterilize them.
- Then remove the ethanol with a suction device.
- Fill the vials with 1 mL of cell medium.
- Seal them with parafilm and put them in the incubator for 72 hours.

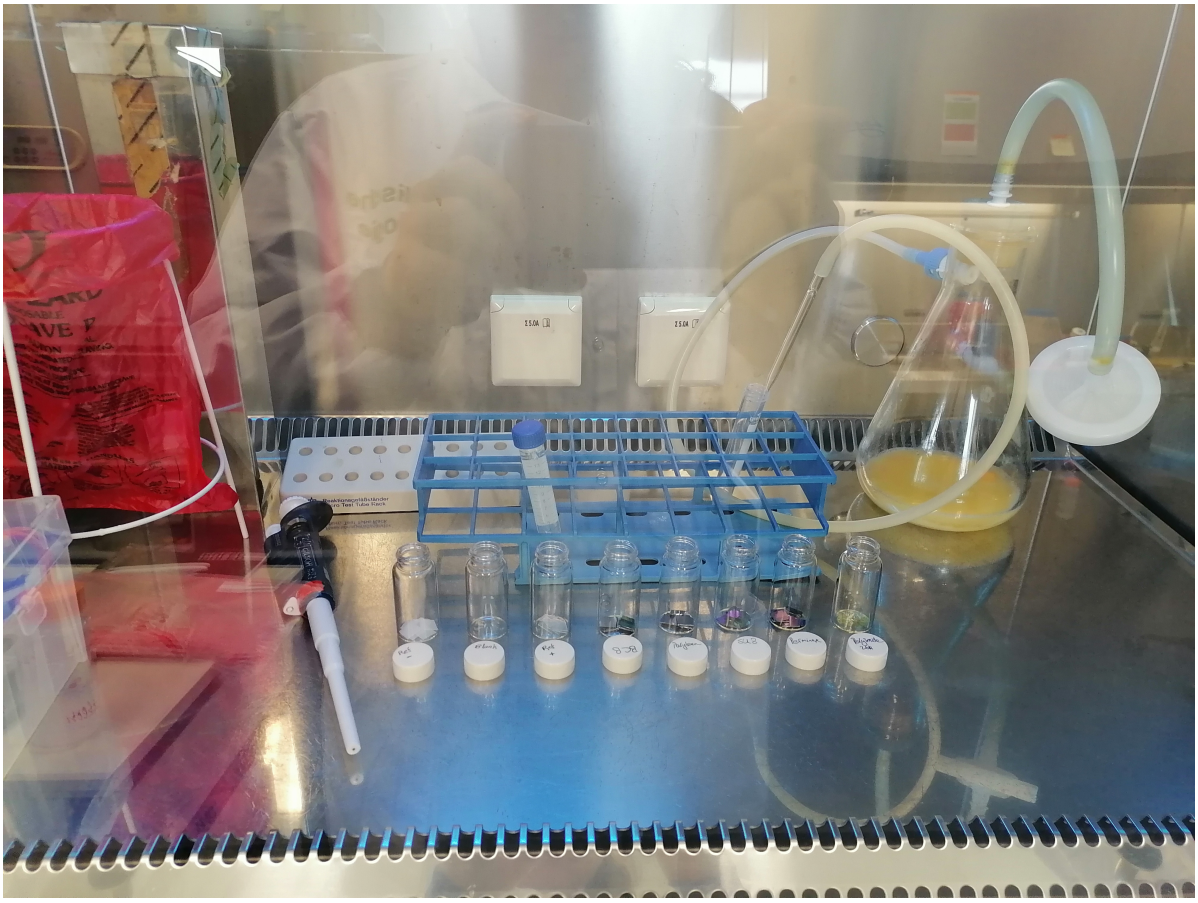

Figure E.1: Sterilization with UV, followed by ethanol.

Day 2: cells from freezer to flask

- Cell medium in waterbath.
- Prepare and clean the pipets.
- Get the cells from the freezer.
- Put them in the waterbath.
- Wipe everything with ethanol.
- Add cells to the medium.
- Rinse the cell vial twice to get all leftover cells as well.
- Adjust volume by adding medium until 10 ml
- Spin the cells in the centrifuge 7 minutes at 130 G.
- Pallet has formed. Remove the medium
- Re-suspend cells with 1 mL medium.
- Pipet an amount of the cells with medium into a flask and cover the bottom plate.

Day 3: cells from flask to wells

- Clean everything with ethanol, the space and the things that go in the closet;
- Check the cells in the flask, inspect the spaces of the cells and presence of dead cells;
- Rinse the cells with PBS, doing this so that the dead cells that float are washed away. For rinsing with PBS, use ½ of the medium. In this case it concerns 2.5 ml PBS;
- Now the cells are dry. Add trypsin to dislodge the cells previously stuck to the bottom by removing the wires. The ammount of trypsin is 1 mL;
- Put the flask with the trypsin in the incubator for 2 min;
- After the 2 min: Check if most cells are floating, if not give the flask a tap;

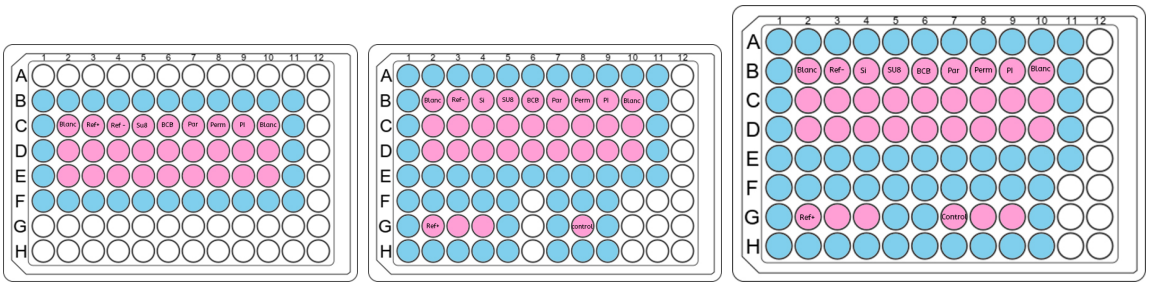

(a) well plate week 1 **(b)** well plate week 2 **(c)** well plate week 3

- Then add cell medium to inactivate the trypsin. The ammount of trypsin is 5 mL;
- Mix it all;
- Then pick up all the flask with the pipette boy and put it in a tube;
- The tube is centrifuged at 130 G for 7 min;
- The result is a pallet;
- Then remove the medium with suction device;
- Add 3 mL medium and make it homogeneous;
- Take 50 μL and put it in an Eppendorf tube;
- Go to the nucleocounter, drop the substance in the Eppendorf tube, then put the chip in the tube and place the chip in the nucleocounter;
- Result = $4.7 \cdot 10^4$ cells/mL;
- Since it is diluted 3x with the medium, we have 3x as many cells. So in total we have 3 x 47,000 = 141,000 cells/mL;
- Fill the cells with 0.34 mL suspension + 2.66 mL cell medium to get 3 mL.

Day 4: add extracts to wells

- Get the wells out of the incubator.
- Check the cells under the microscope and take the photo's.
- Suction all the medium out of the wells, the cells are now on the bottom of the well.
- Add 90 μL extract to the coherent wells.
- Put The well plate back in the incubator for a day.

Day 5: Time for PrestoBlue

- Add 10 μL Prestoblue this could be in a row pattern or in a snake pattern.
- Incubate the plate for at least 15 min. at 37 °C.
- Set the plate reader ready and put the cell plate into the plate reader.

Bibliography

[1] P. engineering solutions, *Mems & amp; micro devices applications*, Apr. 2022. [Online]. Available: https://www.engineeringsolutions.philips.com/looking-expertise/mems-micro-devices/mems-micro-devices-applications/.

[2] J. J. Bancifra, Tarlac State University, Tarlac City, Philippines, and https://orcid.org/0000-0003-0641-1305, "Supervisory practices of department heads and teachers' performance: Towards a proposed enhancement program," *APJAET - Journal ay Asia Pacific Journal of Advanced Education and Technology*, pp. 25–33, Sep. 2022.

[3] *Polymer-based biomems*. [Online]. Available: https://www.egr.msu.edu/mems/projects/polymer-based-biomems.

[4] Kayakuam, *Su-8 2000*, 2020. [Online]. Available: https://kayakuam.com/products/su-8-2000/.

[5] DOW, *Cyclotene* 3000 series advanced electronic resins*, 2005. [Online]. Available: https://wiki.nanotech.ucsb.edu/w/images/7/72/BCB-cyclotene-3000-revA.pdf.

[6] SCS, *Scs parylene properties*, 2022. [Online]. Available: https://scscoatings.com/parylene-coatings/parylene-properties/.

[7] Kayakuam, *Perminex® 1000 and 2000 wafer bonding adhesives*, 2019. [Online]. Available: https://kayakuam.com/products/perminex-wafer-bonding-adhesives/.

[8] H. microsystems, *Pi2600 series*, 2022. [Online]. Available: https://www.hdmicrosystems.com/products/pi-2600-series.html.

[9] T. O. K. product, *Photosensitive permanent films*. [Online]. Available: https://www.tok-pr.com/en/products/structure-forming-material/photosensitive-permanent.html.

[10] Kayakuam, *Lab-on-a-chip*, 2016. [Online]. Available: https://kayakuam.com/products/lab-on-a-chip/.

[11] H. microsystems, *Techniques and considerations in the microfabrication of parylene c microelectromechanical systems*, 2022. [Online]. Available: https://pdfs.semanticscholar.org/d053/90e47a273a39b801239ed23d1a0bc646ed9c.pdf.

[12] X. Zhou and S. Virasawmy, "Wafer-level bcb bonding using a thermal press for microfluidics," *Microsyst. Technol.*, vol. 15, pp. 573–580, Jan. 2009. DOI: 10.1007/s00542-008-0712-2.

[13] C. Cber, "Use of international standard iso 10993-1, "biological evaluation of medical devices-part 1: Evaluation and testing within a risk management process" guidance for industry and food and drug administration staff preface public comment." [Online]. Available: https://www.fda.gov/vaccines-blood-biologics/guidance-compliance-regulatory-information-.

[14] C. P. Constantin, M. Aflori, R. F. Damian, and R. D. Rusu, "Biocompatibility of polyimides: A mini-review," *Materials*, vol. 12, p. 3166, 19 Sep. 2019, ISSN: 1996-1944. DOI: 10.3390/ma12193166. [Online]. Available: https://www.mdpi.com/1996-1944/12/19/3166.

[15] ElveFlow, *How to succeed with your su-8 photoresist spin coating*. [Online]. Available: https://www.elveflow.com/microfluidic-reviews/soft-lithography-microfabrication/su-8-photolithography-spin-coating/.

[16] R. Bashir, "Biomems: State-of-the-art in detection, opportunities and prospects," *Advanced Drug Delivery Reviews*, vol. 56, pp. 1565–1586, 11 Sep. 2004, ISSN: 0169409X. DOI: 10.1016/j.addr.2004.03.002.

[17] M.Abramowitz and M. Davidson, *Fluorochrome data tables*. [Online]. Available: https://www.olympus-lifescience.com/en/microscope-resource/primer/techniques/fluorescence/fluorotable2/.

[18] S. Hosseini, ·. Michelle, A. Espinosa-Hernandez, *et al.*, "Lecture notes in bioengineering." [Online]. Available: http://www.springer.com/series/11564.

[19] B. . Valeur and M. . N. . Berberan-Santos, *Molecular Fluorescence: Principles and Applications*, 2nd ed. Wiley-VCH, Mar. 2013.

[20] B. Lu, S. Zheng, B. Q. Quach, and Y. C. Tai, "A study of the autofluorescence of parylene materials for μtas applications," Tech. Rep., 2010, pp. 1826–1834. DOI: 10.1039/b924855b.

[21] W. Kubicki, R. Walczak, and J. A. Dziuban, "Discussion and summary optical transmittance miniature spectrometer pc with dedicated software," Tech. Rep., 2020. [Online]. Available: www.memslab.eu.

[22] R. Walczak, P. Śniadek, and J. A. Dziuban, "Su-8 photoresist as material of optical passive components integrated with analytical microsystems for real-time polymerase chain reaction lab-on-chip payload as a first step towards development of fully-integrated astrobiological nanosatellite view project su-8 photoresist as material of optical passive components integrated with analytical microsystems for real-time polymerase chain reaction," Tech. Rep., 2011. [Online]. Available: https://www.researchgate.net/publication/267689736.

[23] M. J. Cen, T. Chang, Y. B. Yin, X. L. Li, and Y. W. He, "A novel ratiometric fluorescent sensor for ag+ based on two fluorophores," *Methods and Applications in Fluorescence*, vol. 6, 3 Apr. 2018, ISSN: 20506120. DOI: 10.1088/2050-6120/aabcf1.

[24] Y. Wu, Z. Chen, J. Ji, *et al.*, "Multifunctional polyimides by direct silyl ether reaction of pendant hydroxy groups: Toward low dielectric constant, high optical transparency and fluorescence," *European Polymer Journal*, vol. 132, no. 00143057, 2020. DOI: 0.1016/j.eurpolymj.2020.109742.

[25] ASML, *All about light and lasers in lithography*, 2019. [Online]. Available: https://www.asml.com/en/technology/lithography-principles/light-and-lasers.

[26] Wikipedia-Autoren, *Fotolithografie (Halbleitertechnik)*, Dec. 2003. [Online]. Available: https://de.wikipedia.org/wiki/Fotolithografie_(Halbleitertechnik).

[27] V. V. P. Sreenivas, A. Winkler, S. Harazim, and O. G. Schmidt, "Ultraviolet transmittance of su-8 photoresist and its importance in multi-wavelength photolithography," *Journal of Vacuum Science & Technology B*, vol. 36, p. 051 601, 5 Sep. 2018, ISSN: 2166-2746. DOI: 10.1116/1.5033996.

[28] Y. G. Zhao, W. K. Lu, Y. Ma, S. S. Kim, S. T. Ho, and T. J. Marks, "Polymer waveguides useful over a very wide wavelength range from the ultraviolet to infrared," *Applied Physics Letters*, vol. 77, pp. 2961–2963, 19 Nov. 2000, ISSN: 00036951. DOI: 10.1063/1.1323547.

[29] S. Aryal, *Fluorescence microscopy- definition, principle, parts, uses*, 2022. [Online]. Available: https://microbenotes.com/fluorescence-microscope-principle-instrumentation-applications-advantages-limitations/.

[30] E. S. Solusindo, *Image analysis*. [Online]. Available: http://enigma-saintia.com/image-analysis/.

[31] C. A. Schneider, W. S. Rasband, and K. W. Eliceiri, "NIH Image to ImageJ: 25 years of image analysis," *Nature Methods*, vol. 9, no. 7, pp. 671–675, Jun. 2012. DOI: 10.1038/nmeth.2089. [Online]. Available: http://dx.doi.org/10.1038/nmeth.2089.

[32] *Lambda 850+ uv/vis spectrophotometer-l850*. [Online]. Available: https://www.perkinelmer.com/nl/product/lambda-850-uv-vis-spectrophotometer-l850.

[33] A. K. Gaigalas, L. Wang, S. J. Choquette, Y.-Z. Zhang, and V. Karpiak, "Measurement of scattering cross section with a spectrophotometer with an integrating sphere detector," *Journal of Research of the National Institute of Standards and Technology*, vol. 117, p. 202, 2012. DOI: 10.6028/jres.117.012. [Online]. Available: https://doi.org/10.6028/jres.117.012.

[34] F. Lofink, D. Kähler, and W. Reinert, *Hermeticity tests*, Jan. 2015. DOI: 10.1016/B978-0-323-29965-7.00040-3.

[35] F. . Selbmann, M. . Baum, M. . Wiemer, and T. . Gessner, “Deposition of Parylene C and characterization of its hermeticity for the encapsulation of MEMS and medical devices,” *2016 IEEE 11th Annual International Conference on Nano/Micro Engineered and Molecular Systems (NEMS)*, Apr. 2016. DOI: 10.1109/nems.2016.7758283. [Online]. Available: http://dx.doi.org/10.1109/nems.2016.7758283.

[36] H. . Greenhouse, *Hermeticity of Electronic Packages, Second Edition*, 2nd ed. William Andrew, Nov. 2011.

[37] J. Oberhammer, F. Niklaus, and G. Stemme, “Sealing of adhesive bonded devices on wafer level,” vol. 110, Feb. 2004, pp. 407–412. DOI: 10.1016/j.sna.2003.06.003.

[38] W. . Li, D. . Rodger, P. . Menon, and Y. C. Tai, “Corrosion Behavior of Parylene-Metal-Parylene Thin Films in Saline,” *ECS Transactions*, vol. 11, no. 18, pp. 1–6, Oct. 2008. DOI: 10.1149/1.2897437. [Online]. Available: http://dx.doi.org/10.1149/1.2897437.

[39] S. M. Kani, “Polyimide encapsulation for implantable medical devices,” 2020.

[40] Y. J. Kim, Y.-T. Kang, and Y.-H. Cho, “A poly(ethylene glycol)-modified tapered-slit membrane filter for the efficient release of captured viable circulating tumor cells.,” *Analytical Chemistry*, vol. 88, Jul. 2016. DOI: 10.1021/acs.analchem.5b04927.

[41] Q. . Du, J. . Liu, L. . Guo, M. . Lv, and X. . Zeng, “Tailoring the surface wettability of polyimide by UV laser direct texturing in different gas atmospheres,” *Materials & amp; Design*, vol. 104, pp. 134–140, Aug. 2016. DOI: 10.1016/j.matdes.2016.05.008. [Online]. Available: http://dx.doi.org/10.1016/j.matdes.2016.05.008.

[42] C. Graf, M. Günther, and G. Gerlach, “Biocompatible hermetic encapsulation for implantable miniaturized biomedical sensor system,” *Procedia Technology*, vol. 27, pp. 42–43, Dec. 2017. DOI: 10.1016/j.protcy.2017.04.020.

[43] M. Yoon, K. Ko, S.-W. Min, and S. Im, “Polymer/oxide bilayer dielectric for hysteresis-minimized 1 v operating 2d tmd transistors,” *RSC Advances*, vol. 8, pp. 2837–2843, Jan. 2018. DOI: 10.1039/C7RA12641G.

[44] B. Moon, N. Jun, S. Park, C. S. Seok, and U. S. Hong, “A study on the modified arrhenius equation using the oxygen permeation block model of crosslink structure,” *Polymers*, vol. 11, 1 Jan. 2019, ISSN: 20734360. DOI: 10.3390/polym11010136.

[45] V. Blanco Carballo, J. Melai, C. Salm, and J. Schmitz, “Moisture resistance of su-8 and kmpr as structural material,” *Microelectronic Engineering*, vol. 86, no. 4-6, pp. 765–768, 2009. DOI: 10.1016/j.mee.2008.12.076.

[46] M. Nordström, A. Johansson, E. S. Noguerón, B. Clausen, M. Calleja, and A. Boisen, “Investigation of the bond strength between the photo-sensitive polymer su-8 and gold,” vol. 78-79, Mar. 2005, pp. 152–157. DOI: 10.1016/j.mee.2004.12.021.

[47] R. Dekker, ; V. Henneken, M. Louwerse, P. Restricted, □. Koninklijke, and P. Electronics, “Adhesion of polyimide,” 2013.

[48] M. Ferreira, S. Pinto, F. Aires da Silva, A. Bettencourt, S. Aguiar, and M. Gaspar, “Liposomes as a nanoplatform to improve the delivery of antibiotics into staphylococcus aureus biofilms,” *Pharmaceutics*, vol. 13, p. 321, Mar. 2021. DOI: 10.3390/pharmaceutics13030321.

[49] Z. Chen and J. B. Lee, “Biocompatibility of su-8 and its biomedical device applications,” *Micromachines*, vol. 12, 7 Jul. 2021, ISSN: 2072666X. DOI: 10.3390/mi12070794.

[50] Y. . Sun, S. P. Lacour, R. A. Brooks, N. . Rushton, J. . Fawcett, and R. E. Cameron, “Assessment of the biocompatibility of photosensitive polyimide for implantable medical device use,” *Journal of Biomedical Materials Research Part A*, vol. 90A, no. 3, pp. 648–655, Sep. 2009. DOI: 10.1002/jbm.a.32125. [Online]. Available: http://dx.doi.org/10.1002/jbm.a.32125.

[51] J. . Kim, K. H. Choi, Y. . Kim, B. . Park, and G. . Cho, “Wearable Plasma Pads for Biomedical Applications,” *Applied Sciences*, vol. 7, no. 12, p. 1308, Dec. 2017. DOI: 10.3390/app7121308. [Online]. Available: http://dx.doi.org/10.3390/app7121308.

[52] J. S. Mandelli, J. . Koepp, A. . Hama, S. . Sanaur, G. A. Rae, and C. R. Rambo, “Cell viability and cytotoxicity of inkjet-printed flexible organic electrodes on parylene C,” *Biomedical Microdevices*, vol. 23, no. 1, Jan. 2021. DOI: 10.1007/s10544-020-00542-z. [Online]. Available: http://dx.doi.org/10.1007/s10544-020-00542-z.

[53] G. . Ehteshami, A. . Singh, G. . Coryell, S. . Massia, J. . He, and G. . Raupp, “Glial cell and fibroblast cytotoxicity study on 4026-cyclotene photosensitive benzocyclobutene (BCB) polymer films,” *Journal of Biomaterials Science, Polymer Edition*, vol. 14, no. 10, pp. 1105–1116, Jan. 2003. DOI: 10.1163/156856203769231592. [Online]. Available: http://dx.doi.org/10.1163/156856203769231592.

[54] *Synergy HTX Multi-Mode Microplate Reader: Fluorescence-Luminescence - Features*. [Online]. Available: https://www.biotek.com/products/detection-multi-mode-microplate-readers/synergy-htx-multi-mode-reader/features/.